4-27-2018

Roles of Phospholipases and Ribosomal S6 Kinase in Lipid Remodeling and Growth in Arabidopsis Response to Phosphate Deprivation

Yuan Su
ysyn7@mail.umsl.edu

Roles of Phospholipases and Ribosomal S6 Kinase in Lipid Remodeling and Growth in Arabidopsis Response to Phosphate Deprivation

Yuan Su
B.S., Biology, Xiamen University, 2009

A Dissertation Submitted to The Graduate School at the University of Missouri-St. Louis in partial fulfillment of the requirements for the degree

Doctor of Philosophy in Biology
with an emphasis in Cell and Molecular Biology

May, 2018

Advisory Committee

Xuemin Wang, Ph.D.
Chairperson

Bethany Zolman, Ph.D.

Lon Chubiz, Ph.D.

Wendy Olivas, Ph.D.

Acknowledgement

"Nothing happens unless first a dream." That is what I have learned and believed throughout my Ph.D life at University of Missouri-St. Louis. My best and most exciting experiences so far are always associated with wonderful people around. So first of all, I have to give my deepest respect and sincerest appreciation to my dear advisor Dr. Xuemin Wang, who has supported and guided me unconditionally through my study and research in his lab. Besides the interesting and inspiring research projects that I have been working on with Dr. Wang's tremendous help and trust, he has also influenced me by continuously reminding me how to get things well planned, how to troubleshoot when facing problems and more importantly how to think critically and logically. He is definitely one of my important and beloved persons in my career and life.

I would also like to thank my current committee members Dr. Wendy Olivas, Dr. Bethany Zolman, and Dr. Lon Chubiz and my previous committee member Dr. Mindy Steiniger. They have mentored and supported me all the time by giving me good suggestions on my research, sharing lab equipment and materials, and shaping me with their kind and smart minds. In addition, I want to give my thanks to Dr. Michael Hughes as well as Dr. Jiajia Li and Erin Terry in his lab, for their help with my RNA-seq experiment, and Dr. James Umen for letting me use their devices for the polysome analysis.

I also appreciate countless care from the department of biology, my colleagues,

and my lab mates from UMSL and Donald Danforth Plant Science Center. I feel so lucky to meet and know these kind and brilliant people, especially the people in Wang lab including Dr. Maoyin Li, Dr. Geliang Wang, Dr. Liang Guo, Dr. Sanchul Kim, Dr. Yu Liu, Dr. Yong Zheng, Dr. Sung Chul Bahn, Dr. Guangqin Cai, Dr. Jianwu Li, Dr. Fengjuan Yang, Amanda Tawfall, Brian Fanella, Xinliang Huang, Shanshan Sun, Siyun Su and many undergraduate students, intern students and visiting scholars.

Finally, I want to thank my families who always stand on my side and give me huge love and understanding. All the moments and stories I had so far during my Ph.D study here will be a precious chapter of my life and will continue to encourage me to become a stronger and better person in the future.

Abstract

Phosphate (Pi) is one of three macronutrients for plants, which is vital for plant growth and development. Understanding the mechanism by which plants respond and adapt to Pi deficiency not only unveils functions of genes and pathways involved, but also provides potential tools to manipulate crops to better stand Pi stress in low Pi-containing lands. One of the significant metabolic changes in plants under Pi starvation is the membrane lipid remodeling that converts Pi-containing lipids such as phospholipids to Pi-free lipids, such as glycolipids. To elucidate the metabolism and regulation of lipid remodeling, this dissertation characterized the role of two phospholipases, phospholipase D zeta2 (PLDζ2) and nonspecific phospholipase C4 (NPC4), which hydrolyze phospholipids and their gene expressions are highly induced by Pi limitation. I generated double knockout *pldζ2npc4* Arabidopsis and performed comprehensive growth and membrane lipid analyses in single and double knockout under Pi deprivation. NPC4 contributed DGDG accumulation at an early stage of Pi deprivation in roots while PLDζ2 displayed a dominant effect on lipid remodeling at a later stage of Pi deprivation in leaves. In addition, NPC4 facilitated root hair elongation, but had no effect on root hair density. By comparison, PLDζ2 constrained both root hair elongation and density. The results indicate that PLDζ2 and NPC4 mediate the Pi deprivation-induced lipid remodeling in a tissue- and time-specific manner, and that PLDζ2 negative modulates root hair density and length whereas NPC4 promotes root hair elongation in response to Pi deprivation.

To probe the regulation of membrane lipid remodeling, it was found that phosphatidic acid (PA), a central lipid intermediate and product of the phospholipase reactions, binds to S6 Kinase (S6K). S6K is a ribosomal protein kinase in the TOR (Target of Rapamycin) signaling pathway involved in nutrient sensing and growth control. Knockout of *S6K2* but not *S6K1* in Arabidopsis impeded membrane lipid remodeling and root growth in response to Pi deficiency. In addition, a double mutant was generated between *S6K2 and* the transcription factor *PHR1* (PHOSPHATE RESPONSE 1). Comparative lipidomic profiling and growth analyses indicate that *S6K2* participates in the same pathway as *PHR1* because similar growth phenotypes and membrane lipid composition were observed among *s6k2*, *phr1* and *s6k2phr1*. The results indicate that *S6K2* but not *S6K1* is part of the regulatory pathway that controls lipid remodeling and growth adaption to Pi limitation.

ABBREVIATIONS

4E-BP1, 4E binding protein 1

BHT, butylated hydroxytoluene

DAG, diacylglycerol

DGDG, digalactosyldiacylglycerol

ESI-MS/MS, electrospray ionization–tandem mass spectrometry

ER, endoplasmic reticulum

FA, Fatty acid

G3P, glycerol-3-phosphate

KO, knockout

MGDG, monogalactosyldiacylglycerol

miR399, miscroRNA399

NPC, non-specific phospholipase C

OE, overexpression

P1BS, PHR1 binding sequence

PA, phosphatidic acid

PAH, phosphatidic acid hydrolase

PC, phosphatidylcholine

PE, phosphatidylethanolamine

PG, phosphatidylglycerol

PHR1, phosphate starvation response 1

PHT, phosphate transporter

PI, phosphatidylinositol

PL, phospholipids

PLA, phospholipase A

PLC, phospholipase C

PLD, phospholipase D

PS, phosphatidylserine

PSR, Pi starvation response

qPCR, quantitative real-time PCR

RAPTOR, regulatory associated protein of TOR

S6K, S6 kinase

SPR, surface plasmon resonance

TAG, triacylglycerol

TOR, Target of rapamycin

WT, wild-type

Contents

List of Figures

Chapter 1 Research Background

INTRODUCTION

Of various nutrients for plants, phosphorus (P), nitrogen (N) and potassium (K) are the three macronutrients essential for plant growth and therefore are important fertilizers for crop production in agriculture as they are required by plants in large quantities. The crop yield is highly limited by the deficiency in any of these nutrients. The increasing global demand of N and P fertilizer is due to the rising population and food production. The estimated N and P fertilizer usage reaches 120 metric ton (Mt) and 47 Mt by 2018, respectively (Heuer et al., 2017). Nitrogen fertilizers are made of nitrogen gas from atmosphere which is a huge and recycled resource although the fertilizer production is energy-intensive. By comparison, P fertilizers are produced from phosphate rocks which are a finite natural resource. It is estimated that the easily accessible phosphate rocks will last another 300-400 years and new P resources have to be explored (Rahman et al., 2014; Heuer et al., 2017). The cause of P deficient agricultural soils is either due to insufficient P replacement back into lands or because of little available P form (phosphate) present as it is often fixed by aluminum (Al) or iron (Fe) in soils with low or high PH, or by calcium (Ca) in alkaline soils (Pérez-Torres et al., 2008; Cordell et al., 2009; Haefele et al., 2014).

P is the key element in many biological organic components in cells such as genetic material nucleic acid (DNA and RNA), membrane phospholipids,

signaling cascade participants phosphorylated proteins, and energy molecules (e. g. ATP, NADPH). Therefore, P homeostasis in plants is tightly regulated through mechanisms, such as P acquisition, P translocation, and P metabolism (Ham et al., 2018).

Root system architecture adaptions to low phosphate availability

Plants perceive and absorb water and nutrients from soil through their root systems that locate at the plant-soil interface. Different plant species have evolved and exhibited various root architectures to optimize their needs from lands based on the local environments and soil types. As P, unlike N, is immobile and usually in the surface soil, the capability of plants to access P relies on whether they can form dense and shallow root system. The morphological changes of plant root systems in response to deficient P have been intensely studied in many plant species including model plant Arabidopsis, maize, rice, and tomato (Williamson et al., 2001; López-Bucio et al., 2002; López-Bucio et al., 2003; Pérez-Torres et al., 2008). When transferring Arabidopsis seedlings from a P-sufficient medium to a P-limited medium, the first visible event is the strong reduction of primary root growth with enhanced lateral root and root hair formation. These changes resulted in enlarged root surface to enhance P acquisition (López-Arredondo et al., 2014). One of the proposed underlying mechanisms of root morphological changes under Pi deprivation is due to changes in auxin levels and sensitivity (López-Arredondo et al., 2014).

Phosphate uptake

Besides the ability to alter root morphologies to adapt the low P environment, plants also upregulate phosphate transporters in the epidermal cells that are located on the outer cortex of the root. In Arabidopsis, *PHT* (*Phosphate Transporter*) genes that encode Pi transporters can be grouped into four gene families: *PHT1*, *PHT2*, *PHT3*, and *PHT4*, where high-affinity Pi transporter PHT1 locates on the plasma membrane and transports Pi from root-contacting soil to the inside of root cells, while the Pi distribution and translocation to other subcellular compartments such as chloroplasts, mitochondria and Golgi is carried out by low Pi affinity PHT2, PHT3 and PHT4 proteins (Versaw and Harrison, 2002; Guo et al., 2008; Cubero et al., 2009; Heuer et al., 2017). *PHT1* gene family comprises nine members and has been well characterized in Arabidopsis (Bucher, 2007). When Pi is low, PHT1 proteins uptake Pi mainly in the form $H_2PO^-_4$ and HPO^{2-}_4 from relatively low Pi concentration containing soil to the relatively high Pi concentration containing cytoplasm of root epidermal cells against the ion concentration gradient, which is part of the direct Pi uptake pathway (Raghothama and Karthikeyan, 2005).

In addition to PHT Pi transporters, another well studied protein PHO1 translocates Pi from roots to shoots and plays an important role in keeping Pi homeostasis (Hamburger et al., 2002). Arabidopsis null mutant *pho1* exhibits severe leave growth defect and low seed yield as well as accumulated anthocyanin, which are the typical phenotypes associated with Pi starvation, and

reserves a low Pi level in shoots (Poirier et al., 1991). PHO1 protein contains a N-terminal hydrophilic SPX (named after two yeast proteins Syg1 and Pho81, and a human protein Xpr1) tripartite domain and a EXS domain (ERD1/SYG1/XPR1) at C-terminus (Wang et al., 2004). PHO1 function is tightly regulated by PHO2, a ubiquitin E2 conjugase, via degrading PHO1 protein through its SPX domain (Liu et al., 2012). In addition, plants can exude organic acids or phosphatases into soil to solubilize P complexes or hydrolyze organic P, respectively, to enhance P availability for uptatke (Hammond et al., 2004; López-Arredondo et al., 2014).

Plant metabolic changes in response to P deficiency

One of prominent metabolic modifications during Pi deficiency is that P containing phospholipids are replaced by non-P containing glycolipids including galactolipids and sulfolipids to recycle P from an internal source. This lipid remodeling process was initially identified in non-photosynthetic bacterium *Pseudomonas diminuta*, followed by finding similar phenomena in photosynthetic bacterium *Rhodobacter sphaeroides* (Minnikin et al., 1974; Benning et al., 1993; Benning et al., 1995). Seed plants also showed such changes of P lipids to non-P lipids in response to low P availability. In Arabidopsis, lipid remodeling occurs in two steps: 1) membrane bilayer lipids phospholipids are hydrolyzed by phospholipase D (PLD) or phospholipase C (PLC) to produce phosphatidic acid (PA) or diacylglycerol (DAG), respectively to contribute the DAG pool with PA later converted to DAG by PA phosphohydrolases (PAH). 2) DAG generated by

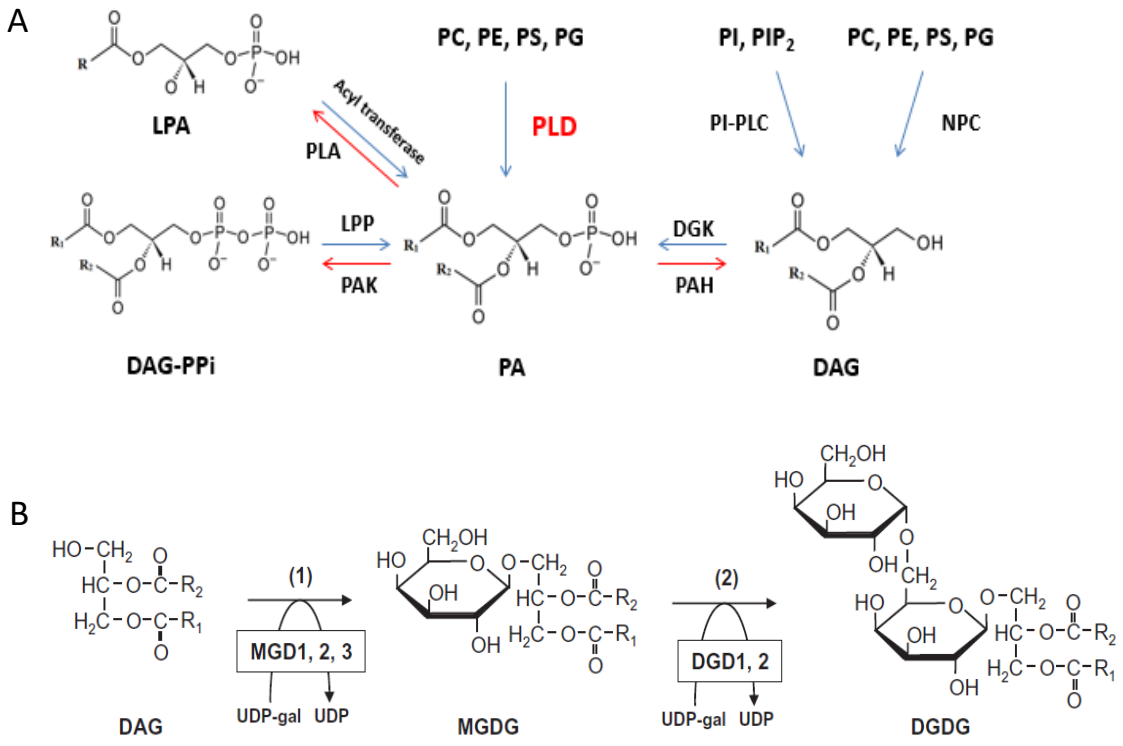

Figure 1-1 Phospholipids and galactolipids metabolism.

A) Phospholipid metabolism. PA is in the central of phospholipid metabolism. The blue arrows indicate PA-producing pathways and the red arrows indicate PA-removing pathways. B) Galactolipid metabolism (modified from Shimojima and Ohta, 2011). Enzymes are abbreviated as follows: PLA phospholipase A, LPAAT LPA acyltransferase, PLD phospholipase D, PI-PLC phosphoinositide-phospholipase C, NPC nonspecific PLC, DGK DAG kinase, LPP lipid phosphate phosphatase, PAK PA kinase, PAH PA phosphohydrolase, MGD MGDG synthase, DGD DGDG synthase. Metabolites are abbreviated as follows: DAG diacylglycerol, DAG-PPi DAG pyrophosphate, LPA lyso-PA, PC phosphatidylcholine, PE phosphatidylethanolamine, PS phosphatidylserine, PG phosphatidylglycerol, PIP2 phosphatidylinositol 4,5-bisphosphate, DAG diacylglycerol, MGDG monogalactosyldiacylglycerol, DGDG digalactosyldiacylglycerol.

phospholipases are used to synthesize monogalactosyldiacylglycerol (MGDG) and digalactosyldiacylglycerol (DGDG) (Nakamura, 2013; Figure 1-1). Several phospholipid-hydrolyzing enzymes such as PLDζ1, PLDζ2, NPC4 (non-specific PLC), and NPC5 are reported to function in the lipid remodeling, while the facilitated MGDG and DGDG synthesis is mediated by MGD2 and MGD3, and DGD1 and DGD2, respectively (Härtel et al., 2000; Kelly and Dörmann, 2002; Li et al., 2006a; Gaude et al., 2008; Kobayashi et al., 2009).

Membrane phospholipids

Phospholipids are the main component of cell membranes including plasma membrane and subcellular organelle membranes such as mitochondria, endoplasmic reticulum (ER), and vacuole along with membrane anchored proteins and carbohydrates in eukaryotes such as yeast, mammals and plants (Wang et al., 2006). The basic structure of a single phospholipid molecule contains a glycerol backbone, with a hydrophilic head group attached to one hydroxyl group and a hydrophobic free fatty acid conjugated to each of other two hydroxyl groups. Phospholipids can be primarily classified as phosphatidic acid (PA), phosphatidylcholine (PC), phosphatidylethanolamine (PE), phosphatidylserine (PS), phosphatidylinositol (PI) and phosphatidylglycerol (PG), with phosphate, choline, ethanolamine, serine, inositol and glycerol as their head groups, respectively (Testerink and Munnik, 2005; Figure 1-2). Besides head groups, the composition of acyl chains also determines the physical and biological properties of phospholipids. For example, 16:0 PA with 16 carbons and

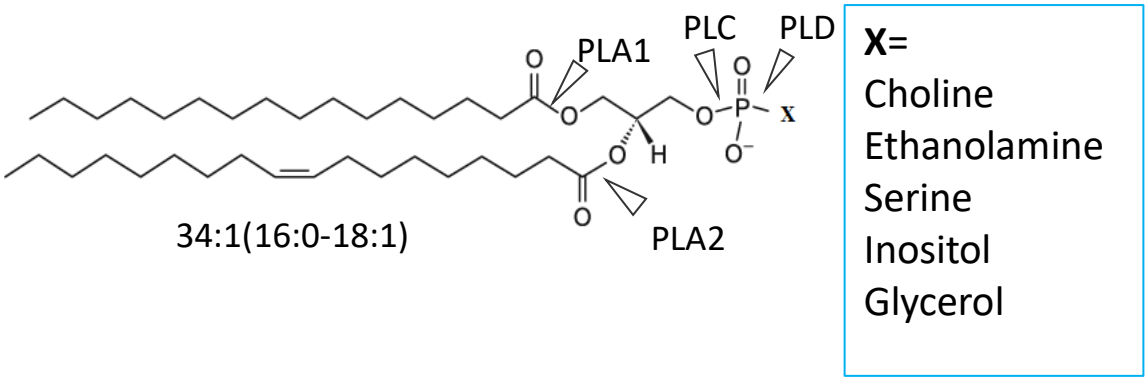

Figure 1-2 The molecular structure of phospholipids and the hydrolysis sites of phospholipases. (Modified from Wang et al., 2006)

Representative phospholipid with 18:1 fatty acid at sn-1 position, 16:0 fatty acid at sn-2 position. The head group could be choline, ethanolamine, serine, inositol or glycerol to make this phospholipid PC, PE, PS, PI or PG, respectively. PLD catalyzes at head group after the phosphate, whereas PLC catalyzes at head group before the phosphate. PLA1 and PLA2 hydrolyzes the sn-1 and sn-2 acyl chain respectively. X, head groups.

no double bond in each acyl chain may have different functions from 18:2 PA with 18 carbons and two double bonds in each acyl chain. Due to the amphipathic character of phospholipids, the phospholipid bilayer builds a stable and flexible membrane system that segregates cells and organelles from the outer environment. In plants, PC is the most abundant phospholipid in the plasma membrane while PA takes up less than 1% of total phospholipids (Wang et al., 2006). However, PA is emerging as a second messenger and plays a vital role in various signaling pathways and physiological processes.

Phospholipases D induced by Pi deprivation

There are four types of phospholipases in Arabidopsis, phospholipase A1 (PLA1), phophoslipase A2 (PLA2), phospholipase C (PLC) and phospholipase D (PLD), differing from each other based on the sites of phospholipids they hydrolyze (Wang et al., 2012; Figure 1-2). Particularly, PLD catalyzes phospholipid substrates such as PC or PE to produce PA and a free head group such as choline or ethanolamine, respectively (Li et al., 2009). Arabidopsis has 12 *PLD* genes in its genome and these *PLD*s can be divided into two distinctive groups. One group has 10 PLDs, PLDα (3), PLDß (2), PLDγ (3), PLDδ, and PLDε, subclassified by their sequence similarities and biochemical identities. These PLDs feature a Ca2+-dependent phospholipid binding C2 domain, which is unique to plants. In contrast, the other group only contains two PLDs, PLDζ (2), which contain phox homology (PX) and pleckstrin homology (PH) domains (Kolesnikov et al., 2012; Li et al., 2009; Wang et al., 2006). Out of 12 PLDs,

PLDζ1 and PLDζ2 were

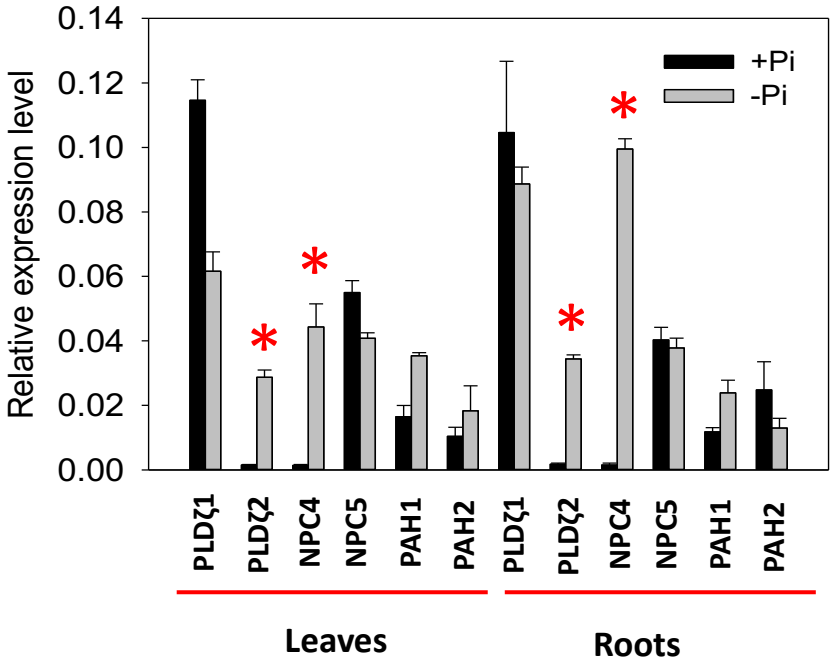

Figure 1-3 Gene expression of selected phospholipase genes in WT Arabidopsis leaves and roots under +Pi and -Pi conditions.

Relative gene expression levels of *PLDζ1*, *PLDζ2*, *NPC4*, *NPC5*, *PAH1* and *PAH2* in WT leaves and roots. The Arabidopsis samples were collected at day 5 after Pi starvation treatment before which seedlings were grown in +Pi medium for 3 days after germination. Values are means ± SD (n = 3). Asterisk indicates the significant ($P < 0.05$) differences between same genotypes under Pi-sufficient or deficient conditions based on Student's *t*-test.

shown to affect primary root growth and mainly hydrolyze PC to release PA (Li et al., 2006b; Li et al., 2006a). Especially, PLDζ2 gene expression is highly promoted by Pi starvation, and the DGDG levels in roots decrease in pldζ2 mutant (Cruz-Ramirez et al., 2006). Besides the function involved in Pi starvation response, PLDζ2 also plays a role in vesicle trafficking and auxin response (Li and Xue, 2007). A later study also found an enhancer element in the promoter region of PLDζ2 as a conserved low-Pi-responsive transcriptional sequence (Oropeza-Aburto et al., 2012).

Nonspecific phospholipase C induced by Pi deprivation

There are two types of PLC: phosphoinositides specific PLC (PI-PLC) and non-specific PLC (NPC) that works on various phospholipid substrates such as PC and PE. Arabidopsis genome contains 6 *NPC*s (*NPC1* to *NPC6*), two out of which *NPC4* and *NPC5* play roles in Pi starvation response. The gene expression of NPC4 is significantly induced by Pi deficiency and the enzyme extracted from Pi-starved plants displayed strong PC-hydrolyzing ability in vitro (Nakamura et al., 2005). Nevertheless, the DGDG level and phospholipid levels in *npc4* shoots was not significantly different from WT under low Pi (Nakamura et al., 2005), resulting in the mystery of NPC4 function. It is possible that NPC4's role is covered up by a redundant phospholipase such as other NPCs or PLDs, or NPC4 may function at a certain period after Pi stress and/or in a tissue specific manner. In contrast, a less Pi-starvation induced NPC5 compared with NPC4 contributes to the DGDG accumulation and PC/PE degradation (Gaude et al.,

2008). It is uncertain that if the cellular localization difference of NPC4 and NPC5 affects their activity in the lipid remodeling as NPC4 primarily locates on the plasma membrane whereas NPC5 is in the cytosol which access to ER and chloroplast envelops, although NPC4 and NPC5 share high amino acid sequence identities (Nakamura, 2013).

It is interesting that PLDζ2 and NPC4 are the only highly induced ones by Pi starvation in both shoots and roots among several candidate phospholipase genes (Figure 1-3). Previous investigations shed some light on the function of PLDζ2 and NPC4 in phospholipid hydrolyzing capability (Nakamura et al., 2005; Li et al., 2006). However, the role of NPC4 is still unknown. Whether PLDζ2 and NPC4 have redundant functions, and how these two enzymes interact with each other in the network of converting phospholipids to DAG and then further to MGDG and DGDG is not clear. In order to further explore the role of PLDζ2 and NPC4, I wanted to generate *pldζ2npc4* double mutant and carry out detailed lipid profiling comparing WT, single mutant *pldζ2*, *npc4*, and double mutant *pldζ2npc4*. Shoot and roots samples collected at 5-day, 10-day and 14-day after Pi starvation treatment will be subject to lipid analysis (as described in chapter 2).

Gene regulation upon P stress

PHR1 (Phosphate Starvation Response 1) is a MYB-like master transcription factor that regulates a large portion of Pi-starvation-response (PSR) genes including phospholipase genes, galactolipid synthesis genes, Pi transporter

genes introduced above and many other genes involved in pathways responsive to Pi limitation. Interestingly, PHR1 itself is not induced by Pi starvation. It binds to the conserved P1BS sequence (GNATATNC) in the promoter of target genes (Franco‐Zorrilla et al., 2004; Bustos et al., 2010). The knockout mutant *phr1* displayed retarded growth compared with wild type (WT) and failed to induce PSR genes (Bustos et al., 2010). Along with microRNA399 (miR399) and PHO2, PHR1 defines a phosphate signaling pathway that communicate Pi status between roots and shoots to keep the phosphate homeostasis (Bari et al., 2006; Pant et al., 2008; Heuer et al., 2017).

TOR-S6K pathway in plants

The TOR (target of rapamycin)-S6K (small ribosomal subunit protein S6 kinase) pathway is a signaling pathway that governs many biological and cellular processes, including nutrient sensing, cell growth, cell apoptosis, cell differentiation and tumor formation in animals (Foster, 2007; Xu et al., 2011). Both PA and PLDs are known to participate in this pathway to regulate the cell growth and proliferation particularly. The mammalian target of rapamycin (mTOR) is a serine/threonine kinase and executes its functions in protein complexes that integrate a wide range of signals such as nutrient, growth factors, and mitogen stimuli (Foster, 2007). mTOR composes two distinct complexes – mTORC1 and mTORC2 (Sarbassov et al., 2004). mTORC1 and mTORC2 have different protein components and biological functions. mTORC1 contains the featured protein Raptor (regulatory associated protein of TOR) and the activated

mTORC1 can phosphorylate and activate its downstream targets S6K1 at Thr-389 and eukaryotic initiation factor 4E binding protein 1 (4E-BP1) at Thr-37/46. Both S6K1 and 4E-BP1 are regulators involved in protein synthesis and subsequently are involved in mTOR mediated cell growth and tumorigenesis (Yoon et al., 2011). In contrast, mTORC2 contains the featured protein Rictor and it can phosphorylate Akt at Ser-473, which is a negative regulator involved in mTOR regulation of cell growth and proliferation (Sun and Chen, 2008; Yoon et al., 2011).

As one of the main downstream targets of TORC, S6K is a Ser/Thr protein kinase that phosphorylates a 40S ribosomal subunit protein S6 (Lehman et al., 2007). S6K tightly regulates the ribosome biogenesis and protein synthesis through TOR and phosphoinositide-dependent kinase-1 (PDK-1) signaling pathways (Wullschleger et al., 2006; Henriques et al., 2010; Fenton and Gout, 2011). The activation of S6K is through the phophorylation by PDK1 on T229 and T389 residues and several other kinases including TOR on T389 residue (Lehman et al., 2007).

Compared with the mTOR pathway in animals, the TOR-S6K pathway and the role of PLD/PA in the pathway are poorly studied in plants. In Arabidopsis, there is one gene copy of TOR and two Raptor genes (RAPTOR1/RAPTOR2) existing in the whole genome based on the sequence similarities to mTOR and Raptor in mammals (Dobrenel et al., 2016). It appears that Arabidopsis TOR (AtTOR) only

forms one protein complex as there are no homologs of hallmark proteins of TORC2 such as AVO1/hSIN1 or AVO3/RICTOR (Dobrenel et al., 2011), whereas both mammals and yeast have two TOR complexes (Xu et al., 2011). AtTOR has conserved protein domains compared with mTOR and they share about 40% sequence identity (Xiong and Sheen, 2012). Interestingly, most higher plants were thought to be resistant to rapamycin while mammal and yeast cells are highly sensitive to rapamycin (Mahfouz et al., 2006). However, a later report indicates that Arabidopsis seedlings are actually sensitive to the rapamycin but at a relatively high concentration of 100-1000 nM compared to 10-50 nM normally used in mammalian and yeast cells (Xiong and Sheen, 2012). The rapamycin treatment as well as other TOR inhibitors such as Torin2 and AZD can inhibit the seedling growth and AtTOR kinase activity on phosphorylating S6Ks, suggesting S6Ks are the substrates of AtTOR in plants as well (Xiong and Sheen, 2012; Xiong et al., 2017; Li et al., 2017).

In Arabidopsis, there are two S6K genes (*S6K1* and *S6K2*), which are tandemly located in chromosome 3. The two genes share 87% sequence identity and have similar functions as in animals and yeast (Mahfouz et al., 2006; Henriques et al., 2010; Yaguchi and Kozaki, 2018). The single knockout of either S6K1 or S6K2 has no obvious growth defects but the homozygous *s6k2* mutants (salk_13334) showed seed abortion (~30%) (Henriques et al., 2010). Further, hemizygous *s6k1s6k2*/++ mutants displayed reduced fertility, increased ploidy level, aborted seeds and smaller cell size in leaves compared with WT (Henriques et al., 2010).

In addition, ectopic overexpression (OE) of Lily S6K gene in Arabidopsis inhibited the cell expansion in petals and stamens by up-regulating genes involved in the flower development (Tzeng et al. 2009). The Arabidopsis S6K1 was indicated to interact with the Retinoblastoma-related 1 (RBR1)-E2FB complex to regulate the expression of E2F-dependent cell cycle genes and thus cell growth and proliferation (Henriques et al., 2010; 2013). Also, the binding motif of AtS6K1 with Raptor has been characterized and a 12-amino acid sequence at N-terminal domain was found critical for the binding (Son et al., 2017). Recently, rice S6K was shown to execute yeast Ypk3 function which is an ortholog of mammalian S6Ks in yeast. However, the conserved TOR phosphorylation at S6K hydrophobic domain was not detected in rice S6K expressed in yeast lacking Ypk3, whereas instead the N-terminal domain of S6K seemed important for its kinase activity (Yaguchi and Kozaki, 2018). The results suggest a more complicated role of plant S6K in the TOR pathway. Overall, all these lines of evidence demonstrate that S6Ks have conserved functions in animals and plants, while plant S6Ks may have their distinct and plant-specific properties. So far, S6K1 has been characterized by a few studies recently, whereas the role of S6K2 is vague.

The TOR pathway is a regulatory master that controls various biological events such as cell growth in response to extracellular hormones, nutrients, and stresses in mammals and yeast. In this pathway, PA has been demonstrated to be important in the regulation of kinase activity, to stabilize protein association,

and initiate protein translocation as a second signaling messenger. In contrast, such a regulatory pathway or signaling sensor that can incorporate environmental information and trigger cellular responses has not been found in plants (Figure 1-4). Unlike animals, plants cannot move and have to deal with complicated environmental cues and regulate internal signaling pathways to adjust their growth and development in response to limited sources. However, how plants integrate various environmental stimuli to correspondingly tune cellular homeostasis is poorly understood. The TOR pathway is a potential candidate to respond to nutrients, stress signals and hormones and optimize sources for cell growth and proliferation by regulating ribosome biogenesis and mRNA translation as many TOR pathway components are discovered in plants. It is very likely that plants utilize such a conserved signaling pathway. Notably, no studies have reported the role of PLD/PA in the plant TOR pathway, though it appears that PLD-derived PA is very likely to participate in the TOR pathway since they are indicated to function in the same biological processes. Therefore, I wanted to investigate the role of PA in the TOR-S6K pathway and the potential functions of TOR/S6K during the plant growth in response to nutrients or stresses in Arabidopsis.

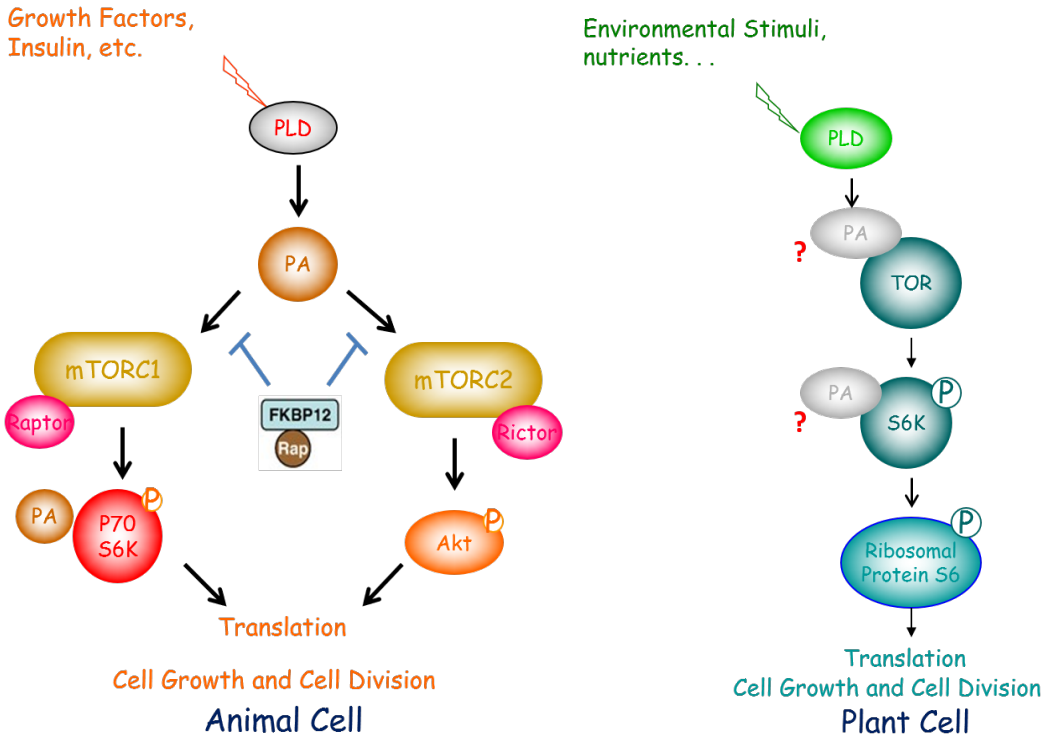

Figure 1-4 Schematic diagram showing TOR-S6K pathways in animal cells and plant cells.

In animals, PA generated by PLD that is activated by stimuli such as growth factors and insulin binds to mTOR complex 1 and 2 and then promotes the following signal cascade including S6K and Akt through a series of phosphorylation events. Therefore, cell growth and division are facilitated as the result. In plants, the details of TOR-S6K pathway are poorly understood. The studies have shown that Arabidopsis TOR protein can phosphorylate tow S6K proteins as substrates. However, it is not clear whether PLD or PA is participate in the pathway (Foster et al., 2014; Bond, 2017).

THE RESEARCH GOAL, HYPOTHESIS, AND SPECIFIC OBJECTIVES

The goal of the dissertation research was to determine the metabolic and regulatory processes of membrane lipid remodeling in plant response to Pi deficiency. One hypothesis was that the two phospholipases PLDζ2 and NPC4 that are highly induced under Pi deficiency play important roles in lipid remodeling and growth adaptation under Pi limitation. Another hypothesis was that the change in phospholipases and lipid remodeling in response to Pi limitation is under the control of a cellular machinery that regulate plant response to nutrient availability. To accomplish the goal and test the hypotheses sense, the objectives were to:

1. Characterize the role of PLDζ2 and NPC4 in lipid remodeling and growth in Arabidopsis response to Pi deficiency;
2. To explore the interaction of PA, the lipid product of PLDζ2 and NPC4, with S6Ks; and
3. To determine the role of S6Ks in Arabidopsis response to Pi deficiency.

REFERENCES

Bari, R., Datt Pant, B., Stitt, M., and Scheible, W.-R. (2006). PHO2, MicroRNA399, and PHR1 Define a Phosphate-Signaling Pathway in Plants. Plant Physiology 141, 988-999.

Benning, C., Huang, Z.H., and Gage, D.A. (1995). Accumulation of a Novel Glycolipid and a Betaine Lipid in Cells of Rhodobacter sphaeroides Grown under Phosphate Limitation. Archives of Biochemistry and Biophysics 317, 103-111.

Benning, C., Beatty, J.T., Prince, R.C., and Somerville, C.R. (1993). The sulfolipid sulfoquinovosyldiacylglycerol is not required for photosynthetic electron transport in Rhodobacter sphaeroides but enhances growth under phosphate limitation. Proceedings of the National Academy of Sciences 90, 1561-1565.

Bond, P. (2017). Phosphatidic acid: biosynthesis, pharmacokinetics, mechanisms of action and effect on strength and body composition in resistance-trained individuals. Nutrition & Metabolism 14, 12.

Bucher, M. (2007). Functional biology of plant phosphate uptake at root and mycorrhiza interfaces. New Phytologist 173, 11-26.

Bustos, R., Castrillo, G., Linhares, F., Puga, M.I., Rubio, V., Pérez-Pérez, J., Solano, R., Leyva, A., and Paz-Ares, J. (2010). A Central Regulatory System Largely Controls Transcriptional Activation and Repression Responses to Phosphate Starvation in Arabidopsis. PLOS Genetics 6, e1001102.

Cordell, D., Drangert, J.-O., and White, S. (2009). The story of phosphorus: Global food security and food for thought. Global Environmental Change 19, 292-305.

Cubero, B., Nakagawa, Y., Jiang, X.-Y., Miura, K.-J., Li, F., Raghothama, K.G., Bressan, R.A., Hasegawa, P.M., and Pardo, J.M. (2009). The Phosphate Transporter PHT4;6 Is a Determinant of Salt Tolerance that Is Localized to the Golgi Apparatus of Arabidopsis. Molecular Plant 2, 535-552.

Dobrenel, T., Mancera-Martínez, E., Forzani, C., Azzopardi, M., Davanture, M., Moreau, M., … Meyer, C. (2016). The Arabidopsis TOR Kinase Specifically Regulates the Expression of Nuclear Genes Coding for Plastidic Ribosomal Proteins and the Phosphorylation of the Cytosolic Ribosomal Protein S6. Frontiers in Plant Science, 7, 1611. http://doi.org/10.3389/fpls.2016.01611

Dobrenel, T., Marchive, C., Sormani, R, Moreau, M., Mozzo, M., MontaneM M.H., Menand, B., Robaglia, C., Meyer, C. (2011) Regulation of plant growth and metabolism by the TOR kinase. Biochem. Soc. Trans. 39, 477-481.

Deprost, D., Yao, L., Sormani, R., Moreau, M., Leterreux, G., Nicolai, M., Bedu, M., Robaglia, C., Meyer, C. (2007) The Arabidopsos TOR kinase links plant growth, yield, stress resistance and mRNA translation. EMBO reports 8, 864-870.

Fenton, T.R., and Gout, I.T. (2011). Functions and regulation of the 70 kDa ribosomal S6 kinases. The Intl J. Biochem & Cell Bio. 43, 47-59.

Foster, DA. Regulation of mTOR by phosphatidic acid. Cancer Res 2007; 67: (1).

Xu, L., Salloum, D., Medlin, PS., Saqcena, M., Yellen, P., Perrella, B., Foster, DA. (2011). Phospholipase D mediumtes nutrient input to mammalian target of rapamycin complex 1 (mTORC 1). Journal of Biological Chemistry 286, 25477-25486.

Foster DA., Salloum, D., Menon, D., and Frias, M. (2014). Phospholipase D and the Maintenance of Phosphatidic Acid Levels for Regulation of Mammalian Target of Rapamycin (mTOR). Journal of Biological Chemistry 289, 22583-22588.

Franco‐Zorrilla, J.M., González, E., Bustos, R., Linhares, F., Leyva, A., and Paz‐Ares, J. (2004). The transcriptional control of plant responses to phosphate limitation. Journal of Experimental Botany 55, 285-293.

Gaude, N., Nakamura, Y., Scheible, W.R., Ohta, H., and Dormann, P. (2008). Phospholipase C5 (NPC5) is involved in galactolipid accumulation during phosphate limitation in leaves of Arabidopsis. Plant J 56, 28-39.

Guo, B., Jin, Y., Wussler, C., Blancaflor, E.B., Motes, C.M., and Versaw, W.K. (2008). Functional analysis of the Arabidopsis PHT4 family of intracellular phosphate transporters. New Phytologist 177, 889-898.

Haefele, S.M., Nelson, A., and Hijmans, R.J. (2014). Soil quality and constraints in global rice production. Geoderma 235-236, 250-259.

Ham,B.K, Chen,J., Yan, Y., Lucas, W.J. (2018) Insights into plant phosphate sensing and signaling, Current Opinion in Biotechnology, 49, 1-9.

Hamburger, D., Rezzonico, E., MacDonald-Comber Petétot, J., Somerville, C., and Poirier, Y. (2002). Identification and Characterization of the Arabidopsis PHO1 Gene Involved in Phosphate Loading to the Xylem. The Plant Cell 14, 889-902.

Hammond, J.P., Broadley, M.R., and White, P.J. (2004). Genetic Responses to Phosphorus Deficiency. Annals of Botany 94, 323-332.

Henriques, R., Magyar, Z., Monardes, A., Khan, S., Zalejski, C., Orellana, J., Szabados, L., Torre, C., Koncz, C., Bogre, L. (2010) Arabidopsis S6 kinase

mutants display chromosome instability and altered RBR1-E2F pathway activity. EMBO J. 29: 2979-2993.

Henriques, R., Magyar. Z., & Bögre, L. (2013) S6K1 and E2FB are in mutually antagonistic regulatory links controlling cell growth and proliferation in Arabidopsis , Plant Signaling & Behavior, 8:6.

Heuer, S., Gaxiola, R., Schilling, R., Herrera-Estrella, L., López-Arredondo, D., Wissuwa, M., Delhaize, E., and Rouached, H. (2017). Improving phosphorus use efficiency: a complex trait with emerging opportunities. The Plant Journal 90, 868-885.

Kolesnikov, YS., Nokhrina, KP., Kretynin, SV., Volotovski, ID., Martinec, J., Romanov, GA., Kravets, VS. (2012). Molecular structure of phospholipase D and regulatory mechanisms of its activity in plant and animal cells. Biochemistry (Moscow) 77, 1-14.

Lehman, N., Ledford, B., Fulvio, M.D., Frondorf, K., McPhail, L.C., and Gomez-Cambronero J. (2007). Phospholipase D2-derived phosphatidic acid binds to and activates p70 S6 kinase independently of mTOR. The FASEB J. 21, 1075-1087.

Li, M., Hong, Y., Wang, X. (2009). Phospholipase D- and phosphatidic acid-mediumted signaling in plants. Biochimica et Biophysica Acta (BBA)-Molecular and Cell Biology of Lipids 1791, 927-935.

Li, M., Welti, R., and Wang, X. (2006). Quantitative profiling of Arabidopsis polar glycerolipids in response to phosphorus starvation. Roles of phospholipases D zeta1 and D zeta2 in phosphatidylcholine hydrolysis and digalactosyldiacylglycerol accumulation in phosphorus-starved plants. Plant Physiol 142, 750-761.

Li, X., Cai, W., Liu, Y., Li, H., Fu, L., Liu, Z., Xu, L., Liu, H., Xu, T., Xiong, Y. (2017) Activation of TOR requires both glucose and auxin Proceedings of the National Academy of Sciences. 114 (10) 2765-2770.

Liu, T.-Y., Huang, T.-K., Tseng, C.-Y., Lai, Y.-S., Lin, S.-I., Lin, W.-Y., Chen, J.-W., and Chiou, T.-J. (2012). PHO2-Dependent Degradation of PHO1 Modulates Phosphate Homeostasis in Arabidopsis. The Plant Cell 24, 2168-2183.

López-Arredondo, D.L., Leyva-González, M.A., González-Morales, S.I., López-Bucio, J., and Herrera-Estrella, L. (2014). Phosphate Nutrition: Improving Low-Phosphate Tolerance in Crops. Annual Review of Plant Biology 65, 95-123.

López-Bucio, J., Cruz-Ramírez, A., and Herrera-Estrella, L. (2003). The role of

nutrient availability in regulating root architecture. Current Opinion in Plant Biology 6, 280-287.

López-Bucio, J., Hernández-Abreu, E., Sánchez-Calderón, L., Nieto-Jacobo, M.a.F., Simpson, J., and Herrera-Estrella, L. (2002). Phosphate Availability Alters Architecture and Causes Changes in Hormone Sensitivity in the Arabidopsis Root System. Plant Physiology 129, 244-256.

Mahfouz MM, Kim S, Delauney AJ, Verma DPS. (2006) Arabidopsis TARGET OF RAPAMYCIN interacts with RAPTOR, which regulates the activity of S6 kinase in response to osmotic stress signals. Plant Cell 18, 477-490.

Minnikin, D.E., Abdolrahimzadeh, H., and Baddiley, J. (1974). Replacement of acidic phospholipids by acidic glycolipids in Pseudomonas diminuta. Nature 249, 268.

Nakamura, Y. (2013). Phosphate starvation and membrane lipid remodeling in seed plants. Progress in Lipid Research 52, 43-50.

Nakamura, Y., Awai, K., Masuda, T., Yoshioka, Y., Takamiya, K., and Ohta, H. (2005). A novel phosphatidylcholine-hydrolyzing phospholipase C induced by phosphate starvation in Arabidopsis. J Biol Chem 280, 7469-7476.

Ora Son, Sunghan Kim, Yoon-Sun Hur, Choong-Ill Cheon, Molecular details of the Raptor-binding motif on Arabidopsis S6 kinase, Biochemical and Biophysical Research Communications, Volume 486, Issue 1,2017, Pages 137-142,

Pant, B.D., Buhtz, A., Kehr, J., and Scheible, W.-R. (2008). MicroRNA399 is a long-distance signal for the regulation of plant phosphate homeostasis. The Plant Journal 53, 731-738.

Pérez-Torres, C.-A., López-Bucio, J., Cruz-Ramírez, A., Ibarra-Laclette, E., Dharmasiri, S., Estelle, M., and Herrera-Estrella, L. (2008). Phosphate Availability Alters Lateral Root Development in Arabidopsis by Modulating Auxin Sensitivity via a Mechanism Involving the TIR1 Auxin Receptor. The Plant Cell 20, 3258-3272.

Poirier, Y., Thoma, S., Somerville, C., and Schiefelbein, J. (1991). Mutant of Arabidopsis Deficient in Xylem Loading of Phosphate. Plant Physiology 97, 1087-1093.

Raghothama, K.G., and Karthikeyan, A.S. (2005). Phosphate Acquisition. Plant and Soil 274, 37.

Rahman, M.M., Salleh, M.A.M., Rashid, U., Ahsan, A., Hossain, M.M., and Ra, C.S. (2014). Production of slow release crystal fertilizer from wastewaters

through struvite crystallization – A review. Arabian Journal of Chemistry 7, 139-155.

Sarbassov DD, Ali SM, Kim DH, Guertin DA, Latek RR, Endjument-Bromage H, Tempst P, Sabatini DM. Rictor, a novel binding partner of mTOR, defines a rapamycin-insensetive and raptor-independent pathway that regulates the cytoskeleton. Current Biology 2004; 14: 1296-1302.

Shimojima, M. and Ohta H. (2011). Critical regulation of galactolipid synthesis controls membrane differentiation and remodeling in distinct plant organs and following environmental changes. Progress in Lipid Research, 258-266.

Sun Y, Chen J. (2008) mTOR signaling: PLD takes center stage. Cell Cycle 7, 3118-3123.

Tzeng TY, Kong LR, Chen CH, Shaw CC, Yang CH. (2009) Overexpression of the Lily p70s6k gene in Arabidopsis affects elongation of flower organs and indicates TOR-dependent regulation of AP3, PI and SUP translation. Plant Cell Physiol. 50: 1695-1709.

Testerink C., Munnik T. (2005) Phosphatidic acid: A multifunctional stress signaling lipid in plants. Trends Plant Sci. 10, 368–375.

Versaw, W.K., and Harrison, M.J. (2002). A Chloroplast Phosphate Transporter, PHT2;1, Influences Allocation of Phosphate within the Plant and Phosphate-Starvation Responses. The Plant Cell 14, 1751-1766.

Wang G, Ryu S, Wang X. (2012) Plant phopholipases: an overview. Methods Mol. Biol. 861, 123-37.

Wang X, Devaiah SP, Zhang W, Welti R. (2006) Signaling functions of phosphatidic acid. Progress in Lipid Research 45, 250-278.

Wang, Y., Ribot, C., Rezzonico, E., and Poirier, Y. (2004). Structure and Expression Profile of the Arabidopsis PHO1 Gene Family Indicates a Broad Role in Inorganic Phosphate Homeostasis. Plant Physiology 135, 400-411.

Williamson, L.C., Ribrioux, S.P.C.P., Fitter, A.H., and Leyser, H.M.O. (2001). Phosphate Availability Regulates Root System Architecture in Arabidopsis. Plant Physiology 126, 875-882.

Wullschleger, S., Loewith, R., and Hall, M.N. (2006). TOR signaling in growth and metabolism. Cell. 124, 471-484.

Xiong, F. , Zhang, R. , Meng, Z. , Deng, K. , Que, Y. , Zhuo, F. , Feng, L. , Guo, S. , Datla, R. and Ren, M. (2017), Brassinosteriod Insensitive 2 (BIN2) acts as a

downstream effector of the Target of Rapamycin (TOR) signaling pathway to regulate photoautotrophic growth in Arabidopsis. New Phytol, 213: 233-249.

Xiong Y, Sheen J. (2012) Rapamycin and glucose-target of rapamycin (TOR) protein signaling in plants. Journal of Biological Chemistry 287, 2836-2842.

Yoon MS, Sun Y, Arauz E, Jiang Y, Chen J. (2011) Phosphatidic acid activates mammalian target of rapamycin complex 1 (mTORC1) kinase by displacing FK506 binding protein (FKBP38) and exerting an allosteric effect. Journal of Biological Chemistry 286: 29568-29574.

Xu B, Chen S, Luo Y, Chen Z, Liu L, et al. (2011) Calcium Signaling Is Involved in Cadmium-Induced Neuronal Apoptosis via Induction of Reactive Oxygen Species and Activation of MAPK/mTOR Network. PLOS ONE 6(4): e19052.

Yaguchi, M. and Kozaki, A. (2018), Plant S6 kinases do not require hydrophobic motif phosphorylation for activity in yeast lacking Ypk3. FEBS Lett, 592: 610-620.

Chapter 2 Different effects of phospholipase Dζ2 and nonspecific phospholipase C4 on lipid remodeling and root hair growth in Arabidopsis response to phosphate deficiency

This chapter has been published in *the Plant Journal* **94**:315-326

Yuan Su[1,2], Maoyin Li[1,2], Liang Guo[1,2,3], and Xuemin Wang[1,2]

[1]Department of Biology, University of Missouri, St. Louis, Missouri 63121
[2]Donald Danforth Plant Science Center, St. Louis, Missouri 63132
[3]National Key Laboratory of Crop Genetic Improvement and College of Plant Science and Technology, Huazhong Agricultural University, Wuhan 430070, China

AUTHOR CONTRIBUTUONS

Y.S. and X.W. designed the study; Y.S. performed the most experiments; M.L. generated homozygous *pldζ2* and *npc4* single mutants and F1 generation of *pldζ2npc4* double mutant. L.G. helped interpret the data. Y.S. and X.W. analyzed the data and wrote the manuscript.

SUMMARY

Phosphate (Pi) deficiency in soils is a major limiting factor for plant growth. In response to Pi deprivation, one prominent metabolic adaptation in plants is the decrease in membrane phospholipids that consume approximately one third cellular Pi. The level of two phospholipid-hydrolyzing enzymes, phospholipase Dζ2 (PLDζ2) and nonspecific phospholipase C4 (NPC4), is highly induced in Pi-deprived Arabidopsis. To determine the role of PLDζ2 and NPC*4* in plant growth under Pi limitation, Arabidopsis plants deficient in both *PLDζ2* and *NPC4* (*npc4pldζ2*) were generated and characterized. Lipid remodeling in leaves and roots was analyzed at three different durations of Pi deficiency. *NPC4* affected lipid changes mainly in roots at an early stage of Pi deprivation, whereas *PLDζ2* exhibited a more overt effect on lipid remodeling in leaves at a later stage of Pi deprivation. Pi deficiency-induced galactolipid increase and phospholipid decrease were impeded in *pldζ2* and *npc4pldζ2* plants. In addition, seedlings of *npc4pldζ2* had the same root hair density as *pldζ2* but shorter root hair length than *pldζ2* in response to Pi deficiency. The loss of *NPC4* decreased root hair length but had no effect on root hair density. These data suggest that PLDζ2 and NPC4 mediate the Pi deprivation-induced lipid remodeling in a tissue- and time-specific manner. PLDζ2 and NPC4 have distinctively different roles in root hair growth and development in response to Pi deprivation; PLDζ2 negative modulates root hair density and length whereas NPC4 promotes root hair elongation.

INTRODUCTION

Phosphate (Pi) is essential for plant growth and development. Pi deficiency in soils is widespread and a major limiting factor for crop production (Grabau et al., 1986; López-Arredondo et al., 2014). In response to Pi deficiency, one of the major metabolic changes is membrane lipid remodeling, a process in which Pi-containing lipids, such as phosphatidylcholine (PC), are decreased whereas non-P-containing lipids, such as digalactosyldiacylglycerol (DGDG), are increased (Andersson et al., 2003; Shimojima and Ohta, 2011; Nakamura, 2013; Pant et al., 2015). Cellular phospholipids contain approximately one third cellular organic Pi. The decrease in phospholipids provides Pi for other critical cellular needs and also diacylglycerol (DAG) as substrate for the synthesis of non-P-containing glycerolipids.

One way to decrease phospholipids is via phospholipase-mediated lipid hydrolysis (Cruz-Ramirez et al., 2006; Li et al., 2006a; Gaude et al., 2008);(Nakamura et al., 2009). Among various families of phospholipases, the expression of phospholipase Dζ2 (*PLDζ2*) and non-specific phospholipase C4 (*NPC4*) is most highly induced in response to Pi deficiency (Nakamura et al., 2005; Cruz-Ramirez et al., 2006; Li et al., 2006b). Analyses of PLDζ2 and its mutant showed that this enzyme plays a role in plant response to Pi deprivation. PLDζ2 hydrolyzes PC to generate phosphatidic acid (PA) that can be dephosphorylated by a phosphatase to release Pi and DAG. In addition, PA is a mediator in various cellular and physiological processes (Hong et al., 2016).

Genetic suppression of PLDζ2 attenuated the Pi-deficiency-induced decrease in PC and increase in DGDG (Cruz-Ramirez et al., 2006; Li et al., 2006a). PLDζ2 plays a positive role in primary root elongation and also root hair morphology under Pi deprivation. The effect of PLDζ2 on membrane lipid remodeling is tissue-specific and also dependent on the Pi-deficiency treatments (Cruz-Ramirez et al., 2006; Li et al., 2006b), suggesting that other phospholipases are involved in lipid remodeling under Pi deprivation.

Analyses of NPC4 *in vitro* showed that NPC4 hydrolyzes various phospholipids, including PC, phosphatidylethanolamine (PE), PA, and phosphatidylserine (PS), to produce DAG (Nakamura et al., 2005; Peters et al., 2010). The knockout mutant *npc4* showed significantly shorter root hairs than wild-type (WT) under Pi-limited conditions (Chandrika et al., 2013). Root hairs play important roles in nutrient absorption, and root hair density and length increase under Pi limitation (Sánchez-Calderón et al., 2006; Bouain et al., 2016). However, previous studies failed to detect significant alterations in the PC to DGDG ratio in the knockout mutant *npc4* under Pi deficiency in leaves and seedlings (Nakamura et al., 2005; Peters et al., 2010) and the metabolic function of NPC4 in lipid remodeling remains unclear. It is unknown whether the two highly Pi-deficiency-induced NPC4 and PLDζ2 have overlapping functions in lipid remodeling. This study was undertaken to determine the relationship between PLDζ2 and NPC4 in lipid remodeling and plant response to Pi deprivation. The effect of *npc4pldζ2* was compared with *npc4* and *pldζ2* single knockout mutants in leaves and roots

under different durations of Pi deficiency. The results reveal that PLDζ2 and NPC4 have distinguishable effects on membrane lipid remodeling and the effects differ between leaves and roots as well as during different stages of Pi deprivation. In addition, PLDζ2 and NPC4 play distinctively different roles in root hair density and growth in response to Pi deficiency.

RESULTS

Isolation of npc4pldζ2 double knockout mutant in Arabidopsis

The double knockout mutant *npc4pldζ2* was generated by crossing *npc4* and *pldζ2* single knockout mutants (Figure 2-1a). The *npc4* and *pldζ2* mutants have been confirmed previously, and these mutants have been genetically complemented by introducing the native *NPC4* and *PLDζ2* to the respective knockouts (Li et al., 2006a; Peters et al., 2010). To verify the loss of *NPC4* and *PLDζ2* expression in the mutants, *NPC4* and *PLDζ2* transcripts were detected using reverse transcription (RT)-PCR using RNA isolated from WT, *npc4*, *pldζ2* and *npc4pldζ2* as templates under Pi-replete and –deficient conditions. Both *NPC4* and *PLDζ2* transcripts in leaves and roots displayed an increase under Pi-deficient over Pi-replete conditions (Figure 2-1b). The *NPC4* transcript was detected in WT and *pldζ2* mutants, but not in *npc4* or *npc4pldζ2* mutants under Pi-deficient or Pi-replete condition in leaves or roots (Figure 2-1b). Likewise, the *PLDζ2* transcript was detected in WT and *npc4* mutants, but not in *pldζ2* or *npc4pldζ2* mutants (Figure 2-1b). These results were consistent with those by real time PCR (qRT-PCR) quantification (Figure 2-1c). *NPC4* or *PLDζ2* transcript

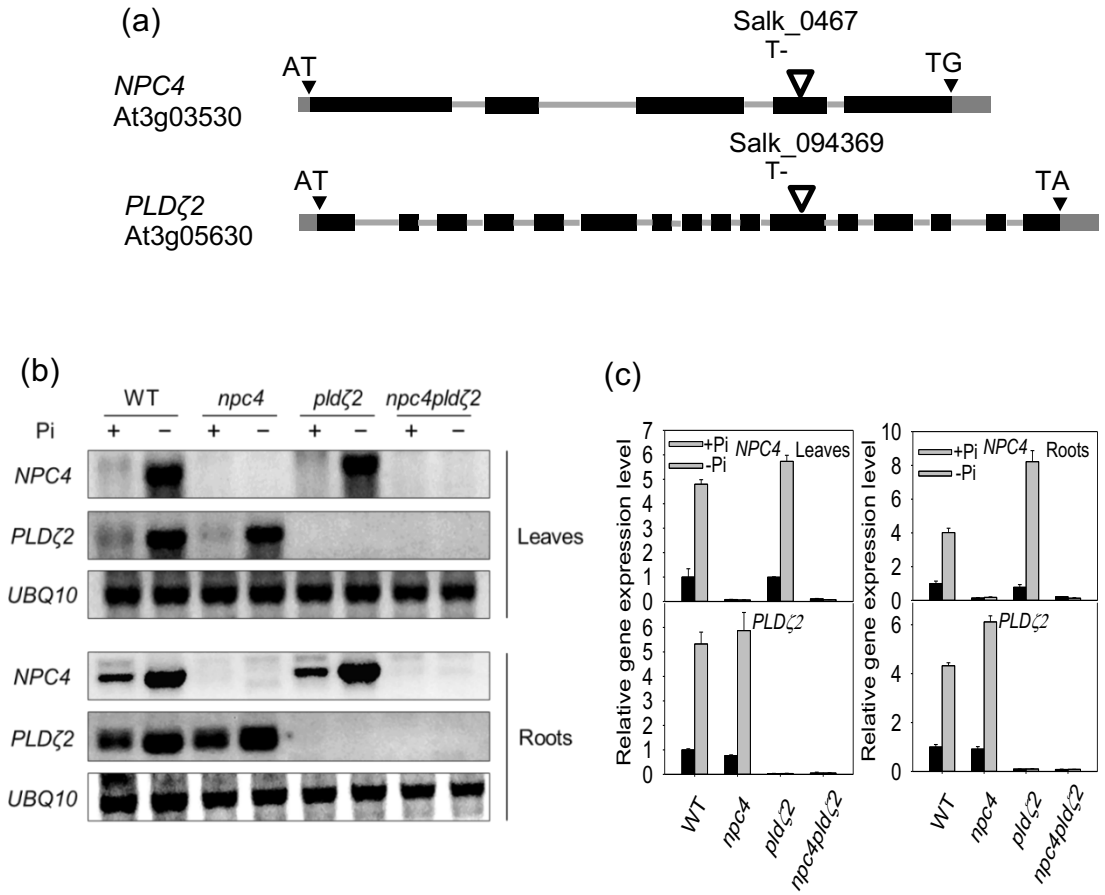

Figure 2-1 Isolation of npc4pldζ2 mutant.

(a) Schematic diagram showing T-DNA insertion mutant lines of *NPC4* (Salk_046713) and *PLDζ2* (Salk_094369). Black boxes, gray horizontal lines and gray boxes indicate exons, introns and UTRs, respectively. Empty triangles indicate T-DNA insertion site. Full triangles indicate start codon or stop codon. (b) Semi quantitative RT-PCR of *NPC4* and *PLDζ2* transcripts from WT, *npc4*, *pldζ2, and npc4pldζ2* in leaves and roots under Pi-sufficient (+, 1 mM) and –deficient (-, 0 mM) conditions. (c) Real-time PCR quantification *of NPC4* and *PLDζ2* transcripts in WT, *npc4*, *pldζ2* and *npc4pldζ2* leaves (left) and roots (right). Levels of expression were normalized to *UBQ10*. Values are means ± SD (n = 3). Total RNA was extracted from leaves and roots of seedlings that were grown in a Pi-sufficient liquid medium for 5 days and then transferred into medium with or without Pi for 5 days.

in *npc4pldζ2* did not show an increase in response to Pi deficiency and were at the background level of the *npc4*- and *pldζ2*-single mutants (Figure 2-1c). The results showed that the *npc4pldζ2* double mutant lost the expression of both *NPC4* and *PLDζ2.*

NPC4 and PLDζ2 mutants affect the expression of genes in lipid remodeling

The qRT-PCR quantification indicated that the *NPC4* transcript level in roots of *pldζ2* was approximately 100% higher than that of WT under Pi deprivation (Figure 2-1c, *right upper panels*) whereas the *PLDζ2* level was approximately 40% higher in *npc4* than WT roots (Figure 1c, *right lower panels*). In leaves, the *NPC4* transcript level in *pldζ2* tended to be higher than that in WT but the *PLDζ2* level was comparable between *npc4* and WT under Pi deprivation (Figure 2-1c, *left panels*). The results indicate that the loss of *PLDζ2* has an impact on *NPC4* expression and *vice versa* in roots.

These changes in *PLDζ2* and *NPC4* expression in *npc4* and *pldζ2*, respectively, prompted the assessment of whether the loss of *NPC4* and/or *PLDζ2* affected the expression of other genes involved in lipid remodeling (Figure 2-2). PA phosphohydrolase (PAH) hydrolyzes PA to produce DAG which is the precursor for glycerolipid production. In leaves, Pi limitation induced the expression of *PAH1* more than *PAH2*, and the magnitude of the induction was similar among

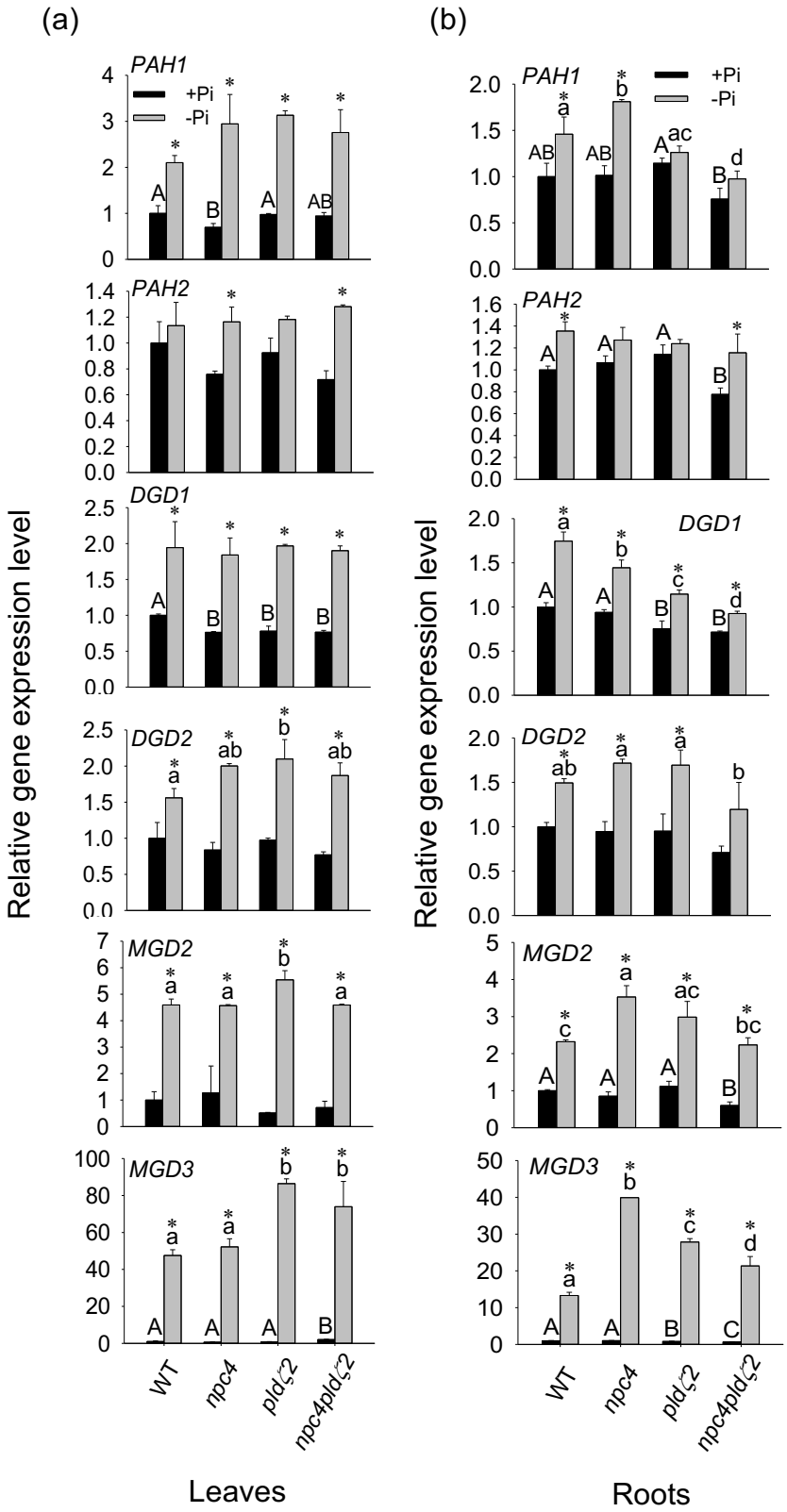
(a)
(b)
PAH1
PAH2
DGD1
DGD2
MGD2
MGD3
+Pi
-Pi
Relative gene expression level
WT
npc4
pldζ2
npc4pldζ2
Leaves
Roots

Figure 2-2 Effect of NPC4 and PLDζ2 mutations on the transcript levels of genes involved in lipid remodeling in leaves and roots.

Seedlings were germinated and grown in Pi-sufficient (1 mM Pi) liquid medium for 5 days, and then transferred into medium with 1 mM Pi (+Pi) or medium without Pi (-Pi) for another 5 days. Total RNA was extracted from leaves (a) and roots (b) and subject to qRT-PCR. Levels of expression were normalized to *UBQ10.* Values are means ± SD (n = 3). Different capital letters indicate differences at $P < 0.05$ among genotypes under sufficient Pi using one way ANOVA. Different lower letters indicate differences at $P < 0.05$ among genotypes under deficient Pi by one way ANOVA. Asterisk indicates the significant ($P < 0.05$) differences between same genotypes under Pi-sufficient or deficient conditions based on Student's *t*-test.

all genotypes except for a higher *PAH2* induction in *npc4* and *npc4pldζ2* mutants than WT. In roots, the low Pi-induced expression of *PAH1* in *pldζ2* and *npc4pldζ2* was lower than WT and *npc4.* Monogalactosyldiacylglycerol (MGDG) synthase (MDG) uses DAG to synthesize MGDG that DGDG synthase (DGD) uses to make DGDG. In leaves, the expression of *MDG2* and *3*, and *DGD1* and *2* was induced by low Pi availability, but *pldζ2* and *npc4pldζ2* leaves exhibited a higher level of *MDG3* induction than *npc4* or WT (Figure 2-2). In roots, all mutants displayed a higher level of *MGD3* induction but a lower level of DGD1 induction than WT (Figure 2-2).

Loss of *NPC4* and *PLDζ2* impedes primary root growth under Pi deprivation

Under Pi-sufficient conditions, the growth of *npc4pldζ2* plants in soil was slower in early stages, and the rosette leaf radiation of three-week-old *npc4pldζ2* plants was smaller than WT and single knockout mutants (Figure 2-3). The overall growth and development of *npc4* and *pldζ2* single KO were similar to WT in later stages (Figure 2-3b). For seedlings grown on a plant nutrient medium with 1% sucrose containing sufficient Pi (1 mM), the primary root length of *pldζ2* and *npc4pldζ2* seedlings was similar to that of WT whereas the primary roots of *npc4* seedlings were approximately 5% shorter than WT at 10 days after germination (Figure 2-4). No difference occurred to the primary root tip of all four genotypes under Pi-replete and deficient conditions (Figure S2-1). Lateral root length and numbers of *npc4* and *pldζ2* single and double mutants were similar to those of WT (Figure 2-4).

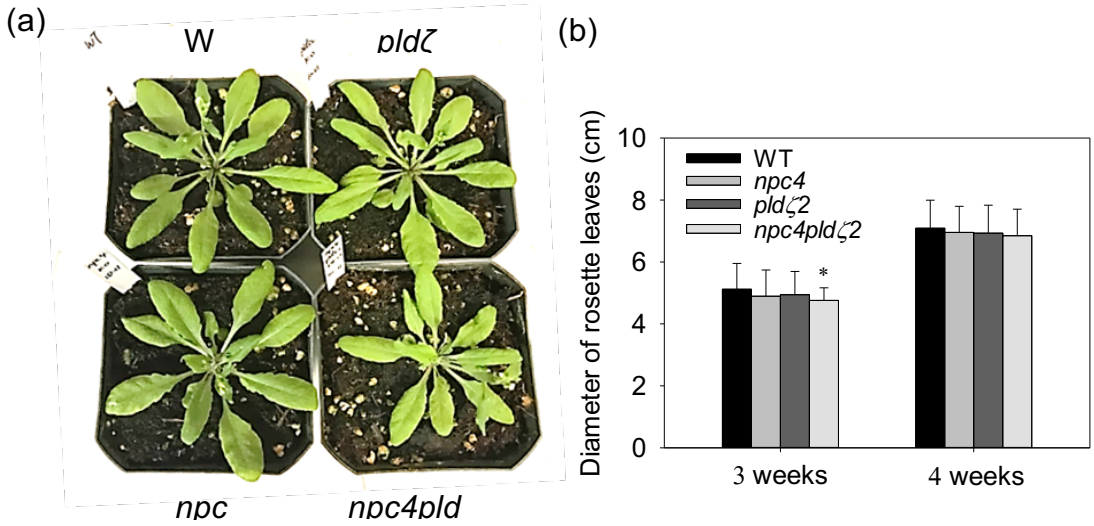

Figure 2-3 Growth phenotype of WT, *npc4*, *pldζ2* and *npc4pldζ2* in soil with sufficient nutrient supply.

(a) Growth phenotype of 3-week plants of WT, *npc4*, *pldζ2* and *npc4pldζ2.* (b) Measurements of diameters of rosette leaves at 3 week and 4 week after germination. Values are means ± SD (n = 20). Asterisk indicates the significant ($P < 0.05$) differences between WT and mutants based on Student's *t*-test.

Under Pi limitation (1 μM), primary root length was decreased. At 10 days after germination, the length of primary roots was WT > *npc4* > *pldζ2* = *npc4pldζ2* (Figure 2-4). The primary root length of *npc4* seedlings was about 10% shorter than WT whereas that of *pldζ2* and *npc4pldζ2* was about 15% shorter than that of WT (Figure 2-4b). There was no significant difference in primary root length between *pldζ2* and *npc4pldζ2* mutants (Figure 2-4b). Lateral root number was comparable among four genotypes. The results indicate that the loss of *NPC4* decreases root growth under both Pi-sufficient and -deficient conditions with the decrease stronger under Pi deficiency whereas the loss of *PLDζ2* reduces primary root growth only under Pi deficiency. The data from single KO indicate that PLDζ2 has a greater effect than NPC4 on promoting primary root growth in response to Pi deficiency.

PLDζ2 and NPC4 have different roles in root hair density and growth

Root hairs are tubular extensions of specific root epidermal cells important for Pi absorption. To determine the effect of NPC4 and PLDζ2 on root hair number and growth, root hair density and root hair length were measured and compared among four genotypes. With sufficient Pi, root hair density and length were comparable among *pldζ2*, *npc4*, and *npc4pldζ2* (Figure 2-5). Under Pi deficiency, all genotypes displayed an increase in root hair numbers at the 0-5 mm region from the root tip compared to sufficient Pi (Figure 2-5a, b). WT and *npc4* had a similar increase (~75%) but *pldζ2* and *npc4pldζ2* had a higher increase (~100%) in root hair density than WT and *npc4* (Figure 2-5b). In addition, root hair length

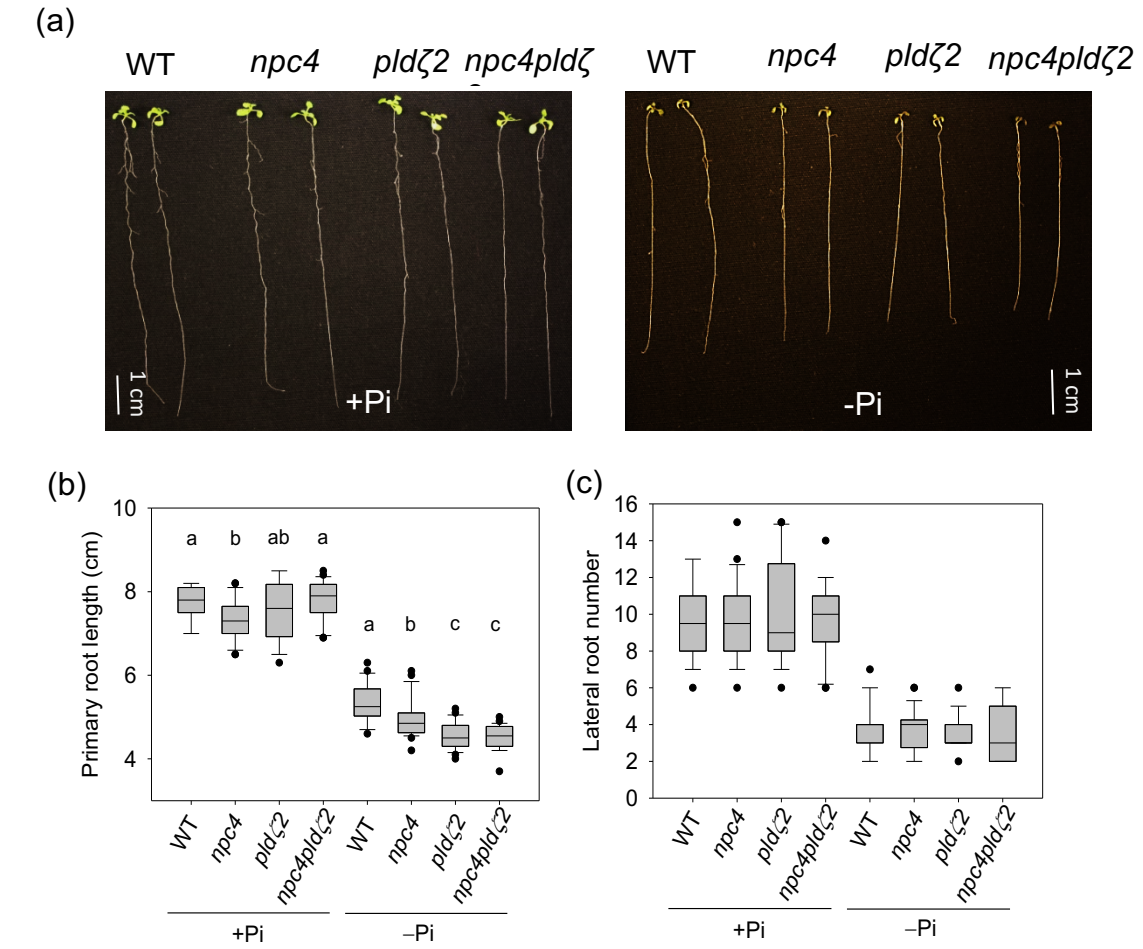

at

Figure 2-4 Primary and lateral roots of Arabidopsis seedlings with or without sufficient Pi.

Seedlings were germinated and grown on PNS agar plates with 1 mM Pi or 1 μM Pi for 10 days after germination. (a) WT, *npc4*, *pldζ2*, and *npc4pldζ2* (dko) seedlings. Bars, 1 cm. (b) Primary root length. Values are means ± SD (n = 24). Bars, 1 cm. Note that different scales are used for 2a and 2b. (c) Lateral roots number. Values are means ± SD (n = 20). Different lower letters indicate statistical differences at $P < 0.05$ between genotypes by one way ANOVA.

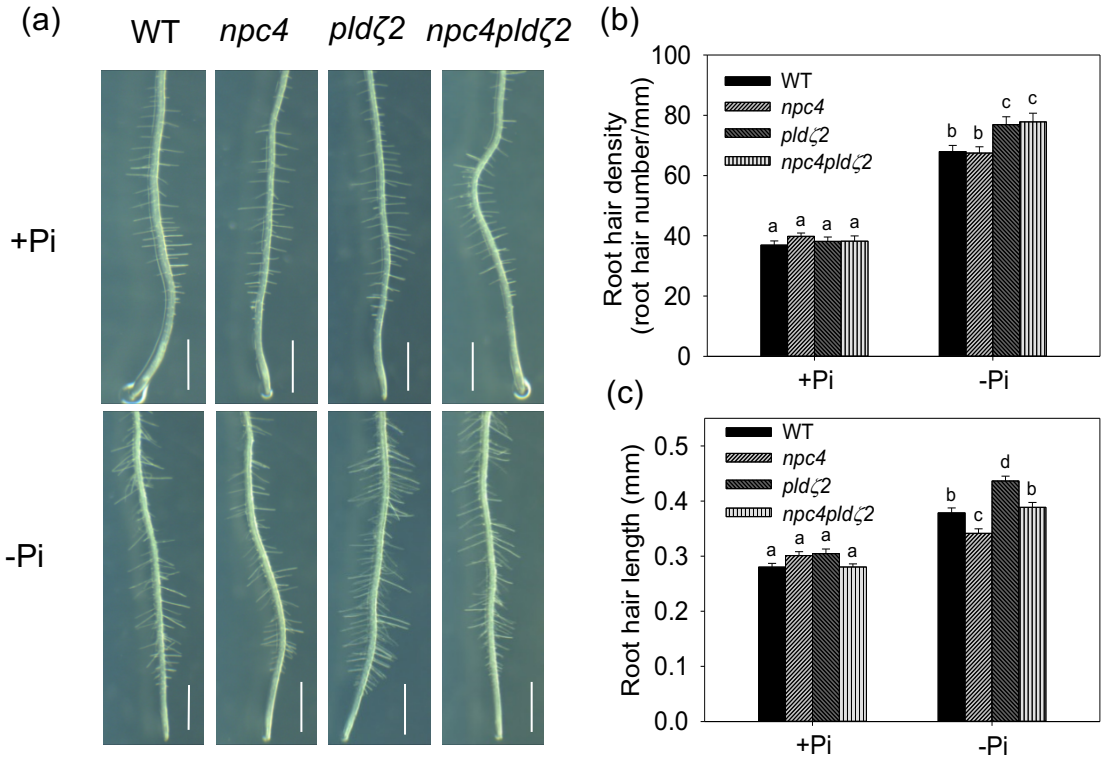

Figure 2-5 Root hairs of WT, *npc4*, *pldζ2*, and *npc4pldζ2* seedlings under +Pi and –Pi conditions.

(a) Roots with hairs at 0-6 mm region from the root tip. Bars, 1 mm. (b) Root hair density at 0-5 mm from the root tip. Values are means ± SE (n = 20). (c) Root hair lengths from root hairs at 3-4 mm from the root tip. Values are means ± SE (n = 200). Different lower letters indicate statistical differences at $P < 0.05$ between genotypes by one way ANOVA. Seedlings were germinated and grown on PNS agar plates with 1 mM Pi or 1 μM Pi for 6 days after germination.

the 3-4 mm region from the root tip in all genotypes increased, with the increase the smallest in *npc4* (~10%) and greatest in *pldζ2* (~50%; Figure 2-5c). The root hair density of WT and *npc4pldζ2* was comparable. The results suggest that PLDζ2 is a negative regulator of both root hair density and length under Pi-deficient conditions. In comparison, NPC4 promotes root hair elongation under Pi deficiency.

PLDζ2 **and** ***NPC4*** **affect lipid remodeling in roots and leaves differently at different stages of Pi deprivation**

To examine the effect of PLDζ2 and NPC4 on lipid remodeling, seedlings were subjected to Pi deprivation for 5, 10 and 14 days, and lipids were then extracted from leaves and roots separately for profiling. After 5 days of Pi deprivation, *npc4pldζ2* roots had significantly less DGDG accumulation and less PE increased than in WT and single mutants (Figure 2-6). DGDG levels in *npc4pldζ2* roots were increased by approximately 3.5-fold whereas those in WT, *npc4,* and *pldζ2* roots were about 5-fold (Figure 2-6a). PE levels were decreased by 25% in WT, *npc4,* and *pldζ2* roots, but 18% in *npc4pldζ2* roots (Figure 2-6d). PC levels were decreased by approximately 7% in four genotypes (Figure 2-6c). PA content significantly decreased in *pldζ2* and *npc4pldζ2* roots but not in WT and *npc4* roots (Figure S2-2). In contrast to roots, lipid levels in 5-day Pi-starved leaves were similar among all genotypes (Figure 2-6). These results suggest that both PLDζ2 and NPC4 contribute to PE decrease and DGDG increase in roots and that PLDζ2 promotes PA production.

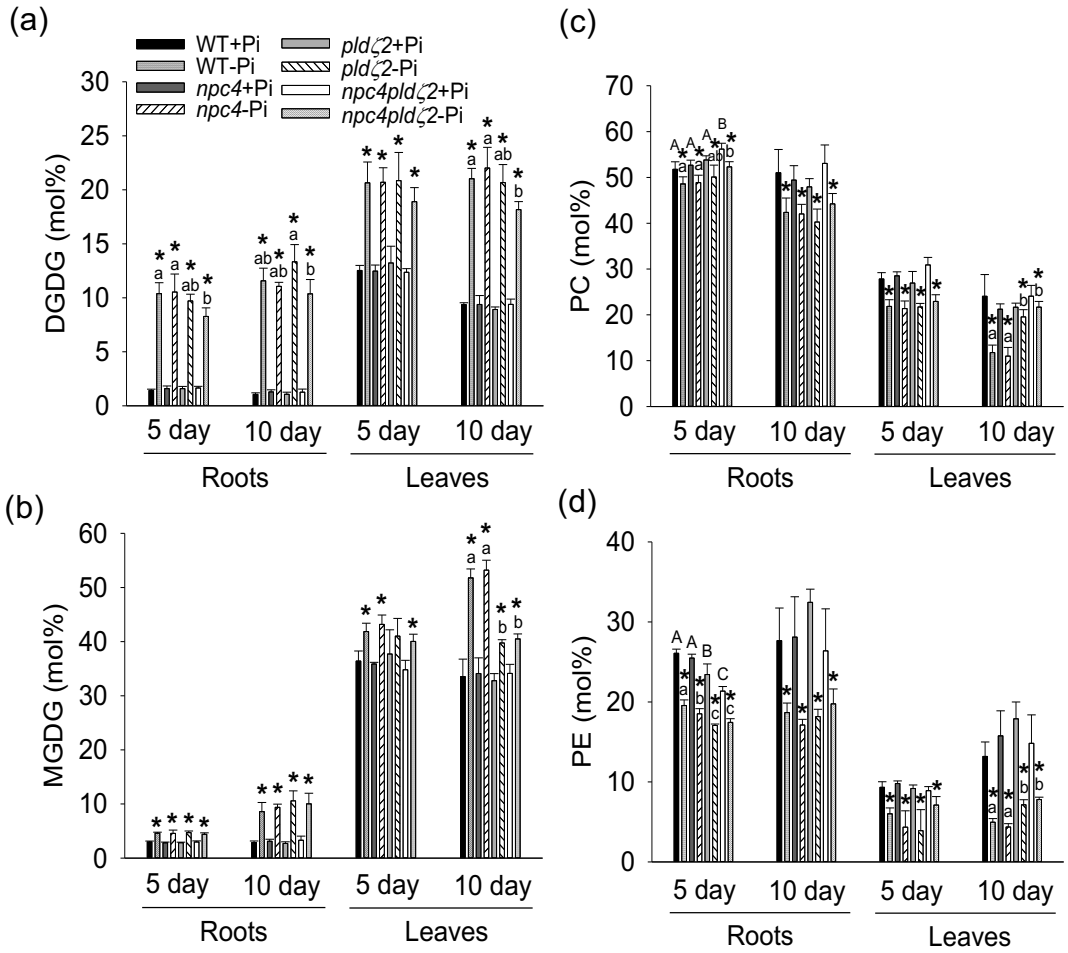

Figure 2-6 Major galactolipid and phospholipid levels of WT, *npc4*, *pldζ2*, and *npc4pldζ2* in roots and leaves at 5-day and 10-day durations of Pi treatments.

(a) DGDG in roots and leaves. (b) MGDG in roots and leaves. (c) PC in roots and leaves. (d) PE in roots and leaves. Seedlings were germinated and grown in Pi sufficient (1 mM) liquid medium for 5 days, and then transferred into medium containing 1 mM Pi or no Pi for indicated days. Values are means ± SD (n = 5). Different capital letters indicate differences at $P < 0.05$ among genotypes under sufficient Pi using one way ANOVA. Different lower letters indicate differences at $P < 0.05$ among genotypes under deficient Pi by one way ANOVA. Asterisk indicates the significant ($P < 0.05$) differences between same genotypes under sufficient Pi or deficient Pi conditions based on Student's *t*-test.

After 10 days of Pi deprivation, the magnitude of lipid changes, such as increase in galactolipids and decrease in phospholipids, was greater than that of the 5-day treatment (Figure 2-6). The double mutant *npc4pldζ2* leaves had a smaller increase in DGDG than WT and single mutants. The level of DGDG in leaves was increased by 90% in *npc4pldζ2,* but approximately 130% in WT and single mutants (Figure 2-6a). For MGDG, a smaller increase occurred in both *pldζ2* and *npc4pldζ2* than WT and *npc4* leaves. The level of MGDG was increased by 20% in *pldζ2* and *npc4pldζ2* but 55% in WT and *npc4* (Figure 2-6b). In roots, the level of MGDG and DGDG is much lower relative to that in leaves (Figure 2-6). No significant difference in MGDG or DGDG levels was observed between WT and mutants under Pi deprivation (Figure 2-6a, b). These results indicate that PLDζ2, but not NPC4, promotes MGDG increases in leaves and that PLDζ2 and NPC4 both contribute to the DGDG increase. For phospholipids, *pldζ2* and *npc4pldζ2* leaves had a higher level of PC than WT and *npc4* under Pi limitation. Pi deficiency induced a 50% decrease of PC in WT and *npc4* leaves but only a 10% decrease in *pldζ2* and *npc4pldζ2* leaves (Figure 2-6c). PE levels in *pldζ2* and *npc4pldζ2* were higher than those in WT and *npc4* leaves, but the *pldζ2* and *npc4pldζ2* effect on PE decrease was not as great as that on PC (Figure 2-6d). In roots, no significant difference in phospholipid levels was observed between WT and mutants under Pi deprivation (Figure 2-6). These results indicate that PLDζ2 promotes PC and PE hydrolysis in leaves.

After 14 days of Pi deprivation, seedling growth was severely retarded and there

were no significant differences of various lipid species in roots and leaves among four genotypes, except PG and PA (Figures S2-3). In roots, PG levels in *npc4pldζ2* and *pldζ2* were lower than that in WT and *npc4* (Figure S2-3g). The PA levels in roots of *pldζ2* and *npc4pldζ2* were significantly lower than those in WT and *npc4* (Figure S2-3e). In leaves, PG levels in *npc4pldζ2* were lower than WT and single mutants (Figure S2-3g). The decrease in PG in *npc4pldζ2* may result from an effect of the double mutant on retarded plant growth because PG is present primarily in photosynthetic, thylakoid membranes.

I further analyzed lipid molecular species to gain insights to the pathways involved in lipid remodeling (Figure 2-7). In 5-day Pi-starved roots, the mole percentage of DGDG molecular species measured was increased to different extents, leading to the change of relative composition of molecular species with the most abundant species switched from 36:6 DGDG to 34:3 DGDG compared with Pi-replete roots (Figure 2-7a). The molecular species composition of newly accumulated DGDG resembles closely that of PC or PE species composition in Pi-replete roots, suggesting that PC and PE provide DAG substrates for DGDG production during Pi deprivation. Among all DGDG molecular species, compared to WT, 34:4 DGDG and 34:2 DGDG accumulated less in *pldζ2* roots while 34:3 DGDG, 34:2 DGDG, and 36:3 DGDG accumulated less in *npc4pldζ2* roots (Figure 2-7a). On the other hand, a smaller decrease of 34:3 PE and 34:2 PE occurred in the double mutant (Figure 2-7c). The results imply that PLDζ2 and NPC4 prefer 34C PC and 34 C PE and produce DAG for DGDG synthesis.

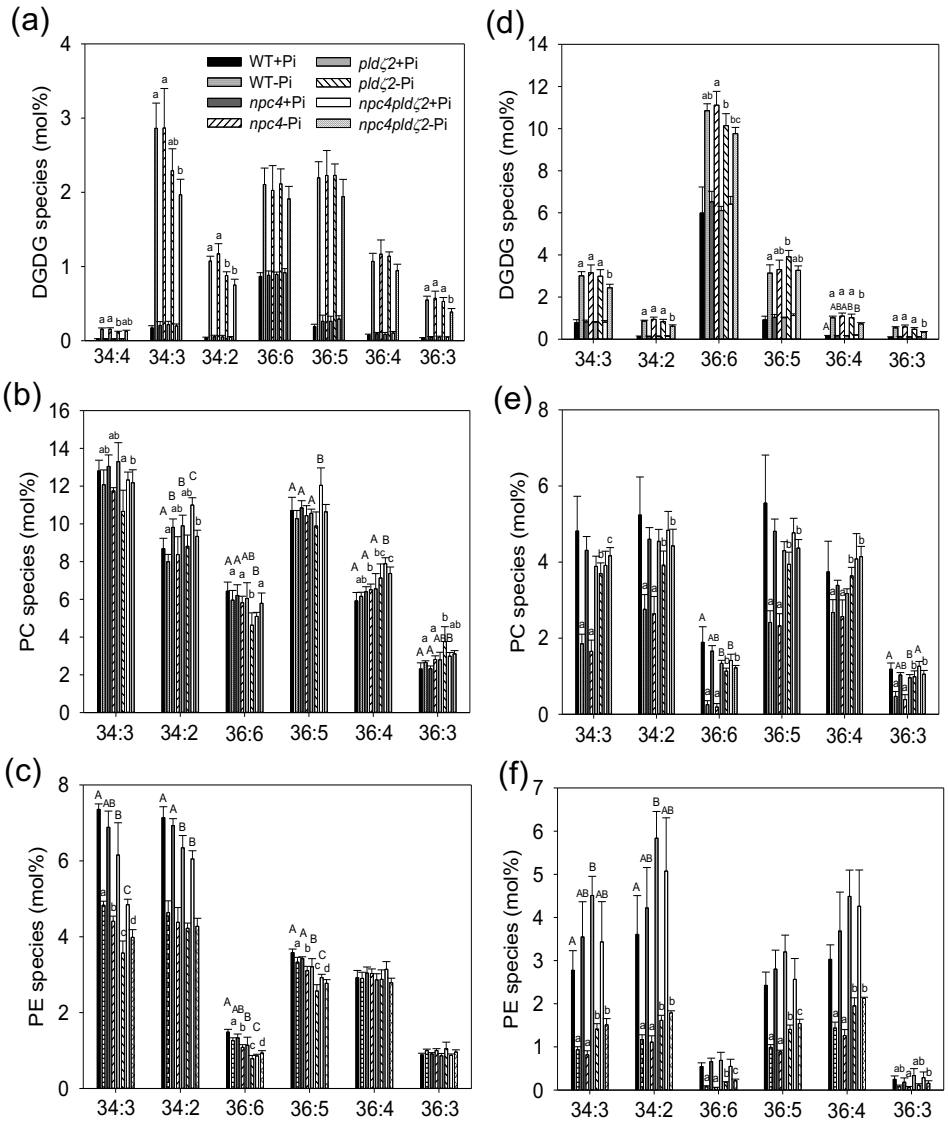

Figure 2-7 Lipid species of 5-day Pi-starved roots and 10-day Pi-starved leaves of WT, *npc4*, *pldζ2*, and *npc4pldζ2* Arabidopsis.

Molecular species of DGDG (a), PC (b), and PE (c) in 5-day roots. Molecular species of DGDG (d), PC (e), and PE (f) in 10-day leaves. Seedlings were germinated and grown in Pi sufficient (1 mM) liquid medium for 5 days, and then transferred into medium containing 1 mM Pi or no Pi for 5- and 10-days. Values are means ± SD (n = 5). Different capital letters indicate differences at $P < 0.05$ among genotypes under sufficient Pi using one way ANOVA. Different lower letters indicate differences at $P < 0.05$ among genotypes under deficient Pi by one way ANOVA.

In 10-day Pi-starved leaves, the lipid remodeling did not change relative molecular species composition of DGDG, MGDG, PC or PE. The accumulation of all DGDG/MGDG molecular species except for 36:5 DGDG/MGDG was suppressed in the *npc4pldζ2* double mutant compared with WT (Figures 2-7d, S2-4). The hydrolysis of all measured PC species and all measured PE species except for 36:3 PE was inhibited in *pldζ2* and *npc4pldζ2* leaves but not in *npc4* leaves (Figure 2-7e,f), suggesting that PLDζ2 plays a dominant role in hydrolyzing PC and PE over NPC4 in Pi-starved leaves. However, by comparing *pldζ2* and *npc4pldζ2*, less accumulation of certain DGDG species (34:3, 34:2, 36:4 and 36:3) and MGDG species (34:6 and 34:4) and less decrease of certain PC species (34:3) and PE species (36:6 and 36:5) indicated that both NPC4 and PLDζ2 were able to hydrolyze PC and PE and contributed to DGDG and MGDG accumulation.

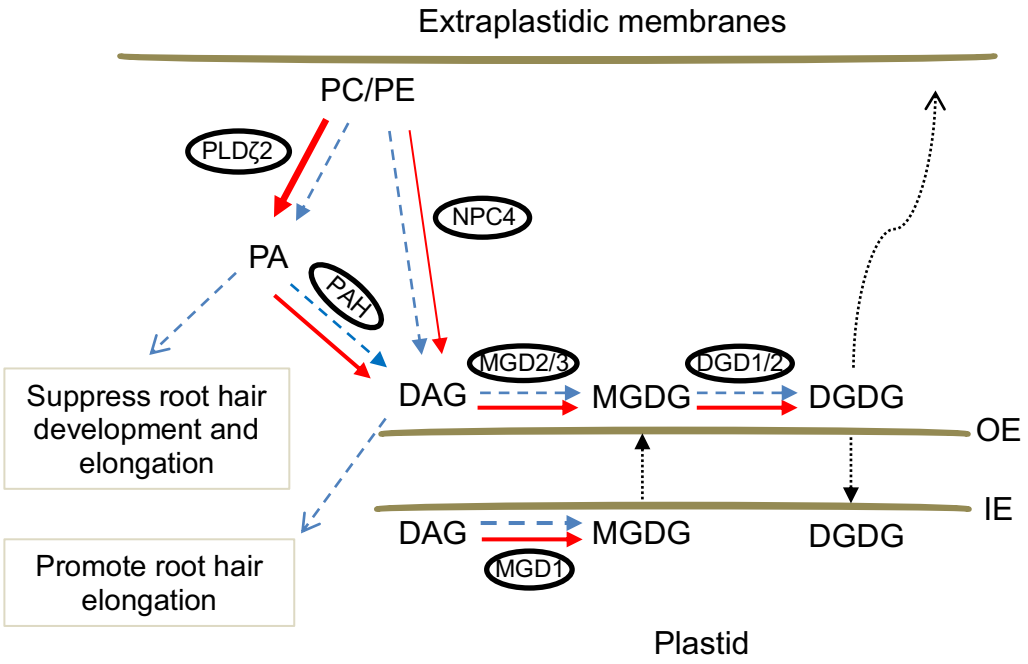

Figure 2-8 A proposed functions of NPC4 and PLDζ2 in lipid remodeling in 5-day Pi-starved roots and 10-day Pi-starved leaves.

Dashed and solid lines highlight NPC4 and PLDζ2 mediated lipid remodeling processes in 5-day Pi-depleted roots and 10-day Pi-depleted leaves, respectively. The thickness of lines indicates the contribution of specific reactions to the remodeling. In response to Pi deficiency, plasma membrane or ER localized PC and PE are hydrolyzed by PLDζ2 or NPC4 to generate PA or DAG, respectively. Such eukaryotic pathway-derived DAG is used to synthesize MGDG by MDG2 and MDG3 on the chloroplast outer envelope membrane (OE), while MDG1 on the chloroplast inner envelope membrane (IE) synthesizes MGDG which is transported to OE where DGD1 and DGD2 catalyze the synthesis of DGDG which is transported back into IE or transported to the extraplastidic membranes. Dotted lines indicate lipid movements.

DISCUSSION

Using Arabidopsis lines with the loss-of-function for *NPC4* and *PLDζ2,* separately and together, this study examined the contribution of NPC4 and PLDζ2 to membrane lipid remodeling and plant growth under Pi deficiency (Figure 8). In addition, I determined whether NPC4 and PLDζ2 acted in a tissue- and/or a time-specific manner in response to Pi deprivation. In 5-day Pi-starved roots, the magnitude of increase in DGDG in WT, *npc4* and *pldζ2* was similar, but a significantly smaller increase occurred in *npc4pldζ2*. The *npc4pldζ2* roots also displayed a weaker degradation of phospholipids than that of WT, *npc4*, and *pldζ2*. These results indicate that both NPC4 and PLDζ2 contribute to the attenuated phospholipid hydrolysis, decreasing DAG for DGDG production during the earlier phase of Pi deficiency (Figure 2-8). The differences between the single and double mutants suggest that NPC4 and PLDζ2 compensate for one another in phospholipid hydrolysis under Pi deficiency in roots. Consistent with the results, I found that the low Pi-induced level of the *PLDζ2* transcript was higher in *npc4* whereas the *NPC4* transcript was higher in *pldζ2* than WT. The reciprocal increase in *PLDζ2* and *NPC4* expression in the *npc4* and *pldζ2* single mutants, respectively, may explain the compensation for the loss of *NPC4's or PLDζ2's* effect on lipid hydrolysis in the early phase of Pi deprivation in roots. By comparison, the knockout of *PLDζ2* or *NPC4* did not alter each other's expression in leaves. This is consistent with the lipid remodeling data, and the double mutant *npc4pldζ2* and single *npc4* and *pldζ2* mutants exhibit similar lipid composition in leaves under Pi deprivation for 5 days, indicating no apparent

compensation of *PLDζ2* for *NPC4* and vice versa in leaves at this stage.

However, the mutant effects on lipid changes vary at different durations of Pi deprivation. After 10 days of Pi deficiency, lipid changes in *npc4* plants were almost identical to those in WT. In contrast, *pldζ2* leaves were lower in MGDG but higher in PC and PE compared to WT, and the lipid changes in *npc4pldζ2* leaves were like those of *pldζ2*, except for a lower level of DGDG compared to WT. PC levels decreased by 50% in WT and *npc4* but only 10% in *pldζ2* and *npc4pldζ2*, indicating that PLDζ2 is primarily responsible for the PC decrease in leaves at this stage. The attenuated decrease in PC in both *pldζ2* and *npc4pldζ2* indicates that the loss of *PLDζ2* cannot be compensated by *NPC4*. However, it might be possible that the loss of *NPC4* in 10 days of Pi limitation might be compensated by the function of *PLDζ2*. In addition, comparison between *pldζ2* and *npc4pldζ2,* especially on MGDG, DGDG, PC, and PE molecular species, revealed the additive effect of NPC4 and PLDζ2 on galactolipid synthesis and phospholipid hydrolysis. For instance, in 10-day Pi-starved leaves, *npc4pldζ2* had less decreased 36:6 PE and 36:5 PE than *pldζ2* even though the total PE levels in the two mutants were similar, indicating a role of NPC4 in PE hydrolysis on certain species. The results indicate that the effect of PLDζ2 and NPC4 on membrane lipid remodeling is tissue- and time-specific, with the effect of NPC4 being apparent mainly in roots at 5 days whereas that of PLDζ2 being highly overt in leaves at 10 days after Pi deprivation (Figure 2-8). In addition, at 14 days of Pi limitation, the difference of membrane lipids among four genotypes

disappeared except for PA and PG. The different effects of NPC4 and PLDζ2 on lipid remodeling at different durations of Pi limitation suggest that PLDζ2- and NPC4-mediated lipid hydrolysis contributes to membrane lipid remodeling at relatively early stages whereas after prolonged Pi limitation, changes in lipid biosynthesis, such as increased galactolipid synthesis and decreased phospholipid production, play a predominate role in altering membrane lipid composition.

Such lipid remodeling phenotypes result from a combination of redundant and unique functions of PLDζ2 and NPC4, as well as other genes involved in lipid remodeling. Our earlier studies showed that 7 days after Pi starvation the transcript level of *PLDζ2* in leaves and roots was more than 10-fold than that in Pi-sufficient WT (Li et al., 2006a). In roots, the Pi-induced expression of *PAH1* in *pldζ2* and *npc4pldζ2* was lower than WT and *npc4,* consistent with the finding that the loss of *PLAζ2* reduces the production of PA so that less *PAH* is required to hydrolyze PA to DAG. In leaves, *npc4* and *npc4pldζ2* mutants displayed a higher *PAH2* induction than WT, which could mean that the loss of NPC4 leads to a higher production of PA by another PLD, such as PLD*ζ1,* thus requiring more *PAH2* expression, as suggested by our previous studies which showed that the transcript of *PLDζ1* increased under Pi deprivation (Li et al., 2006a). The higher level of *MDG3* induction under low Pi availability found in *pldζ2* and in *npc4pldζ2* compared to *npc4* and WT leaves could mean that when the lipid remodeling capability is compromised by the loss of *PLDζ2*, the galactolipid

biosynthesis activity is up-regulated to compensate for the loss of PA and DAG source caused by the defect in *PLDζ2*-mediated phospholipid hydrolysis. The need for increasing MGDG synthesis is indicated by lipid data that showed *pldζ2* and *npc4pldζ2* leaves had only about 20% of low-Pi-induced MGDG in WT and *npc4*. In roots, all mutants displayed a higher level of *MGD3* induction because roots have a low level of galactolipids under normal growth, and a drastic increase in MGD3 expression may help to compensate for the loss of DAG produced from both NPC4 and PLDζ2. Compared to WT, the low Pi-induced *DGD1* expression was WT > *npc4* > *pldζ2* > *npc4pldζ2*. This gene expression pattern correlates with DGDG molecular species changes under Pi deficiency. For example, the low Pi- induced 34:3 DGDG was significantly lower in the double mutant while the induced 34:2 DGDG was less in *pldζ2* and *npc4pldζ2* because DGD1 is the key enzyme for synthesizing DGDG from MGDG in the prokaryotic pathway (Klaus et al., 2002; Kelly et al., 2016). One possible mechanism for the effect of *PLDζ2* and *NPC4* on gene expression is the regulatory function of their lipid products PA and DAG. For example, PA and DAG production was suggested to repress the stress transcription factor DREB2 genes (Djafi et al., 2013). PA was shown to bind to a MYB transcription factor WER and facilitate its nuclear translocation and thus its gene targets (Yao et al., 2013).

The distinguishable effects of *PLDζ2* and *NPC4* on lipid remodeling are consistent with the alterations in root and root hair phenotypes under Pi

deprivation. Under Pi deficiency, all mutants displayed slower primary root elongation than WT whereas the root growth of *pldζ2* and *npc4pldζ2* was similar but retarded more than *npc4*, suggesting that *PLDζ2* promotes the primary root growth. For root hairs, loss of NPC4, PLDζ2 or both had no effect on root hair density or length under Pi-sufficient conditions. In contrast, under Pi limitation, *npc4* has similar root hair density to WT, but decreased root hair length, indicating that NPC4 promotes root hair elongation. However, *pldζ2* showed an increase in root hair density and length under Pi starvation, compared to Pi-sufficient conditions, indicating that PLDζ2 is a negative regulator of root hair density and elongation in response to Pi starvation. A similar effect on the root hair phenotype by *pldζ2* was reported in another study (Cruz-Ramirez et al., 2006). Compared to *pldζ2, npc4pldζ2* seedlings had similar root hair density, but shorter hairs. The results indicate that under Pi deficiency, NPC4 promotes, but PLDζ2 suppresses, root hair elongation*;* whereas on root hair density, PLDζ2 suppresses root hair numbers but NPC4 has no effect (Figure 2-8).

The lipid changes in these mutants also shed some light on the role of PLDζ2 and NPC4 in root and root hair phenotypes. One potential mechanism by which PLDζ2 and NPC4 modulate root and root hair growth and development is via their reaction products PA and DAG used as signaling molecules. In addition, NPC-produced DAG can be phosphorylated to PA by DAG kinase. Previous reports have indicated that PA generated by PLDζ2 and NPC4 promotes primary root elongation (Li et al., 2006a; Peters et al., 2010). PA was reported to bind

PDK1 to mediate root hair growth (Anthony et al., 2004). PA derived from PLDζ1 and PLDζ2 was also shown to bind a MYB transcription factor WEREWOLF (WER) to translocate its cellular location and thus regulate root hair density (Yao et al., 2013). Nod factor was reported to activate PLC and PLD in turn to produce DAG and PA, respectively, to induce root hair deformation in *Vicia sativa* (Den Hartog et al., 2001). NPC4- and NPC5-generated DAG participates in lateral root growth and development in response to ABA or salt stress, respectively (Peters et al., 2010; Peters et al., 2014). DAG content in *npc4-1* roots and rosette was about 20% and 15%, respectively, lower than that in WT (Peters et al., 2010). Moreover, DAG levels were found to increase under Pi starvation (Pant et al., 2015). It has been proposed that DAG in itself has regulatory functions in root development (Peters et al., 2010; 2014). Thus, it is likely that DAG produced by NPC4 and PA produced by PLDζ2 may function as signaling messengers in Pi-starvation-induced molecular pathways. It is tempting to suggest that PLDζ2 and its product PA modulate root hair density, whereas NPC4 and its lipid product DAG promote root hair elongation (Figure 2-8). However, establishing the direct link is challenging because DAG and PA can be interconverted by lipid kinases and phosphatases. In addition, the present results on tissue- and duration-effects suggest that the temporal and spatial regulation of PLDζ2 and NPC4 plays an important role in their effect on plant response to Pi deficiency.

EXPERIMENTAL PROCEDURES

Plant Materials and Growth Conditions

Seeds of T-DNA insertion mutants *npc4* (Salk_046713) and *pldζ2* (Salk_094369) in the *Arabidopsis thaliana* ecotype Columbia-0 were obtained from *Arabidopsis* Biological Resource Center (ABRC) at The Ohio State University. The homozygous *npc4pldζ2* double mutant was identified by PCR using one specific primer from T-DNA (LBa1) and one specific primer from *NPC4 or PLDζ2 gene*. The primer for T-DNA left border is 5'-TGGTTCACGTAGTGGGCCATCG-3', and the primers for *NPC4* and *PLDζ2* were 5'- CTACGAGGCATTGAGATCGAG -3' and 5'- CGGCATTTACCTCTGGTACAG -3', respectively. For plants grown in soil, seeds were sowed and germinated in a plastic pot under a long-day condition (16 h light 22°C/8 h dark 18°C) in a growth chamber with 70% relative humidity and 170 μmol $m^{-2}s^{-1}$ fluorescent light intensity. The plants were supplied with sufficient water and nutrients.

Pi Treatments

For Pi-deficiency treatments, seedlings were either grown in agar plates vertically under the long-day condition or in a hydroponic medium with mild agitation under continuous light in 6-well plates. A plant nutrient sucrose (PNS) medium was modified to adjust Pi concentrations. The PNS medium contained 2.5 mM KH_2PO_4, 5 mM KNO_3, 2 mM $MgSO_4$, 2 mM $Ca(NO_3)_2$, micronutrient solution (Sigma M0529), and 1% sucrose with pH adjusted to 5.7. The modified PNS

contained 1 mM, 1 μM or 0 mM of KH_2PO_4 as Pi source and the resulting lack of K was supplemented with proper amounts of 1 mM KCl. Pi-free agar at 0.8%-1.2% was added to make solid plates. Arabidopsis seeds were surface sterilized using 70% (v/v) ethanol for 1 minute and then 30% bleach for 7 minutes. The seeds were washed 5 times by sterilized water and subjected to 4°C for 2 days before being sowed on agar plates or hydroponic medium. Seeds were germinated and grown in agar plates for the number of days indicated. For hydroponic culture, seedlings were first grown in Pi-sufficient (1 mM Pi) medium for 5 days and then transferred into Pi-sufficient or Pi-starved (0 mM Pi) media for the number of days indicated. The hydroponic medium was replaced with fresh medium every 2 days.

Membrane lipid analysis

Lipids were extracted from fresh seedlings, leaves or roots and analyzed by electrospray ionization–tandem mass spectrometry (ESI-MS/MS) as described previously (Welti et al., 2002). Briefly, the leaf or root materials were collected and put into hot isopropanol (75°C) with 0.01% BHT (butylated hydroxytoluene) immediately for 15 minutes to inhibit phospholipase activity. Then, the tissues were extracted five times by chloroform/methanol (2:1 v/v), followed by a one-time wash with 1 M KCL and water, respectively. The lipids were dried under nitrogen gas and diluted appropriately based on the dry weight of materials with chloroform. Lipids were analyzed using an electrospray ionization tandem spectrometer (ESI-MS/MS) for phospholipids and galactolipids. The lipid profiling

data were analyzed using software Analyst 1.5.1, and lipid levels were determined by comparison to internal standards (Li et al., 2006b). Five biological replicates of each genotype were analyzed. One-way ANOVA analysis using the Holm-Sidak method was applied to determine the significant (P<0.05) differences between genotypes of same Pi treatments. Differences between the same genotypes under Pi-sufficient or -deficient conditions were compared to test significance (P<0.05) using Student's t-test.

RNA extraction, semi-quantitative RT-PCR, and qRT-PCR

RNA extraction and qRT-PCR analysis of gene expression were previously described (Li et al., 2011). Total RNAs were extracted from leaves or roots using an RNeasy Plant Mini Kit (Qiagen 74904), followed by DNase treatment using an RNase-free DNase set (Qiagen 79254). Then 1 μg RNA was reverse transcribed into cDNAs using a qScript cDNA Synthesis Kit (Quanta 95047) according to the user's manual. SYBR green fluorescent dye was applied in each PCR reaction and the samples were loaded into the MyiQ real-time PCR detection system (Bio-Rad). The concentrations of samples were normalized based on the expression of internal control *Ubiquitin 10* (*UBQ10*). Expression levels of target genes were normalized to *UBQ10*. The qRT-PCR program was as follows: one cycle of 95°C for 3 min; 40 cycles of 95°C for 30 s, 56°C for 30 s, 72°C for 30 s; and final extension at 72°C for 10 min, followed by melting curve analysis. Normalized cDNAs of WT, *npc4*, *pldζ2* and *npc4pldζ2* were used to run semi-qRT-PCR using 30 cycles. All the primers used were listed in Supplemental Table 1.

Root trait measurement

For root phenotype observations, seedlings were germinated and grown in PNS agar (1.0%-1.2%) plates with 1 mM Pi or 1 μM Pi for the number of days indicated. Seedlings at 10 days after germination were measured for primary root length and lateral root number. For root hair density and length measurements, seedlings at 6 days after germination were used and roots were photographed under a microscope. Root hairs at 0-5 mm from the root tip were counted and the length of root hairs at 3-4 mm from the root tip was determined using image J (http://imagej.nih.gov/ij/).

ACKNOWLEDGMENTS

I thank Qun Zhang for help on root tip imaging. This work is supported by Agriculture and Food Research Initiative (AFRI) award no. [2016-67013-24429/project accession number 1007600] from the USDA National Institute of Food and Agriculture and the National Science Foundation [MCB-1412901]. Lipidomic instrumentation is supported by the National Science Foundation [DBI-1427621]. The authors have no conflicts of interest to declare.

SHORT LEGENDS FOR SUPPORTING INFORMATION:

Table S1. Primers used for semi qRT-PCR and real time PCR.

Figure S2-1. Root tips of WT, *npc4*, *pldζ2*, and *npc4pldζ2* under Pi-replete and deplete conditions.

Figure S2-2. PA, PG, PI, and PS levels of WT, *npc4*, *pldζ2*, and *npc4pldζ2* in roots and leaves with 5-day and 10-day Pi treatments.

Figure S2-3. Lipid profiling of WT, *npc4*, *pldζ2*, and *npc4pldζ2* roots and leaves

with 14-day Pi treatment.

Figure S2-4. MGDG molecular species of 10-day Pi-starved WT, *npc4*, *pldζ2*, and *npc4pldζ2* leaves.

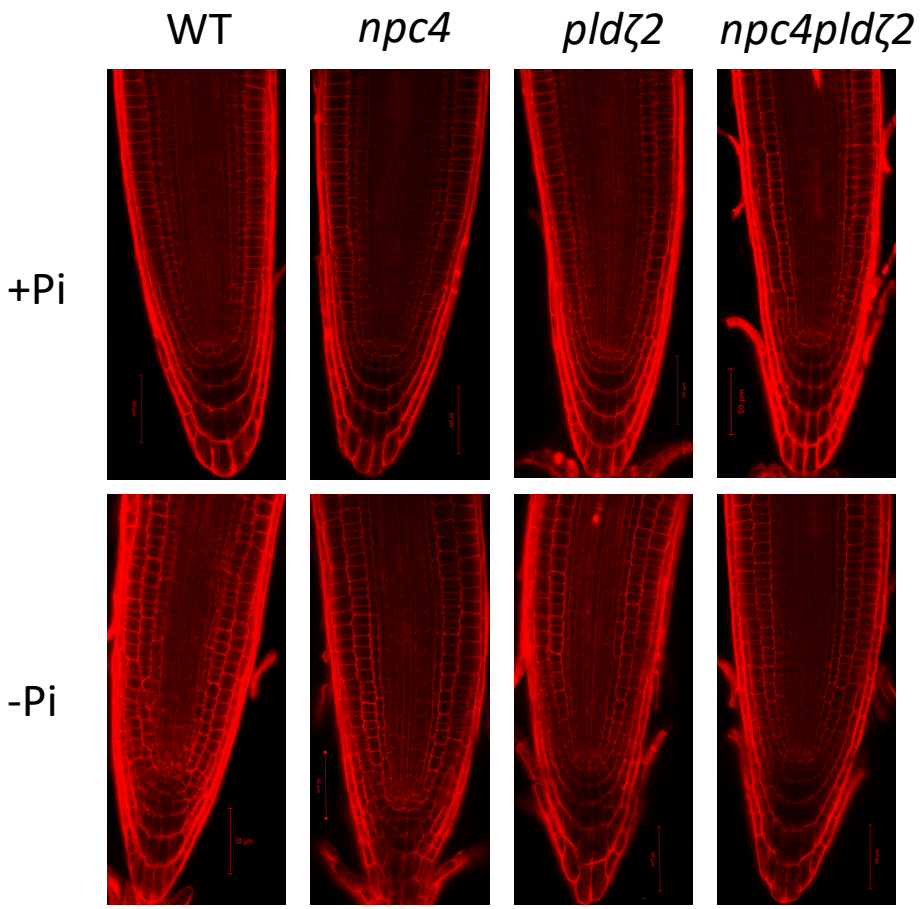

Figure S2-1. Root meristem morphology of WT, *npc4*, *pldζ2*, and *npc4pldζ2* seedlings.

Seedlings were germinated and grown on +Pi medium or –Pi medium for 6 days after germination. The roots were stained with 10 ug/ml propidium iodide and subject to confocal microscope for observation. Bars, 50 μm.

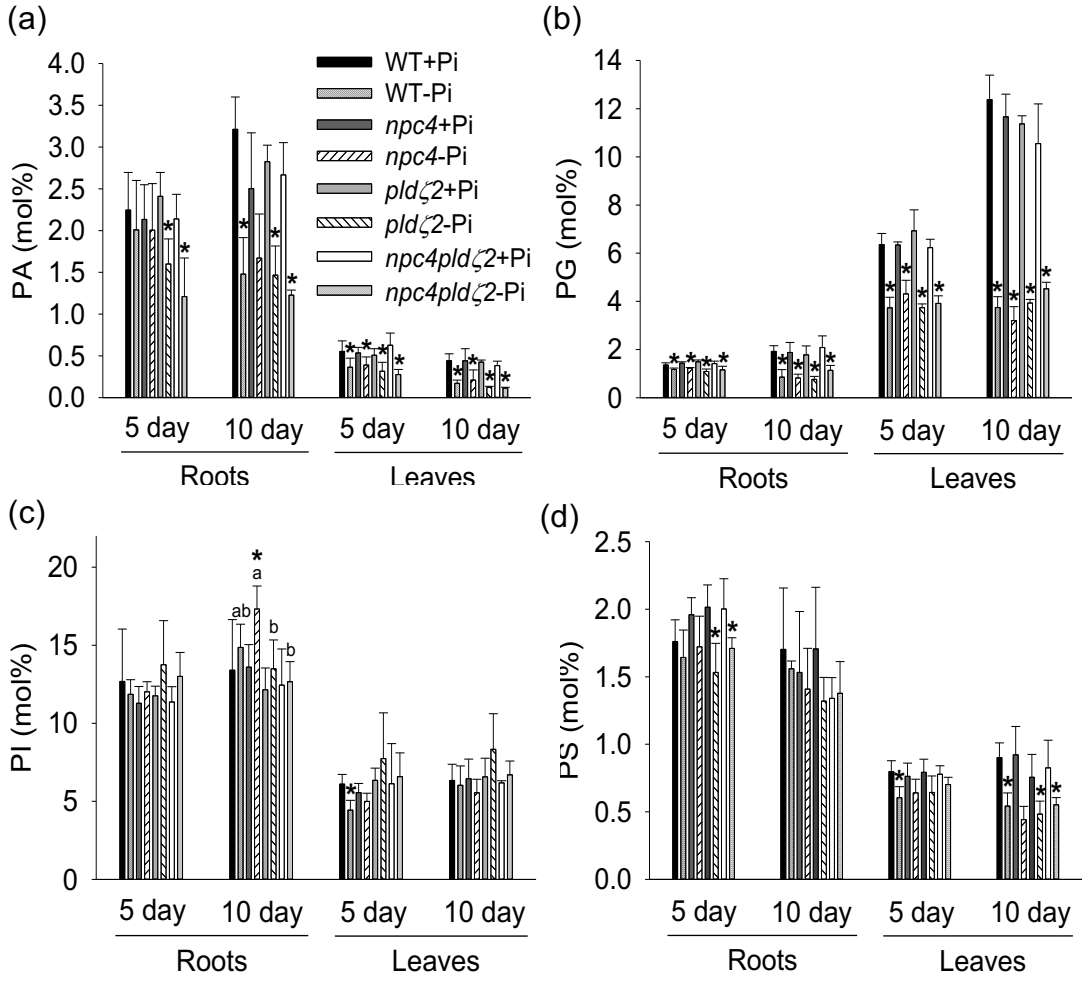

Figure S2-2. PA, PG, PI, and PS levels of WT, *npc4*, *pldζ2*, and *npc4pldζ2* in roots and leaves with 5-day and 10-day Pi treatments.

Seedlings were germinated and grown in Pi sufficient (1mM) liquid medium for 5 days, and then transferred into medium containing 1 mM Pi or no Pi for indicated days. PA (a), PG (b), PI (c) and PS (d) levels of WT, *npc4*, *pldζ2*, and *npc4pldζ2* roots and leaves with 5-day and 10-day Pi treatments. Values are means ± SD (n = 5). Lower-case letters indicate the statistically significant ($P < 0.05$) differences between genotypes by one way ANOVA analysis using the Holm-Sidak method. Asterisk indicates the significant ($P < 0.05$) differences between same genotypes under sufficient Pi or deficient Pi conditions based on Student's *t*-test.

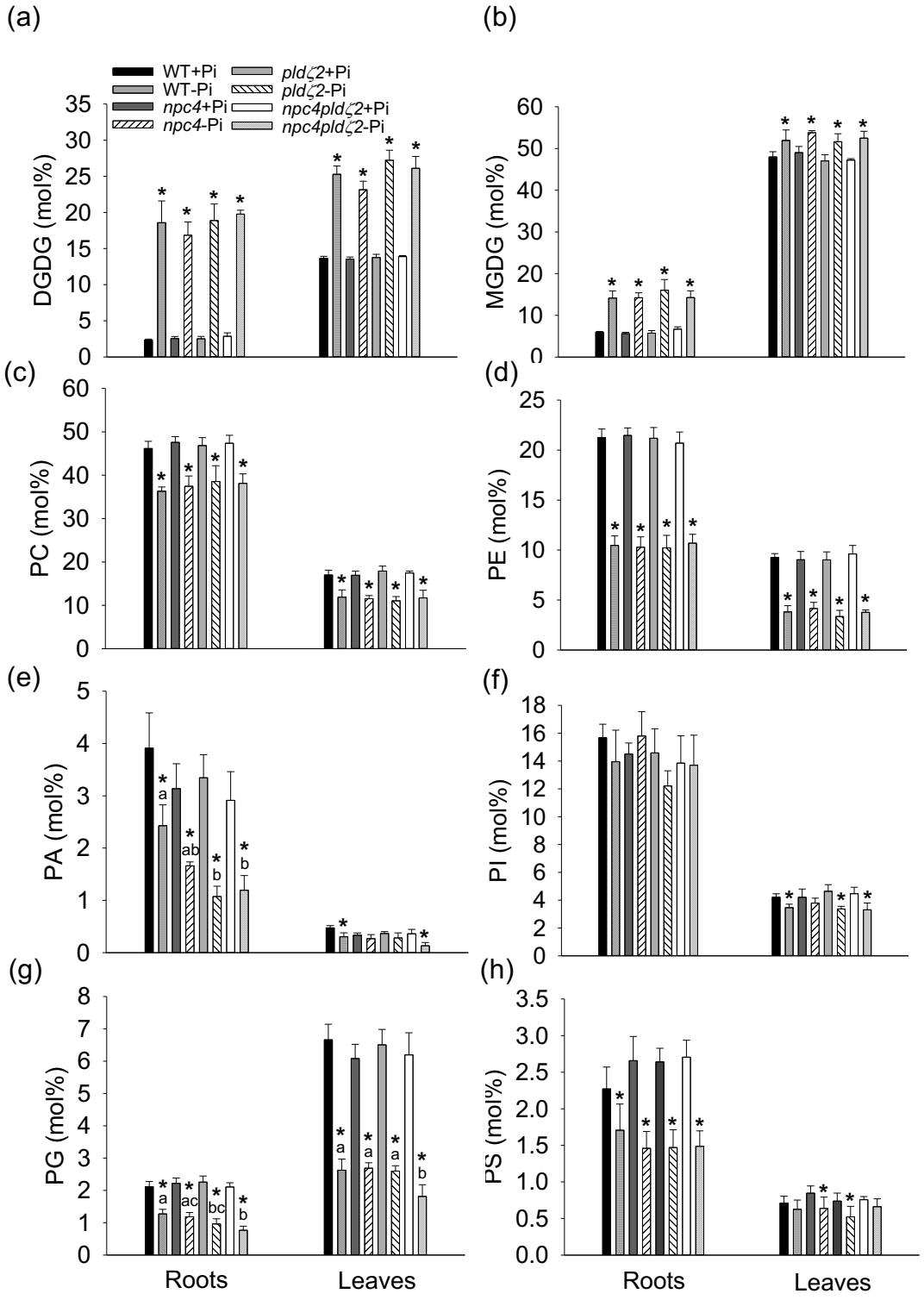
(a)
(b)
(c)
(d)
(e)
(f)
(g)
(h)
WT+Pi
WT-Pi
npc4+Pi
npc4-Pi
pldζ2+Pi
pldζ2-Pi
npc4pldζ2+Pi
npc4pldζ2-Pi
DGDG (mol%)
MGDG (mol%)
PC (mol%)
PE (mol%)
PA (mol%)
PI (mol%)
PG (mol%)
PS (mol%)
Roots
Leaves

Figure S2-3. Lipid profiling of WT, *npc4*, *pldζ2*, and *npc4pldζ2* roots and leaves with 14-day Pi treatment.

Seedlings were germinated and grown in Pi sufficient (1mM) liquid medium for 5 days, and then transferred into medium containing 1 mM Pi or no Pi for 14 days. DGDG (a), MGDG (b), PC (c), PE (d), PA (e), PI (f), PG(g) and PS (h) levels in WT, *npc4*, *pldζ2*, and *npc4pldζ2* roots and leaves. Values are means ± SD (n = 5). Lower-case letters indicate the statistically significant ($P < 0.05$) differences between genotypes by one way ANOVA analysis using the Holm-Sidak method. Asterisk indicates the significant ($P < 0.05$) differences between same genotypes under sufficient Pi or deficient Pi conditions based on Student's *t*-test.

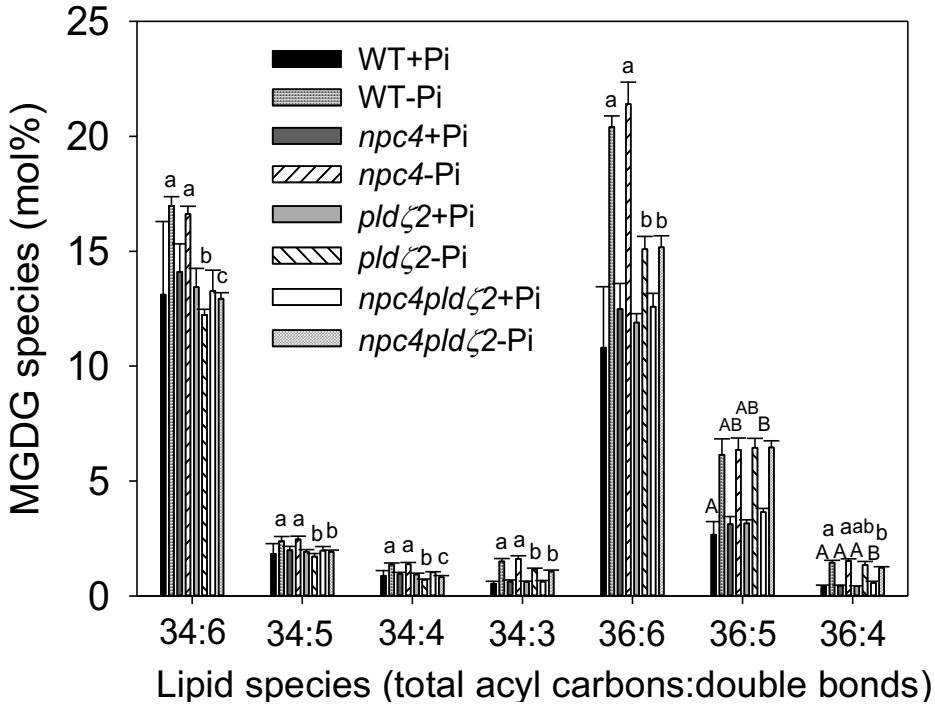

Figure S2-4. MGDG molecular species of 10-day Pi-starved WT, *npc4*, *pldζ2*, and *npc4pldζ2* leaves.

Seedlings were germinated and grown in Pi sufficient (1mM) liquid medium for 5 days, and then transferred into medium containing 1 mM Pi or no Pi for 10 days. Values are means ± SD (n = 5). Different capital letters indicate differences at $P < 0.05$ among genotypes under sufficient Pi using one way ANOVA. Different lower letters indicate differences at $P < 0.05$ among genotypes under deficient Pi by one way ANOVA.

Table S2-1. Primers used for semi qRT-PCR and quantitative real time PCR.

Gene ID	Gene name	Forward primer (5' to 3')	Reverse primer (5' to 3')	
At3g03530	NPC4	CCGTACCCAAGGTCACAATATG	TCAATCATGGCGAATAAAGCAAGAG	Semi-qRT-PCR
At3g05630	PLDζ2	ACCACCACATGGTTCTTCCTCACTA	CTTCATGAGCCTTCAGAATGC	
At4g05320	UBQ10	TCACCGGAAAGACCATCACT	TTAGAAACCACCACGAAGACGCAG	
At3G09560	PAH1	CTGTTGAGCATACGGGAAGTAA	CTGTTGAGCATACGGGAAGTAA	qRT-PCR
At5G42870	PAH2	GGATGCAGCAGCTCCTATTA	TCATTCCGGTCAACAGCTATC	
At5g20410	MGD2	AACATGTCTCCCTTAGTAGTTCTTTTGTC	GTTGATATTGTTAATGGCTAACAATAATGC	
At2g11810	MGD3	GGATATCCATCATCTATCCCAACAA	GATAAAAGAATGACAAACCACTAGAGAATATAC	
At3g11670	DGD1	GTGTGGGCTAAAGGATACAGAG	CATCTTCACCGTTCCCATATACA	
At4g00550	DGD2	GTCTGGAGCAAAGGGTACAA	AGTCCTCTCCATCACCGTATAA	
At4g05320	UBQ10	TCACCGGAAAGACCATCACT	CGGTGGGATACCCTCTTTG	
At3g03530	NPC4	AGCATCAAATGCTGCTGCTCAACC	TCCACCCACACACAAGAGAAGTGA	
At3g05630	PLDζ2	ACGATGTCCACTGCGCTCTATG	GGTGGTGAGGCATCAACAATGG	

REFERENCES

Andersson, M.X.,Stridh M.H., Larsson K.E., Liljenberg C., and Sandelius A.S. (2003). Phosphate-deficient oat replaces a major portion of the plasma membrane phospholipids with the galactolipid digalactosyldiacylglycerol, FEBS Letters, 537, 128-132.

Anthony, R.G., Henriques, R., Helfer, A., Mészáros, T., Rios, G., Testerink, C., Munnik, T., Deák, M., Koncz, C., and Bögre, L. (2004). A protein kinase target of a PDK1 signalling pathway is involved in root hair growth in Arabidopsis. The EMBO Journal 23, 572-581.

Bouain, N., Doumas, P., and Rouached, H. (2016). Recent Advances in Understanding the Molecular Mechanisms Regulating the Root System Response to Phosphate Deficiency in Arabidopsis. Current Genomics 17, 308-304.

Chandrika, N.N., Sundaravelpandian, K., Yu, S.M., and Schmidt, W. (2013). ALFIN-LIKE 6 is involved in root hair elongation during phosphate deficiency in Arabidopsis. New Phytol 198, 709-720.

Cruz-Ramirez, A., Oropeza-Aburto, A., Razo-Hernandez, F., Ramirez-Chavez, E., and Herrera-Estrella, L. (2006). Phospholipase DZ2 plays an important role in extraplastidic galactolipid biosynthesis and phosphate recycling in Arabidopsis roots. Proc Natl Acad Sci U S A 103, 6765-6770.

Den Hartog, M., Musgrave, A., and Munnik, T. (2001). Nod factor-induced phosphatidic acid and diacylglycerol pyrophosphate formation: a role for phospholipase C and D in root hair deformation. The Plant Journal 25, 55-65.

Djafi, N., Vergnolle, C., Cantrel, C., Wietrzyñski, W., Delage, E., Cochet, F., Puyaubert, J., Soubigou-Taconnat, L., Gey, D., Collin, S., Balzergue, S., Zachowski, A., and Ruelland, E. (2013). The Arabidopsis DREB2 genetic pathway is constitutively repressed by basal phosphoinositide-dependent phospholipase C coupled to diacylglycerol kinase. Frontiers in Plant Science 4, 307.

Gaude, N., Nakamura, Y., Scheible, W.R., Ohta, H., and Dormann, P. (2008). Phospholipase C5 (NPC5) is involved in galactolipid accumulation during phosphate limitation in leaves of Arabidopsis. Plant J 56, 28-39.

Grabau, L.J., Blevins, D.G., and Minor, H.C. (1986). P nutrition during seed development : leaf senescence, pod retention, and seed weight of soybean. Plant Physiol., 82, 1008–1012.

Hong, Y., Zhao, J., Guo, L., Kim, S., Deng, X., Wang, G., Li, M., and Wang X.

(2016). Plant Phospholipases D and C and Their Diverse Functions in Stress Responses. Prog. Lipid Res. 62, 55-74.

Kelly, A.A., Kalisch, B., Hölzl, G., Schulze, S., Thiele, J., Melzer, M., Roston, R.L., Benning, C., and Dörmann, P. (2016). Synthesis and transfer of galactolipids in the chloroplast envelope membranes of Arabidopsis thaliana. Proc Natl Acad Sci U S A 113, 10714-10719.

Klaus, D., Härtel, H., Fitzpatrick, L.M., Froehlich, J.E., Hubert, J., Benning, C., and Dörmann, P. (2002). Digalactosyldiacylglycerol Synthesis in Chloroplasts of the Arabidopsis dgd1 Mutant. Plant Physiol 128, 885-895.

Li, M., Welti, R., and Wang, X. (2006a). Quantitative profiling of Arabidopsis polar glycerolipids in response to phosphorus starvation. Roles of phospholipases D zeta1 and D zeta2 in phosphatidylcholine hydrolysis and digalactosyldiacylglycerol accumulation in phosphorus-starved plants. Plant Physiol 142, 750-761.

Li, M., Qin, C., Welti, R., and Wang, X. (2006b). Double knockouts of phospholipases Dzeta1 and Dzeta2 in Arabidopsis affect root elongation during phosphate-limited growth but do not affect root hair patterning. Plant Physiol 140, 761-770.

Li, M., Bahn, S.C., Guo, L., Musgrave, W., Berg, H., Welti, R., and Wang, X. (2011). Patatin-Related Phospholipase pPLAIIIβ-Induced Changes in Lipid Metabolism Alter Cellulose Content and Cell Elongation in Arabidopsis. The Plant Cell 23, 1107-1123.

López-Arredondo, D.L., Leyva-González, M.A., González-Morales, S.I., López-Bucio, J., and Herrera-Estrella, L. (2014). Phosphate Nutrition: Improving Low-Phosphate Tolerance in Crops. Annu. Rev. Plant Biol., 65, 95-123.

Nakamura, Y. (2013). Phosphate starvation and membrane lipid remodeling in seed plants. Prog Lipid Res 52, 43-50.

Nakamura, Y., Awai, K., Masuda, T., Yoshioka, Y., Takamiya, K., and Ohta, H. (2005). A novel phosphatidylcholine-hydrolyzing phospholipase C induced by phosphate starvation in Arabidopsis. J Biol Chem 280, 7469-7476.

Nakamura, Y., Koizumi, R., Shui, G., Shimojima, M., Wenk, M.R., Ito, T., and Ohta, H. (2009). Arabidopsis lipins mediate eukaryotic pathway of lipid metabolism and cope critically with phosphate starvation. Proc Natl Acad Sci U S A 106, 20978-20983.

Pant, B.D., Burgos, A., Pant, P., Cuadros-Inostroza, A., Willmitzer, L., and Scheible, W.R. (2015). The transcription factor PHR1 regulates lipid remodeling

and triacylglycerol accumulation in Arabidopsis thaliana during phosphorus starvation. J Exp Bot 66, 1907-1918.

Peters, C., Kim, S.-C., Devaiah, S., Li, M., and Wang, X. (2014). Non-specific phospholipase C5 and diacylglycerol promote lateral root development under mild salt stress in Arabidopsis. Plant, Cell & Environment 37, 2002-2013.

Peters, C., Li, M., Narasimhan, R., Roth, M., Welti, R., and Wang, X. (2010). Nonspecific phospholipase C NPC4 promotes responses to abscisic acid and tolerance to hyperosmotic stress in Arabidopsis. Plant Cell 22, 2642-2659.

Sánchez-Calderón, L., López-Bucio, J., Chacón-López, A., Gutiérrez-Ortega, A., Hernández-Abreu, E., and Herrera-Estrella, L. (2006). Characterization of low phosphorus insensitive Mutants Reveals a Crosstalk between Low Phosphorus-Induced Determinate Root Development and the Activation of Genes Involved in the Adaptation of Arabidopsis to Phosphorus Deficiency. Plant Physiology 140, 879-889.

Shimojima, M., and Ohta, H. (2011). Critical regulation of galactolipid synthesis controls membrane differentiation and remodeling in distinct plant organs and following environmental changes. Prog Lipid Res 50, 258-266.

Welti, R., Li, W., Li, M., Sang, Y., Biesiada, H., Zhou, H.-E., Rajashekar, C.B., Williams, T.D., and Wang, X. (2002). Profiling membrane lipids in plant stress responses: role of phospholipase Dα in freezing-induced lipid changes in Arabidopsis. Journal of Biological Chemistry 277, 31994-32002.

Yao, H., Wang, G., Guo, L., and Wang, X. (2013). Phosphatidic acid interacts with a MYB transcription factor and regulates its nuclear localization and function in Arabidopsis. The Plant Cell 25, 5030-5042.

Chapter 3 S6 kinase 2 is required for the membrane lipid remodeling and growth response to phosphate starvation in Arabidopsis

The manuscript is in preparation.

Yuan Su,[a,b] Sung Chul Bahn,[a,b] Liang Guo[c], Xuemin Wang[a,b,1]

[a] Department of Biology, University of Missouri, St. Louis, Missouri 63121

[b] Donald Danforth Plant Science Center, St. Louis, Missouri 63132

AUTHOR CONTRIBUTUONS

Y.S. and X.W. designed the project; Y.S. performed the most experiments; S.C.B. generated S6K overexpression lines. L.G. helped discuss the experimental design and interpret the data. Y.S. and X.W. analyzed the data and wrote the manuscript.

SUMMARY

Ribosomal protein S6 kinase (S6K) is a conserved component in the Target of Rapamycin (TOR) signaling pathway, which plays important roles in organismal response to nutrient availability, growth factors, and hormones in animals and sugar network in plants. However, the role of S6K in regulating plant growth in response to environmental nutrient availability is still unclear. Here, I demonstrate that S6K2 plays an important role in plant response to phosphate（Pi） deprivation in *Arabidopsis thaliana*. The T-DNA insertional mutant *s6k2* but not *s6k1* exhibited retarded growth development compared with wild type (WT), including shorter primary roots, fewer lateral roots, and less biomass under low or no Pi conditions, while *S6K2* overexpression enhanced the seedling growth. The transcription of *S6K2* but not *S6K1* was induced by the Pi shortage. Membrane lipid remodeling with a decrease in phospholipid levels and an increase in galactolipid levels was largely inhibited in *s6k2* mutant under Pi starvation condition. The accumulation of galactolipids and degradation of phospholipids were almost abolished under severe Pi starvation, whereas the lipid remodeling could occur but strongly suppressed in both shoots and roots under relatively moderate Pi deficiency. In addition, the induction of genes encoding for key enzymes involved in lipid remodeling by Pi starvation were highly reduced in *s6k2* mutant. Overall, our findings demonstrate that S6K2 plays an essential role in the lipid remodeling and growth response to Pi starvation.

INTRODUCTION

Inorganic phosphate (Pi) is one of essential macronutrients for plant growth, development, and proliferation. The availability of Pi in the soil is critical for the crop growth and production worldwide as orthophosphate, the absorbable phosphorus form by roots, is often low at the soil/root interface, whereas a large part of Pi interacts with elements such as calcium or aluminum to form partially soluble particles (Raghothama, 1999; Poirier and Bucher, 2002). When plants suffer Pi starvation, root architecture will be adapted to acquire more Pi source from the limited Pi pool, including the increase of lateral root density and root hairs to expand the interaction with soil (Lopez-Bucio et al., 2002; Perez-Torres et al., 2008). Meanwhile, plants broke down Pi-containing organic compounds such as membrane phospholipids as the endogenous source to maintain Pi homeostasis (Nakamura, 2013). The morphological and metabolic alterations in response to Pi starvation are achieved by the regulation of a wide range of gene expressions and phytohormones (Briat et al., 2015).

Under Pi limitation, membrane lipids undergo extensive remodeling where the level of phosphorus-containing phospholipids decreases, whereas the level of non-phosphorus containing galactolipids increases (Shimojima and Ohta, 2011; Nakamura, 2013; Pant et al., 2015). Based on head-groups, phospholipids can be classified into phosphatidylcholine (PC), phosphatidylethanolamine (PE), phosphatidylinositol (PI), phosphatidylserine (PS), phosphatidylglycerol (PG), and phosphatidic acid (PA) (Wang et al., 2006). Similarly, galactolipids can be sorted into monogalactosyldiacylglycerol (MGDG) and digalactosyldiacylglycerol (DGDG). In response to Pi deficiency, several

key phospholipid hydrolyzing enzymes have been characterized to degrade phospholipids to generate PA or diacylglycerol (DAG) in Arabidopsis, including phospholipase D ζ1 (PLDζ1) and ζ2 (PLDζ2) (Cruz-Ramirez et al., 2006; Li et al., 2006), non-specific phospholipase C 4 and 5 (NPC4 and NPC5) (Nakamura et al., 2005; Gaude et al., 2008), and PA phosphohydrolase 1 and 2 (PAH1 and PAH2) (Nakamura et al., 2009). On the other hand, the synthesis of galactolipids can utilize phospholipids-derived diacylglycerol (DAG) or DAG originated from glycerol-3-phosphate (G3P) through de novo pathway (Dörmann and Benning, 2002; Bates and Browse, 2012). Several synthases are induced to produce MGDG and DGDG under Pi deprivation, including chloroplast outer envelope membrane localized MGDG synthase 2 and 3 (MGD2 and MGD3) and DGDG synthase 1 and 2 (DGD1 and DGD2) (Awai et al., 2001; Kelly and Dörmann, 2002; Kelly et al., 2003; Kobayashi et al., 2009; Shimojima and Ohta, 2011; Pant et al., 2015) . In addition, DAG and triacylglycerol (TAG) accumulation recently has been discovered in Arabidopsis when low Pi level is present (Pant et al., 2015).

PHOSPHATE STARVATION RESPONSE 1 (PHR1) is a MYB transcription factor that plays a vital role in regulating many Pi-responsive gene expressions, including membrane lipid-altering enzyme genes mentioned above (Jain et al., 2012; Briat et al., 2015; Pant et al., 2015). Most Pi starvation responsive genes have one or multiple PHR1 binding sequence (P1BS) (GNATATNC) motifs in their promoters and/or gene sequences (Rubio et al., 2001; Pant et al., 2015). Particularly, PHR1 regulates the induction of microRNA399 (miR399) that negatively affects *PHO2* expression in

response to Pi limitation. *PHO2* encodes an ubiquitin E2 conjugase that targets phosphate transporters PHT1 and PHO1 for proteasome degradation, hence together communicating Pi status between shoots and roots via PHR1-miR339-PHO2 signaling pathway (Briat et al., 2015). Besides PHR1, some other transcription factors such as PHR1-like 1 (PHL1), PHL2 and PHL3 were reported to have some redundancy with PHR1 in regulating Pi-responsive gene expressions (Bustos et al., 2010; Sun et al., 2016a). Interestingly, *PHR1* itself is not induced by Pi starvation, and the evidence shows that its regulation is through post-translational modification or binding proteins (Briat et al., 2015). Arabidopsis SUMO E3 ligase SIZ1 was shown to sumoylate PHR1 to regulate Pi signaling, however the underlying mechanism is not known (Miura et al., 2005). The SPX [suppressor of yeast gpa1 (SYG1), the yeast cyclin-dependent kinase inhibitor (PHO81), and the human xenotropic and polytropic retrovirus receptor 1 (XPR1)] domain-containing nuclear protein SPX1 was demonstrated to physically interact with PHR1 in a Pi dependent manner to block PHR1 binding with P1BS on promoters in *Arabidopsis* (Puga et al., 2014). Similarly, rice SPX1 and SPX2 also bind to AtPHR1 homolog OsPHR2 to inhibit its function when Pi is present (Wang et al., 2014). However, it is unclear whether PHR1 is regulated translationally or if other components are involved in PHR1 regulation.

S6 kinase (S6K) phosphorylates the 40s small ribosomal subunit protein S6 that is one of numerous ribosomal proteins involved in the protein translation machinery (Ruvinsky and Meyuhas, 2006). S6K belongs to the AGC (named after the cAMP-dependent protein kinase A, cGMP-dependent protein kinase G and phospholipid-dependent

protein kinase C) serine/threonine protein kinase family (Bögre, 2003). The Arabidopsis genome contains two *S6K* genes (*S6K1* and *S6K2*). The catalytic kinase domain of S6K is very conserved throughout organisms including mice, human, *Drosophila*, yeast, and *Arabidopsis.* S6K protein also retains the homologous phosphorylation residues by regulatory proteins 3-phosphoinositide-dependent protein kinase-1 (PDK1) and Target of Rapmycin (TOR) kinase (Stolovich et al., 2002; Turck et al., 2004; Mahfouz et al., 2006; Ruvinsky and Meyuhas, 2006; Jacinto and Lorberg, 2008). AtPDK1 was shown to phosphorylate the activation loop domain of S6K1, while the residues Asp-167, Thr-176, Ser-177, Thr-211, and Ser-276 in AtPDK1 are important for phosphorylating S6K2 (Mahfouz et al., 2006; Otterhag et al., 2006). However, the regulation mechanism and the effect of phosphorylation of S6K by PDK1 is unknown. The TOR-S6K signaling pathway has been well studied in mammals and yeast, and plays an important role in coordinating nutrients, energy level, growth factors, hormones and stress signals with cell growth, division, and proliferation (Jacinto and Lorberg, 2008; Henriques et al., 2014). However, the knowledge of TOR-S6K pathway in plants is still limited. In Arabidopsis, the homologs of key components in TOR-S6K pathway can be found, including TOR, TOR adaptor protein RAPTOR, a TOR partner protein LST8, the downstream target S6K and S6K target S6. Except TOR is encoded by the single gene, all other components are encoded by two loci (Robaglia et al., 2012b; Henriques et al., 2014). AtS6K was reported to be phosphorylated and activated by AtTOR at carboxy-terminal domain during early growth stage with sugar induction. The conserved and most studied downstream target of S6K, S6, is also proved to be phosphorylated by S6K1 (Mahfouz et al., 2006; Schepetilnikov et al., 2011; Xiong and Sheen, 2012;

Schepetilnikov et al., 2013). It appears that TOR accomplishes many functions through S6K, whereas other TOR direct target such as E2F transcription factor E2Fa has also been identified in Arabidopsis (Xiong et al., 2013). *S6K1* overexpressing transgenic seedlings were shown to be hypersensitive to osmotic stress in a TOR dependent manner (Mahfouz et al., 2006). S6K1 was also indicated to interact with Retinoblastma-related 1 (RBR1) and regulate its nuclear localization to negatively control cell size and proliferation. The hemizygous *s6k1s6k2*/++ mutant and gene silenced mutant *S6K1*-RNAi displayed increased ploidy and aneuploidy, causing enlarged flowers, trichome branches and abnormal leave development. In contrast, *S6K1* and *S6K2* single knockout mutants did not display visible growth defect (Henriques et al., 2010). However, the mutants *tor*, *raptor1B*, *lst8-1.1* and *rps6a* or *rps6b* exhibited largely overlapping growth phenotype, including reduced biomass, compromised meristem, and slower root grow development, suggesting a more complex relationship among TOR, S6K and S6 rather than a liner pathway (Anderson et al., 2005; Deprost et al., 2005; Creff et al., 2010; Ren et al., 2011; Moreau et al., 2012; Ren et al., 2012; Henriques et al., 2014). In spite of high similarities of two S6K proteins, the different kinetics of regulation of transcript levels in response to fresh medium/nutrients were observed (Turck et al., 2004). Hence, it seems that two AtS6Ks may have distinct functions as the downstream integrators of TOR or possess its own properties in sensing the nutrient availability. A previous reported genome-wide transcriptional analysis identified *S6K2* as a Pi starvation response gene (Misson et al., 2005).

In this study, in order to understand the functions of S6Ks in plants, I analyzed T-DNA

insertional mutants defective in *S6K1* and *S6K2*. The results uncover that S6K2 but not S6K1 plays a key role in plant response to Pi deficiency. The findings reveal a new role of S6K2 in the Pi starvation signaling and bring up the potential bridge between TOR-S6K pathway and PHR1 regulated Pi-starvation signaling.

RESULTS

s6k2 but not *s6k1* impairs seedling growth response to phosphate starvation

S6K1 (At3g08730) and *S6K2* (At3g08720) tandemly localize on *Arabidopsis* chromosome 3 with 286 base pairs between two genes. S6K1 and S6K2 share 86% protein sequence identity, mainly differing from each other at N-terminal domain. Based on the data from Genevestigator (https://genevestigator.com/gv/index.jsp) and *Arabidopsis* eFP browser (http://bar.utoronto.ca/efp/cgi-bin/efpWeb.cgi), *S6K1* and *S6K2* are ubiquitously expressed in almost all tissues throughout various developmental stages, with some overlapping and distinct patterns. The expression of *S6K1* is pretty evenly distributed in all organs, except for strong expression in pollen cells. In contrast, *S6K2* is highly expressed in roots, dry seeds, and later phases of embryo development (Figure S3-1). The transcript level of *S6K1* is increased in response to ultraviolent light and oxidative stress especially in shoots, while the level of *S6K2* transcript is increased under phosphate deficiency especially in roots (Misson et al., 2005; Müller et al., 2007; Bustos et al., 2010; Henriques et al., 2010). The transcript level of both *S6K*s are highly induced by cold and salt treatment, and moderately induced by an exogenous ABA treatment (Mizoguchi et al., 1995).

Homozygous *S6K* single knockout (KO) mutant was isolated from T-DNA insertion line SALK_112945 (*s6k1-1*) for S6K1 and Salk_026472 (*s6k2-1*) for S6K2. The T-DNA insertion site of *S6K1* is in the second exon, while that of *S6K2* is in the first exon (Figure 3-1A). To test the T-DNA insertion effect on S6K transcript, reverse transcript polymerase chain reaction (RT-PCR) was applied using *S6K1* and *S6K2* specific primers. No complete transcript of *S6K1* or *S6K2* was detected in homozygous *s6k1-1* or *s6k2-1* mutants (Figure 3-1B). The homozygous *s6k1s6k2* double mutant could not be successfully isolated as the homozygous *s6k1s6k2* is lethal (Henriques et al., 2010). In agreement with previous observations, *s6k1-1* and *s6k2-1* single mutants had largely normal growth similarly to WT in soil (Figure S3-2). In addition, I overexpressed *S6Ks* in Arabidopsis under the control of the 35S cauliflower mosaic virus promoter. S6Ks were tagged with GFP at the C terminus and the protein level of S6K-OE was detected in the total protein extract from leaves using anti-GFP antibody. S6K1-OE 8 and S6K2-OE 7 are strong overexpression lines, whereas S6K1-OE 3 and S6K2-OE 6 are relatively weak overexpression line (Figure 3-1C).

To investigate the potential function of S6Ks in plant response to nutrient availability, I tested S6K-KO and OE seedlings' response to different levels of nitrogen (N) and Pi. Under sufficient N condition (6 mM N), similar primary root growth was observed between WT and mutants, except S6K2-OE line 7 has longer primary root than WT and S6K-KO. In response to N deficiency (0.6 mM N), *s6k1-1* and *s6k2-1* seedlings responded similarly as wild-type (WT) seedlings. The strong overexpression lines S6K1-OE 8 and S6K2-OE 7 exhibited slightly better primary root growth than WT (Figure S3-

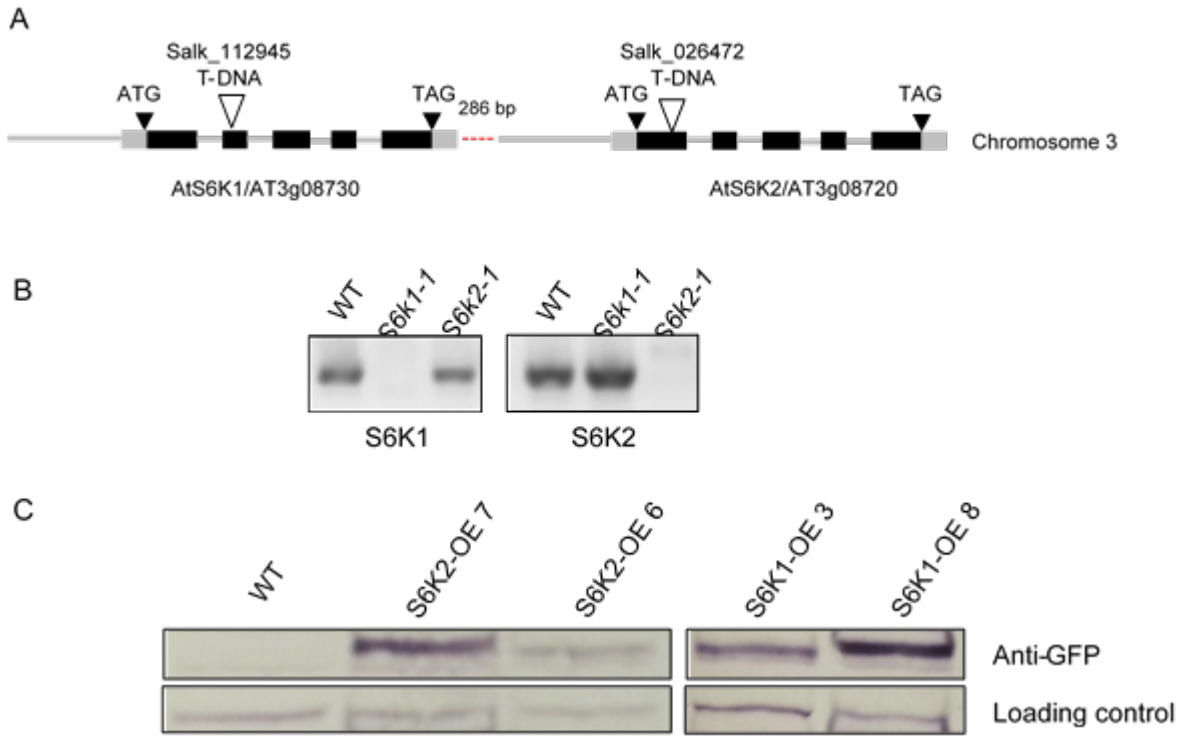

Figure 3-1 Isolation of *s6k1*, *s6k2* and S6K-OE transgenic Arabidopsis.

A. The schematic diagram of S6K gene structure. T-DNA insertions in *S6K1* (Salk_112945) and *S6K2* (salk_026472*)* are indicated by empty triangles. The T-DNA insertion site in salk_026472 was verified by sequencing. Black boxes, gray horizontal lines and gray boxes represent exons, introns and UTRs, respectively. Full triangles indicate start codon or stop codon. B. RT-PCR verification of T-DNA disruption of *S6K1* and *S6K2* transcript. C. Western blotting verification of S6K1 and S6K2 overexpression plants. The construct 35S::*S6K*-GFP was made to generate S6K overexpression lines. Anti-GFP antibody was used to detect S6K-GFP protein from total protein extracted in leaves.

-3). In contrast, with sufficient Pi (1 mM Pi), WT, *s6k2-1* and *s6k2-1* seedlings displayed similar growth and biomass, whereas two S6K2-OE lines accumulated ~10% more biomass than WT. When transferred from Pi replete medium to Pi depleted (0 mM Pi) medium for 6 days, the leaf size and root mass of WT seedlings became smaller. The dry weight of WT seedlings was reduced to almost half of that grown in Pi replete medium. The change in growth of *s6k1-1* seedlings was similar to that of WT, while *s6k2-1* mutant revealed stronger growth retardation than WT and *s6k1-1* (Figure 3-2A and 3-2B). The dry weight of *s6k2-1* seedlings was ~60% of WT dry weight. S6K2 overexpress line 6 did not show significant difference from WT, while overexpression line 7 increased ~30% dry weight than WT seedlings (Figure 3-2B).

The detection of *S6K1* and *S6K2* transcript level over time after the Pi starvation treatment unveiled the different expression patterns between *S6K1* and *S6K2*. The *S6K1* expression level decreased at 8 hour (h) and continued going down till 48 h after Pi starvation. At 72h time point, its level went up back to levels at 0h and 2h time points. On the other hand, the transcript level of *S6K2* increased to ~2.5 folds compared with initial transcript level at 0h. The *S6K2* transcript level then stayed at ~2 folds from 8h to 48h, and went up to ~2.5 folds at 72h of initial transcript level (Figure 3-2C). The *S6K2* transcript levels were also compared in shoots and roots with and without Pi at 8 h after transferred to Pi replete and Pi limited medium, respectively. The transcript level of *S6K2* in roots was ~2 folds of that in shoots under sufficient Pi condition. The Pi deprivation induced *S6K2* expression by ~170% and ~70% in shoots and roots, respectively (Figure 3-2D). The results suggested that S6K2 seems to play a more

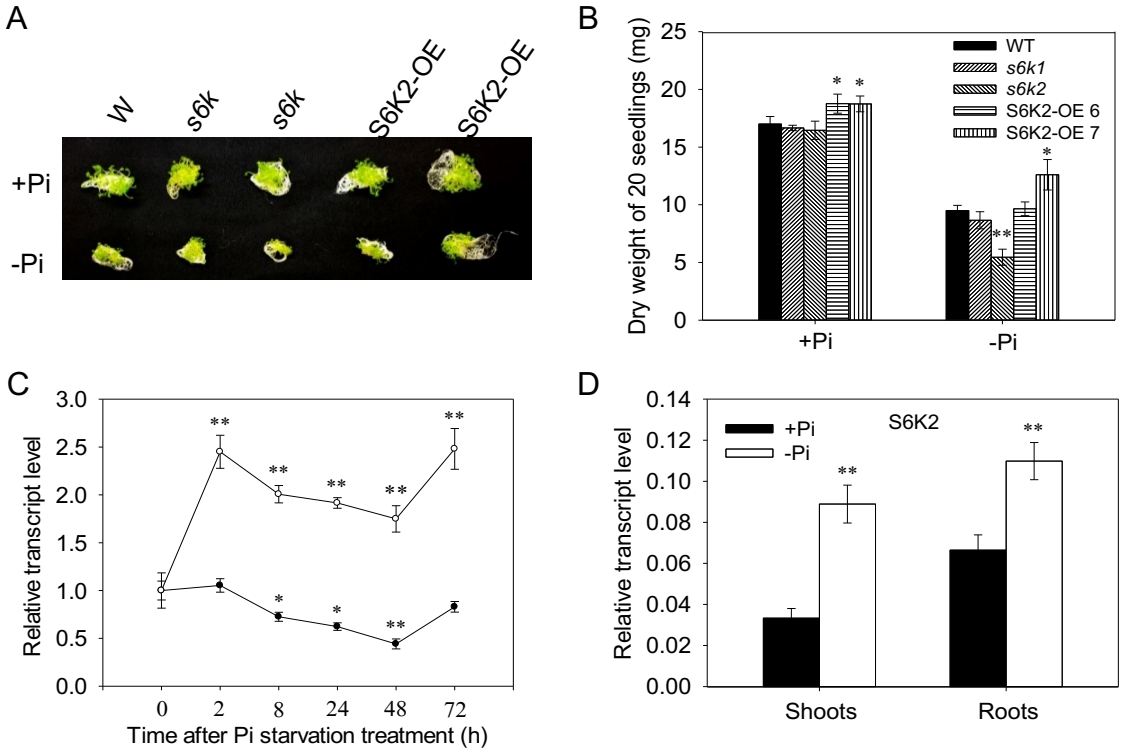

Figure 3-2 *S6k2*, but not *S6k1*, is induced by Pi deprivation. Pi-starved *s6k2* seedlings display more growth retardation than WT.

A. The growth phenotype of *s6k1*, *s6k2* and S6K2-OE seedlings under Pi-sufficient and deficient conditions. Seedlings were grown in 1 mM Pi hydroponic medium for 6 days, and then transferred into Pi sufficient medium or Pi starvation medium for another 6 days. B. Dry weight of 20 seedlings grown under Pi-sufficient and deficient conditions. Transcript level of S6K1 and S6K2 in WT under different times of transferring to Pi-deficient conditions. Values are means ± SD (n ≥ 6). Single and double asterisks mark differences between WT and mutants at $P < 0.05$ and at $P < 0.01$, respectively, based on Student's t test. C. S6K transcript level in WT seedlings at 0h, 2h, 8h, 24h, 48h and 72h after Pi starvation treatment. Values are means ± SD (n = 3). Single and double asterisks indicate significant difference from 0h at $P < 0.05$ and at $P < 0.01$, respectively, based on Student's t test. D. S6K2 transcript level in WT shoots and roots with and without Pi starvation determined by quantitative real-time PCR. The shoots and roots samples were collected at 8h after Pi deprivation. Values are means ± SD (n = 3). Double asterisks indicate significant difference from control at $P < 0.01$ based on Student's t test.

important role than S6K1 in plant response to Pi deprivation.

S6K2 is essential for root architecture formation in response to Pi deficiency

One characteristic plant response to Pi deprivation is the adaption of root morphology including inhibited primary root elongation and facilitated lateral root growth. To study the role of S6K in root growth and development, the root morphology of WT and S6K mutant seedlings was compared when germinated and grown on plant nutrient (PN) plates vertically containing various Pi concentrations (0 mM Pi, 0.01 mM Pi, 0.1 mM Pi, and 1 mM Pi). With decreasing Pi concentration, the growth of leave and primary root was arrested, whereas the later root growth was promoted (Figure 3-3A and S3-4). Under 1 mM Pi condition, the primary root growth was similar among WT, *s6k1-1*, *s6k2-1*, and weak overexpression line S6K2-OE 6 from day 3 to day 7 after germination. S6K2-OE 6 seedlings had significant longer primary root than WT at day 8. The strong overexpression line S6K2-OE 7, however, exhibited a slightly faster primary root elongation than WT (Figure 3-3B and S3-4). No significant difference of later root number was observed among all genotypes (Figure 3-3C). Under low (0.01 mM Pi) or no Pi conditions, the primary root elongation and later root formation were strongly depressed in *s6k2-1*, while both S6K2-OE lines showed enhanced primary root elongation and lateral root growth over days after germination. On the other hand, *s6k1-1* mutant had very similar root growth pattern as WT in response to Pi deprivation (Figure 3-3 and S3-4). The results indicate that S6K2 is important for the root adaption in Pi-starved plants.

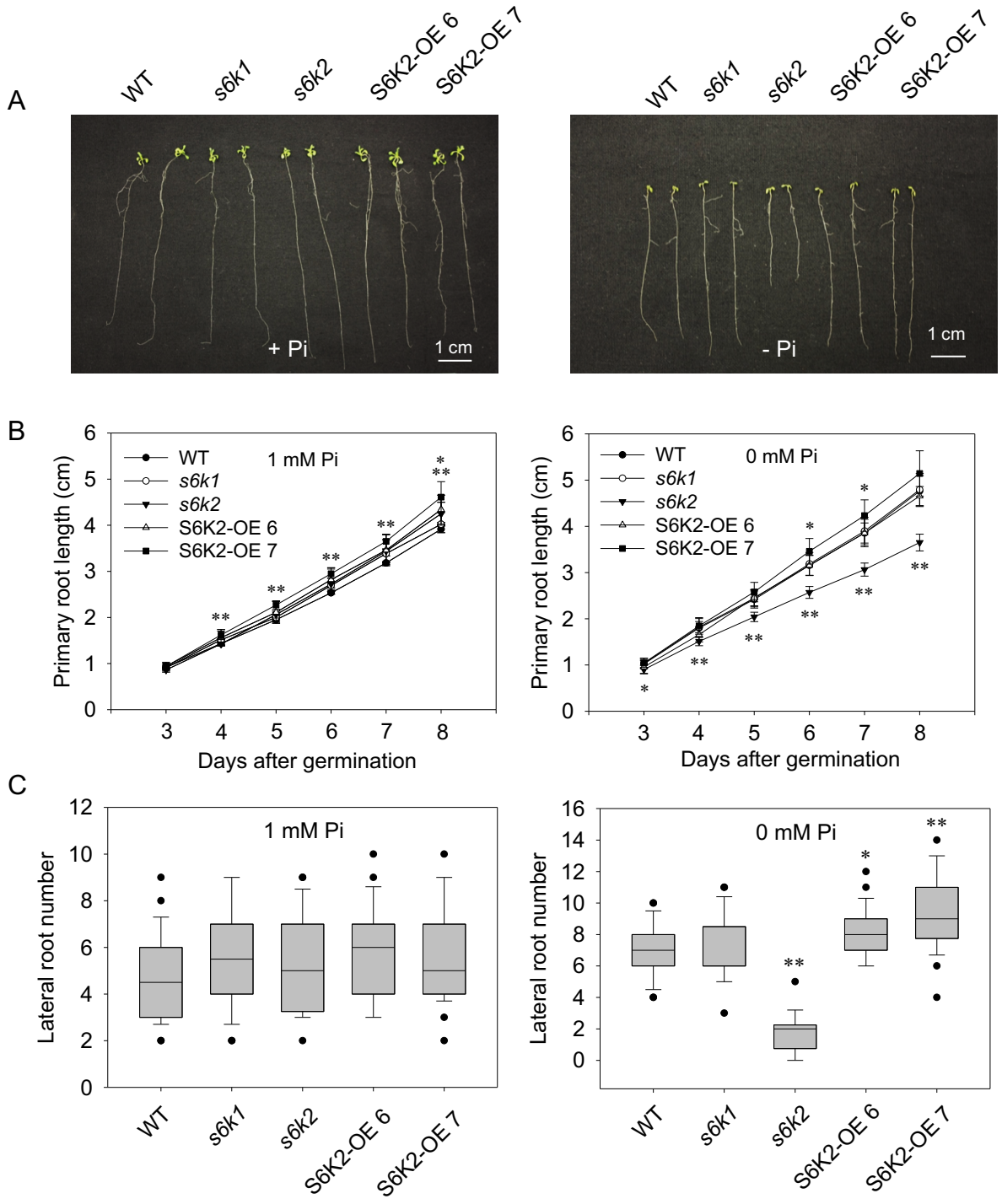
A
WT
s6k1
s6k2
S6K2-OE 6
S6K2-OE 7
+ Pi
1 cm
- Pi
B
1 mM Pi
0 mM Pi
Primary root length (cm)
Days after germination
C
Lateral root number

Figure 3-3 *s6k2* decreased primary and lateral root growth, whereas S6K-OE had opposite effects.

Seedlings were grown on the plant nutrient (PN) medium with or without Pi for indicated days vertically in the growth chamber. *s6k2* mutant was similar to WT with sufficient Pi, whereas *s6k2* mutant was more sensitive to Pi starvation compared with WT. A. The growth phenotype of *s6k1*, *s6k2* and S6K2-OE seedlings grown on the plant nutrient (PN) plates with or without Pi for 6 days after germination vertically in the growth chamber. Bars, 1cm. B. The primary root elongation of *s6k1*, *s6k2* and S6K2-OE seedlings from day 3 to day 8 after germination grown in Pi replete plates or Pi free plates. Values are means ± SD ($n \geq 20$). Single and double asterisks indicate significant difference compared with WT at $P < 0.05$ and at $P < 0.01$, respectively, based on Student's t test. C. The later root number of *s6k1*, *s6k2* and S6K2-OE seedlings grown under Pi replete or Pi starved conditions for 6 days after germination. Values are means ± SE ($n \geq 20$). Single and double asterisks represent the significant difference between WT and mutants at $P < 0.05$ and at $P < 0.01$, respectively, based on Student's t test.

by which Pi-containing phospholipid level decreases whereas galactolipid level increases. To investigate the function of S6K in the membrane lipid remodeling, lipid molecular species were quantitatively profiled using ESI-MS/MS in WT and S6K mutant seedlings grown in Pi replete and Pi free hydroponic media. The seedlings were directly germinated and grown in Pi-sufficient medium or medium without Pi for 14 days to initiate a strong Pi starvation treatment. The total lipids were then extracted from the whole seedlings and subject to load into the mass spectrometry. The membrane lipid profiling analysis showed that *s6k2* KO failed to maintain the membrane lipid remodeling process. In WT, the mole percentage of DGDG was increased from ~25% to ~40% in response to Pi deprivation (Figure 3-4A). Levels of phospholipids including PC, PE, PI, PG, PS and PA decreased by ~32%, ~46%, ~63%, ~52%, ~56% and ~53%, respectively (Figure 3-4B and 3-4C). Similar lipid alterations also occurred in *s6k1* KO and S6K2-OE mutants. However, the lipid remodeling was largely abolished in *s6k2* KO. The galactolipid and phospholipid levels in *s6k2* KO stayed unchanged or the change was much weaker than WT except for PS when compared Pi replete condition and Pi starvation condition. Specifically, in *s6k2* KO, DGDG level was not significantly changed, while MGDG level dropped by ~10%. PC, PE, and PA levels increased, whereas PI, PG, lysophosphatidylcholine (lysoPC) and lysophosphatidylethanolamine (lysoPE) kept the similar levels as in Pi replete medium. Interestingly, PS level in *s6k2* KO decreased almost as much as that in WT. Furthermore, the lipid changes in S6K2-OE seedlings was comparable with WT (Figure 3-4).

The lipid molecular species analysis reveals that the arrested membrane lipid

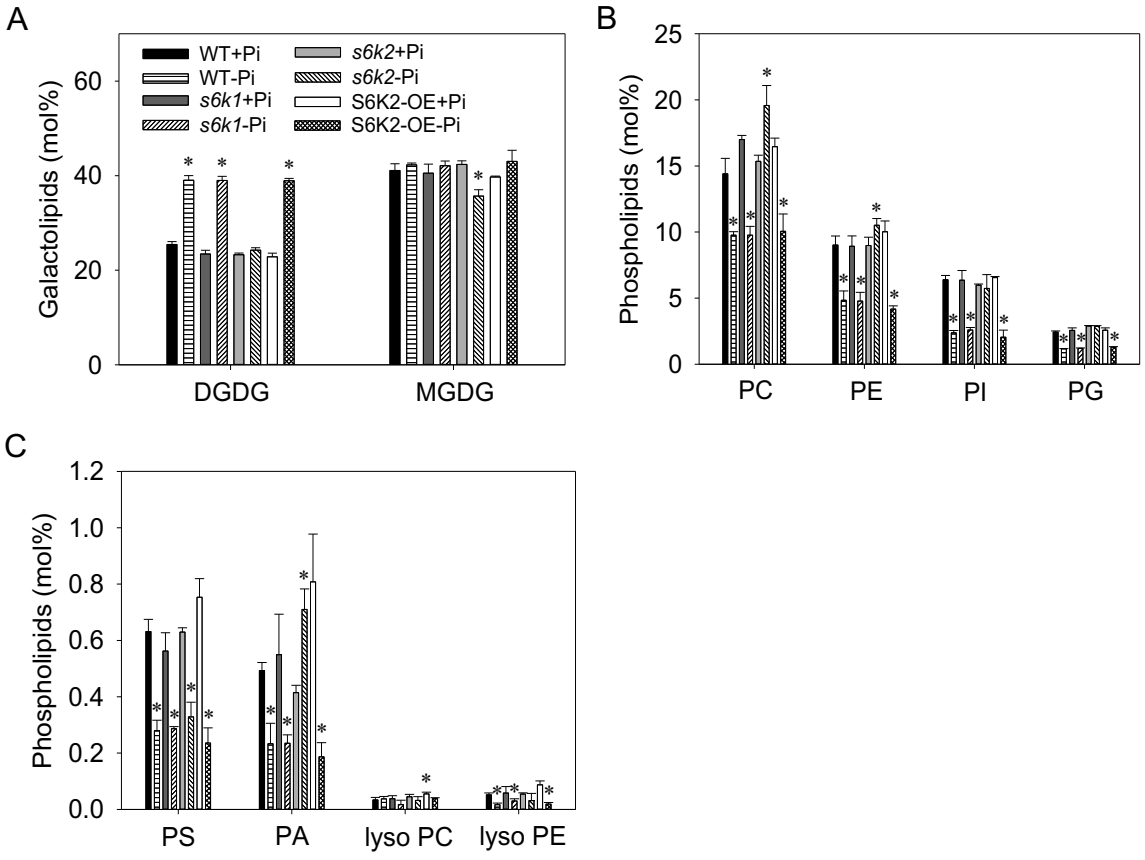

Figure 3-4 *s6k2* seedlings failed to remodel membrane lipids under Pi deprivation.

Seedlings were grown in the hydroponic PNS medium with 1 mM or without Pi under continuous light for 14 days with gentle shaking. A. Galactolipid content in *s6k1*, *s6k2* and S6K2-OE seedlings. B. Major phospholipid content in *s6k1*, *s6k2* and S6K2-OE seedlings. C. Minor phospholipid content in *s6k1*, *s6k2* and S6K2-OE seedlings. Values are means ± SD (n = 3). Asterisks indicate significant difference between +Pi and –Pi conditions at $P < 0.05$ based on Student's t test.

remodeling in *s6k2* KO was lipid molecular species dependent. In other words, the inhibition of lipid alterations was not due to every molecular species unchanged, but came from the inhibition of majority lipid molecular species. For example, the increased level of total DGDG content in WT was contributed by all DGDG molecular species detected except for 34:6 (34 carbons: 6 double bonds) DGDG under Pi starvation condition. However, in *s6k2* KO, the level of most DGDG molecular species (34C and 36C) was not induced as much as WT. Interestingly, the levels of 38:5 and 38:6 DGDG increased similarly as WT by Pi deprivation, suggesting a unique regulation of DGDG synthesis with very long polyunsaturated acyl chains (Figure 3-5A and 3-5B). For phospholipids, most PC and PE molecular species decreased by ~50% except for 36:3 PC/PE and 36:6 PC/PE in WT seedlings under Pi starvation. By comparison, most 34C PC species kept unchanged, while 36C PC species increased in *s6k2* KO seedlings. Unlike 34C PC, most 34C PE species decreased slightly, while majority of 36C PE species increased as 36C PC did (Figure 3-5C and 3-5D). Collectively, the loss of S6K2 resulted in the failure of the membrane lipid remodeling during Pi starvation in a lipid molecular species-specific manner.

Shoots and roots of *s6k2* KO displayed different patterns of lipid changes in response to Pi-deprivation

The expression level of *S6K2* was higher in roots than leaves (Figure 2D). To investigate if S6K2 may function differently in shoots and roots, lipids from shoots and roots were analyzed in the presence and absence of Pi. The lipid profiling data revealed that the lipid remodeling was occurring in both WT shoots and roots. The accumulation

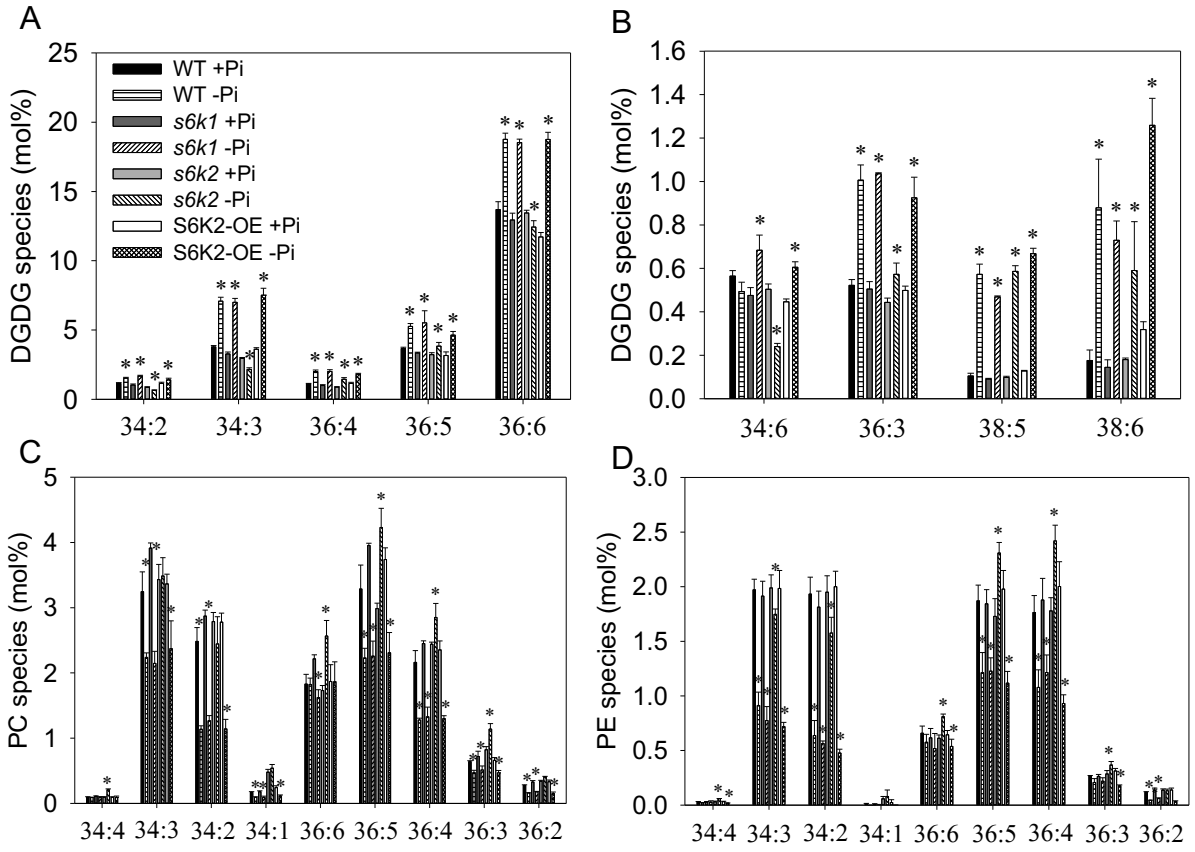

Figure 3-5 Membrane lipid molecular species changes in WT, *s6k*, and S6K-OE seedlings in response to Pi starvation.

A. Major DGDG molecular species content. B. Minor DGDG molecular species content. C. PC molecular species content. D. PE molecular species content. Values are means ± SD (n =3). Asterisks indicate significant difference between +Pi and –Pi conditions at $P < 0.05$ based on Student's t test.

of galactolipids was weaker in shoots than in roots, whereas the degradation of phospholipids was stronger in shoots than in roots. However, the lipid remodeling was highly repressed in *s6k2* KO (Figure 3-6). Specifically, both DGDG and MGDG levels were increased in WT shoots and roots when exposed to Pi free medium. The level of DGDG in shoots was induced to ~2.5 folds by Pi starvation, while in roots, DGDG level increased more than 10 folds. In contrast, the DGDG level in *s6k2* shoots was induced by 100% of that in WT, whereas in *s6k2* shoots it increased ~3 folds (Figure 3-6A). For phospholipids, PC level in WT shoots decreased by ~50% and ~20% in roots respectively under Pi deprivation. However, PC level did not significantly change in both *s6k2* shoots and roots after Pi starvation. PE level dropped dramatically in WT shoots by ~ 80%, while it decreased ~40% in *s6k2* shoots. By comparison, PE level in WT roots went down by ~30%, while PE level in *s6k2* roots decreased by less than 10% under Pi deprivation (Figure 3-6B). The change of PI, PG and PA levels in WT stayed similar to those in *s6k2* mutant in both shoots and roots (Figure 3-6B and 3-6C). Interestingly, PS level in WT shoots decreased by ~40% while it was not significantly altered in *s6k2* shoots. On the other hand, in roots, PS level decreased in both WT and *s6k2* mutant although the decrease in *s6k2* was less than that in WT (Figure 3-6C). The lipid composition in S6K-OE was pretty similar to WT. Overall the data demonstrate the distinct impacts of S6K2 on lipid remodeling in shoots and roots.

The induction of lipid-remodeling genes by Pi starvation was suppressed in *s6k2* mutant

To understand the mechanism by which the knockout of S6K2 inhibits lipid changes in

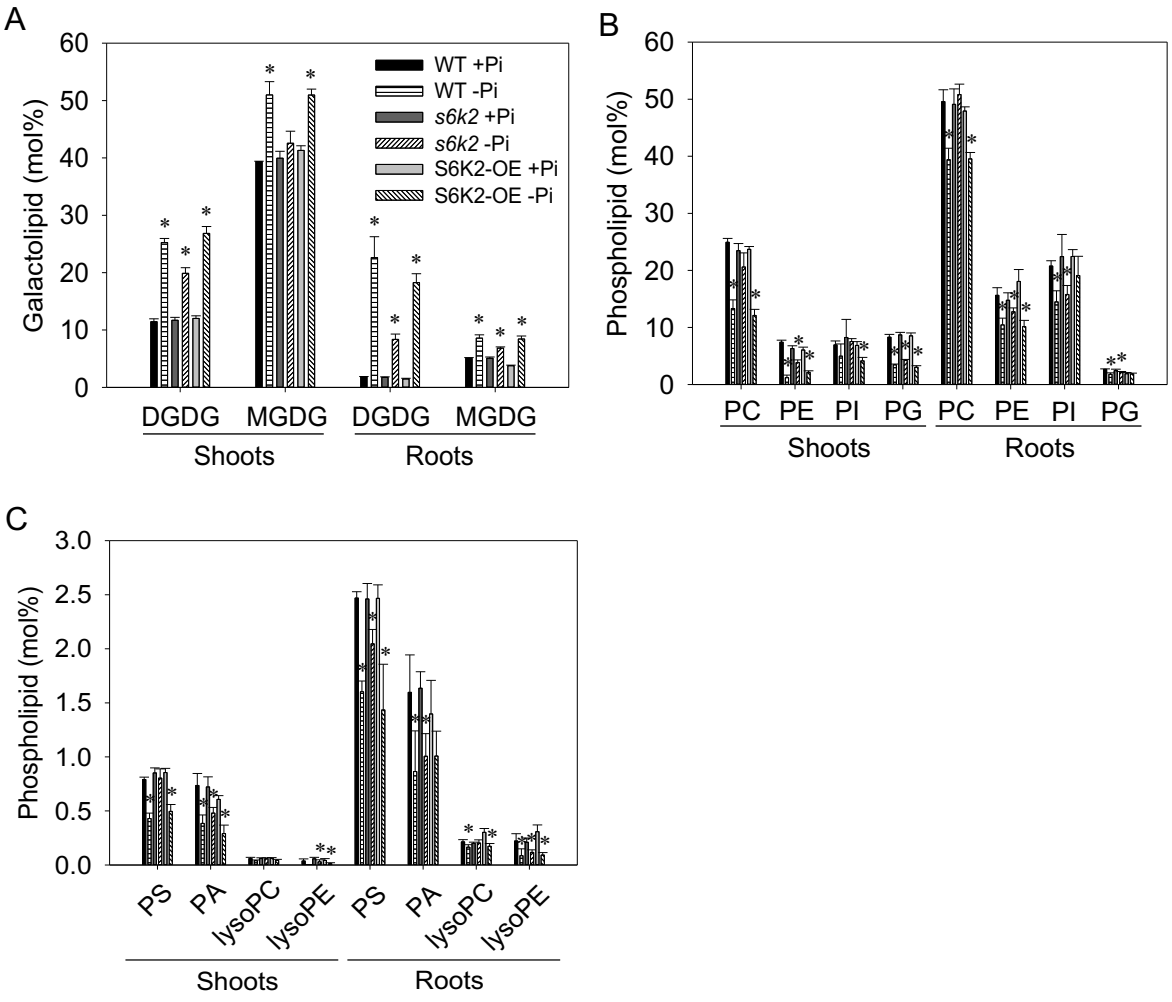

Figure 3-6 The *s6k2* mutant showed highly reduced lipid remodeling in shoots and roots during Pi starvation.

Seedlings were grown in the hydroponic PNS medium containing 1 mM Pi for 5 days and then transferred into Pi sufficient or no Pi medium for another 7 days. A. Galactolipid content in shoots and roots. B. Major phospholipid content in shoots and roots. C. Minor phospholipid content in shoots and roots. Values are means ± SD (n = 5). Asterisks indicate significant difference between +Pi and –Pi conditions at $P < 0.05$ based on Student's t test.

response to Pi starvation, quantitative real-time PCR (qRT-PCR) was applied to analyze the transcript levels of key genes encoding lipid-remodeling enzymes. The shoots and roots materials were collected as those used in lipid analysis to extract total mRNA. The gene expression analysis showed that MGDG synthase genes, *MGD2* and *MGD3*, DGDG synthase genes, *DGD1* and *DGD2,* and phospholipid hydrolyzing enzyme genes *NPC4*, *PLDζ2* and PAH1 were highly induced by Pi starvation in WT shoots and roots. However, in *s6k2* KO, corresponding to lipid changes, the induction of these genes was largely suppressed during Pi depletion. Notably, the transcript levels of these genes except for DGD1 and PAH1 in *s6k2* KO were more abundant than those in WT in both shoots and roots under Pi replete condition (Figure 3-7). The gene expression evidence well explained the alleviated lipid remodeling triggered by Pi deprivation in *s6k2*.

PHR1 expression was partially inhibited in *s6k2* KO, whereas the S6K2 expression was slightly affected in *phr1* KO during Pi starvation

Transcription factor PHR1 is a master regulator of Pi-responsive genes. PHR1 homologs PHL1 was shown to have redundancy with PHR1 in Pi starvation response. There are two P1BS motifs in the first intron of *S6K2* gene (Figure 3-8A). I tested if PHR1 and S6K2 had any effect on each other's expression. The level of *PHR1* transcript was not much altered by Pi starvation, which is similar to the previously report. However, the level of *PHR1* transcript decreased by ~45% and ~38% in *s6k2* shoots, and by ~40% and ~27% in *s6k2* roots compared with WT under Pi replete and Pi deficient conditions, respectively. The transcript level of PHL1 in WT, on the other hand, did not differ significantly from *s6k2* mutant in either shoots or roots with or

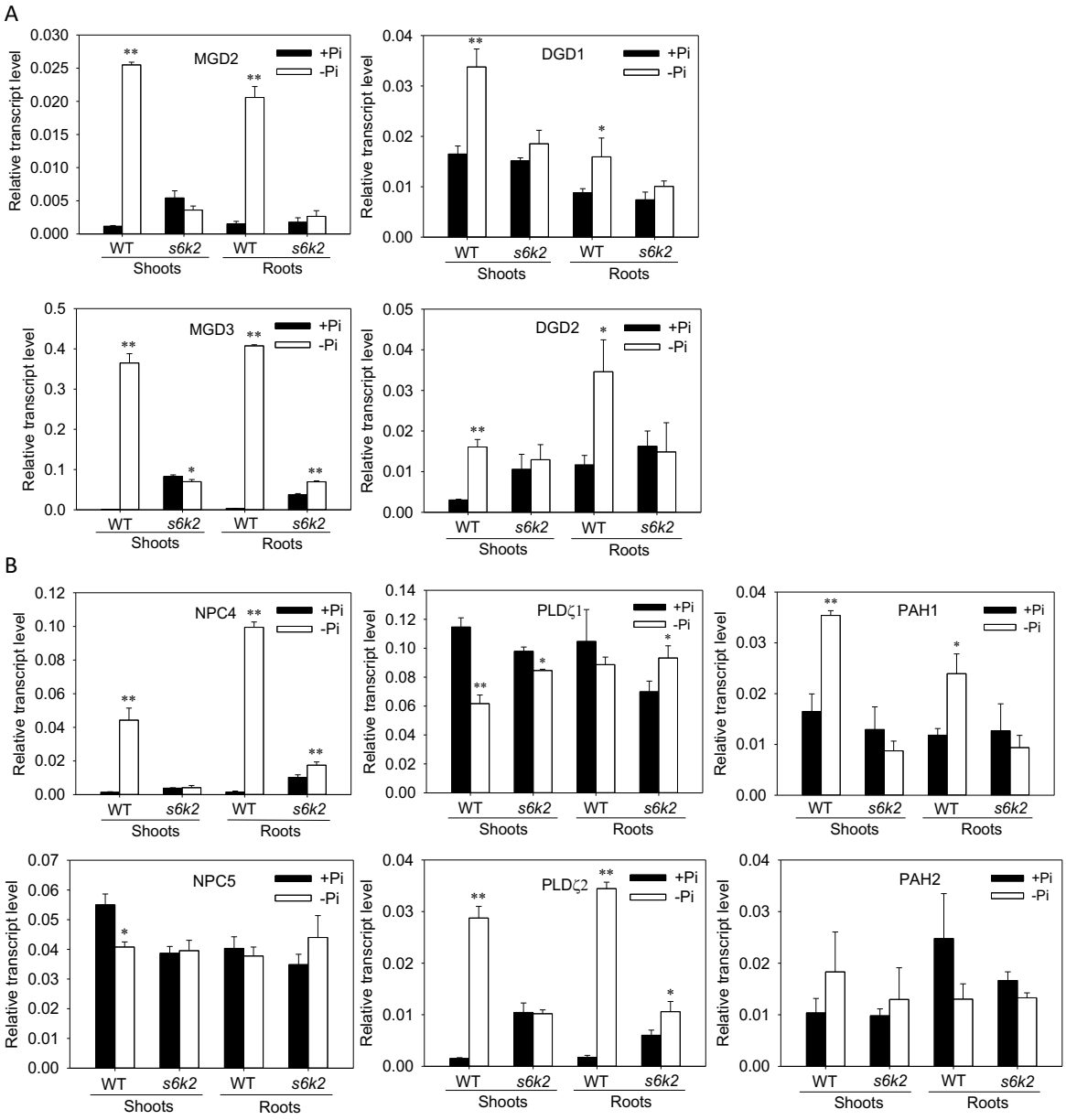

Figure 3-7 The expressions of key genes involved in lipid remodeling were not highly induced in *s6k2* mutant during Pi starvation.

A. Gene expression level of MGDG synthase genes *MGD2/3* and DGDG synthase genes *DGD1/2*. B. Gene expression level of phospholipid hydrolyzing enzyme genes including *NPC4/5*, *PLDζ1/2*, and *PAH1/2*. Values are means ± SD (n = 3). Asterisks indicate significant difference between +Pi and –Pi conditions at $P < 0.05$ based on Student's t test.

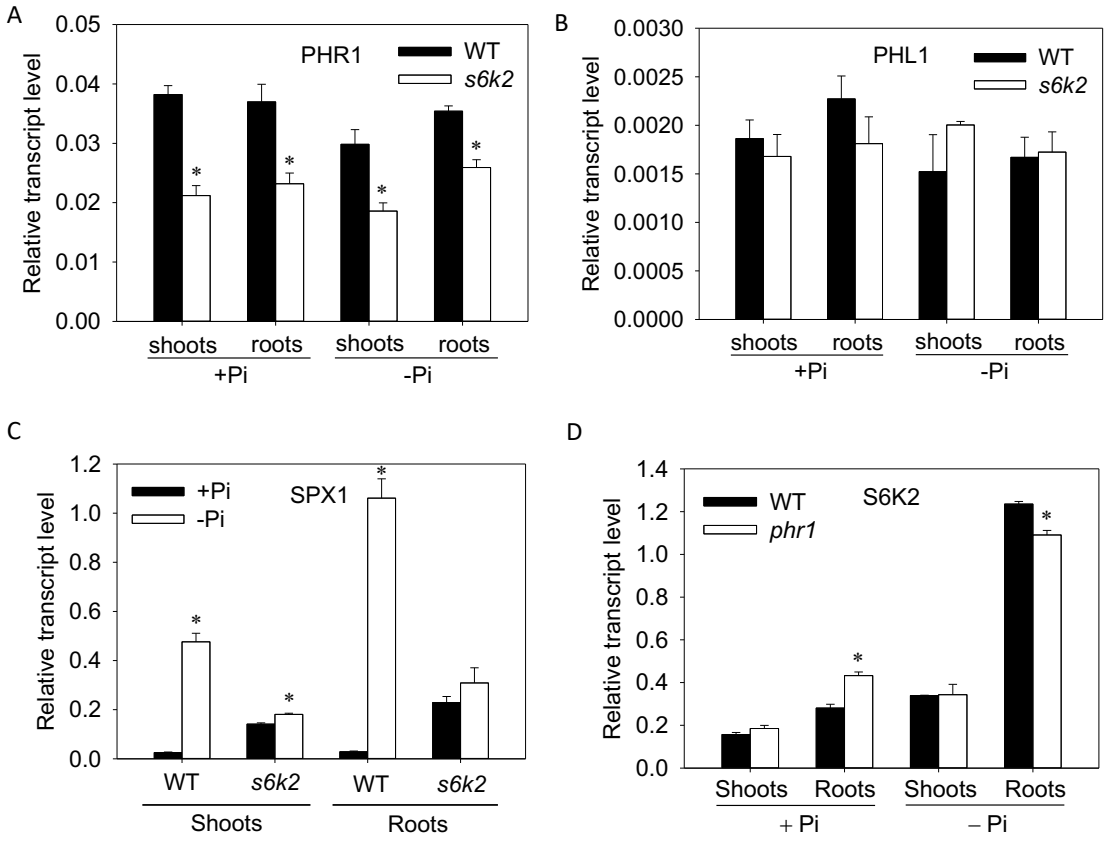

Figure 3-8 The effect of S6K2 and PHR1 on each other's transcription.

A. and B. The expression of *PHR1* and *PHR1* like gene (*PHL1*) in shoots and roots of WT and *s6k2* under indicated conditions. C. The expression of *SPX1* in shoots and roots of WT and *s6k2* under indicated conditions. D. The expression of *S6K2* in shoots and roots of WT and *phr1* under indicated conditions. Values are means ± SD (n = 3). Asterisks indicate significant difference between WT and mutants or between +Pi and –Pi conditions at $P < 0.05$ based on Student's t test.

without sufficient Pi (Figure 3-8B). In contrast, *S6K2* expression level was not altered in Pi replete shoots or roots, whereas S6K2 expression increased by ~35% in *phr1* Pi-replete roots and decreased ~10% in *phr1* Pi-starved roots (Figure 3-8C).

s6k2phr1 **double knockout mutant displayed similar growth phenotype and lipid remodeling as** ***s6k2*** **and** ***phr1*** **in response to Pi deprivation**

To further investigate the relationship between S6K2 and PHR1 genetically, double knockout (DKO) mutant *s6k2phr1* was generated. When grown in soil, no differences were observed between WT and mutants (Figure S3-6). The homozygous *s6k2phr1* DKO seedlings were then tested in the Pi sufficient and deficient media. Under Pi replete condition, WT seedlings displayed similar growth as single mutants and double mutant. No significant difference was observed on primary root length between WT and mutants. Under Pi starvation condition, all the mutants showed strongly retarded primary root growth compared with WT. However, double mutant did not have additive effect (Figure 3-9).

To further confirm the relationship between S6K2 and PHR1, lipid analysis was utilized to compare lipid composition between single mutants *s6k2*, *phr1* and double mutant *s6k2phr1*. Interestingly, *s6k2* and *phr1* responded to Pi deprivation in a very similar way, both inhibiting the lipid remodeling to a comparable extent. The *s6k2phr1* double mutant did not show additive lipid phenotype either, similar to the growth phenotype (Figure 3-10; Figure S3-7). The data suggest S6K2 and PHR1 may functions in the same molecular pathway to regulate growth response and lipid alterations to Pi limitation.

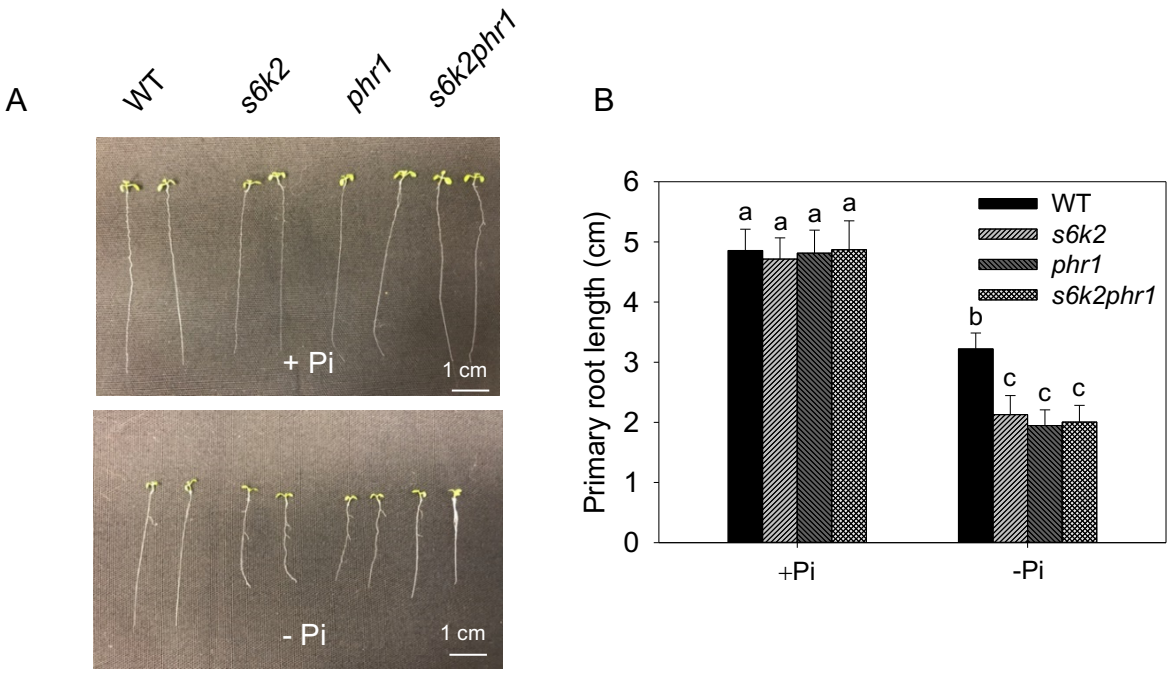

Figure 3-9 *s6k2phr1* showed no additive growth defect.

A. Growth phenotype of WT, *s6k2*, *phr1*, and *s6k2phr1* in response to different Pi concentrations. B. Primary root growth of WT, *s6k2*, *phr1*, and *s6k2phr1* in response to different Pi concentrations. Lower-case letters indicate the statistically significant ($P < 0.05$) differences between samples under +Pi and –Pi conditions by one way ANOVA analysis.

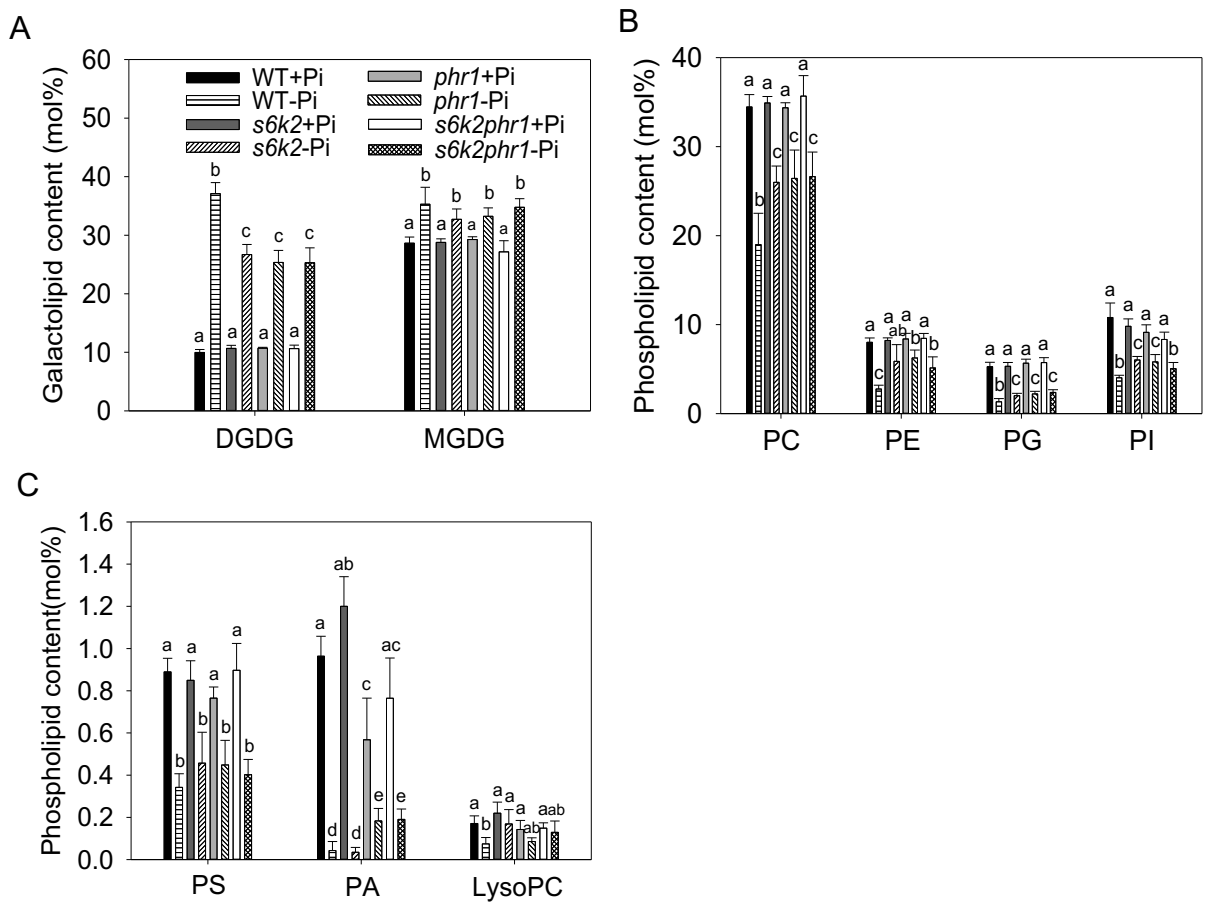

Figure 3-10 *s6k2phr1* had similar inhibited lipid remodeling as *s6k2* and *phr1* single mutants.

A. Galactolipid content in WT, *s6k2*, *phr1*, and *s6k2phr1* seedlings. B. Major phospholipid content in WT, *s6k2*, *phr1*, and *s6k2phr1* seedlings. C. Minor phospholipid content in WT, *s6k2*, *phr1*, and *s6k2phr1* seedlings. Values are means ± SD (n = 5). Lower-case letters indicate the statistically significant ($P < 0.05$) differences between genotypes under sufficient Pi or deficient Pi treatments by one way ANOVA analysis.

DISCUSSION

Although S6K in Arabidopsis is highly conserved to S6K in animals which closely regulates growth and development in response to nutrient signals, the understanding of S6K functions is poor in plant nutrient signaling. Also, due to similarities between S6K1 and S6K2, it is hard to find out distinct roles of S6K1 and S6K2. Our study unveils the unique role of S6K2 in regulating Arabidopsis response to Pi deprivation. Knockout of *S6K2* impaired the root system development and membrane lipid remodeling. Further, S6K2 affected expression pattern of Pi starvation responsive genes. In contrast, *S6K1* KO mutant did not display apparent phenotypes to Pi deprivation, suggesting two S6Ks may have specific functions in certain physiological processes. Discoveries in the study offer potential link between S6K2 and nutrient sensing and assimilation in plants.

S6K1 and S6K2 contain a conserved protein kinase domain and a AGC-kinase C-terminal domain. They share 86% amino acid sequence identities and mainly differ from each other at N-terminal sequences (first exon). The viability of *s6k1* and *s6k2* single KO mutants, but gametophytic leathyl of *s6k1s6k2* DKO suggests S6K1 and S6K2 have redundant functions that are essential for the plant survival (Henriques et al., 2010). On the other hand, the different cellular localizations of two S6Ks that S6K1 localizes in both cytosol and nucleus while S6K2 is mainly in nucleus, as well as the distinct gene expression patterns of S6Ks throughout various tissues and growth developmental stages may hint the unique functions of S6K1 and S6K2 due to spatial and temporal effects (Mahfouz et al., 2006; Figure S3-1). Indeed, in our study, S6K2 displayed its specific role in Pi starvation response. *S6K2* but not *S6K1* was induced by Pi

deprivation and alterations of *S6K2* exhibited different responses to Pi limitation compared with WT, whereas *s6k1* mutant and S6K1-OE did not (Figure S3-5). In contrast, neither S6K1 nor S6K2 responded to N deprivation (Figure S3-3). The results clearly demonstrate different duties of S6Ks in the specific pathway. What makes S6K2 different from S6K1 could be due to their promoters, their protein sequences especially at N-terminus, their interactions with regulatory proteins and their substrates. Further investigations are needed to figure out details of S6K1 and S6K2 mediated signaling pathways.

Some other S6K2 T-DNA insertion mutant lines were used to confirm the phenotype caused by S6K2 disruption. However, the lines tested other than Salk_026472 did not reveal growth retardation or inhibition of lipid remodeling under Pi deprivation. This includes Salk_128183, Salk_013334, and Salk_039937. Interestingly, I could not get homozygous seeds from lines Salk_083818, Salk_083821, Salk_083810 and Salk_083812, suggesting the homozygous of lines are lethal. These lines have the T-DNA insertions in the first exon and are the lines with closest insertion site to the line Salk_026472 (Figure S3-8). One of the lines Salk_083818 was embryo lethal and confirmed by another group (Xiong et al., 2017), suggesting the importance of the first exon of S6K2. The reason other S6K2 T-DNA insertion lines did not reveal the same Pi-responsive phenotype as Salk_026472 could be there is still expression of S6K2 first exon in those lines, which is critical for normal Pi-starvation adaption. Another possibility is that the line Salk_026472 creates a new truncated S6K2 mRNA and further truncated S6K2 protein that mediates Pi-starvation response.

In yeast and animals, TOR signaling pathway is tightly related to available nutrients and energy levels as the addition of amino acids or growth factors can activate TOR followed by the activation of S6K. The activation of TOR can enhance the translation of 5′ terminal oligopyrimidine motif containing mRNAs (5'TOP mRNAs). Most 5' TOP mRNAs encoded proteins involved in protein components of the translational machinery such as ribosomal proteins, translation elongation factors, translation initiation factors and poly (A) binding proteins (Meyuhas and Kahan, 2015). In yeast, nutrient starvation including carbon, nitrogen and phosphorus was reported to inhibit TOR complex 1 (TORC1) activity (Robaglia et al., 2012a). In animal cells, AMP-activated kinase (AMPK/SnRK1) repressed TOR pathway at multiple points to suppress translation in response to carbon/glucose limitation (Henriques et al., 2014).

In Arabidopsis, TOR was shown to be crucial for the metabolic activation of root meristems, and the inhibition of seedling growth by TOR inhibitor rapamycin seems to relay on the phosphorylation status of S6K. The activation of TOR activity was dependent on the exogenous sugar supply (Xiong and Sheen, 2012; Xiong et al., 2013). Here, I showed that *s6k2* mutant exhibited retarded root growth under Pi-deprived condition. Although no evidence has been reported to demonstrate that TOR pathway is involved in Pi signaling in plants, it is possible that S6K2 regulates root development of Pi-deprived seedlings through the TOR activation. On one hand, *s6k2* mutant seems sensitive to sucrose starvation and the inhibition of lipid remodeling in *s6k2* KO disappeared when sucrose was absence in the Pi deplete medium (data now shown). Also, sugar input has been indicated to be necessary for Pi signaling, whereas the

activity of TOR relies on the sugar (Karthikeyan et al., 2007; Xiong et al., 2013). Thus, to maintain normal function of S6K2 in Pi signaling may need the activation of TOR which is mediated by sugar signaling. On the other hand, more insights can be gained if TOR mutant such as TOR-RNAi or S6 mutants can be tested under Pi starvation. It will provide direct evidence whether S6K upstream regulator TOR or S6K downstream target is involved in Pi signaling as well. Further, the TOR inhibitor rapamycin can be applied to WT seedlings to observe if rapamycin-treated seedlings can mimic *s6k2* KO mutant on lipid change under Pi starvation. Besides, the phosphorylation residue of S6K2 by TOR is Thr-455. If phosphorylated S6K2 by TOR is required for the Pi signaling, the TOR phosphorylation site-mutated S6K2 version can be transformed into *s6k2* KO to test if the mutated S6K2 can rescue the phenotype. In addition, truncated S6K2 versions can be transformed into *s6k2* KO as well to determine the key domain(s) of S6K2 is necessary for the function in Pi starvation. The potential S6K2 substrates other than S6 or S6K2 regulators other than TOR are of interest to study as it will provide information on possible pathways S6K2 may be involved in.

PHR1 is a master transcription factor in Pi starvation responses, regulating a large bunch of Pi-responsive genes. Intriguingly, similar to *s6k2* mutant, *phr1* mutant displayed inhibited lipid remodeling and suppressed induction of lipid remodeling genes with Pi depletion (Pant et al., 2015). Thus, I generated *s6k2phr1* double mutant to test if double knockout has additive effect. By comparing *s6k2* and *phr1* single KO and double KO, all mutants showed similar growth and lipid phenotypes under Pi starvation, which indicates that S6K2 and PHR1 are likely in the same signaling pathway. One possibility

is that S6K2 perhaps post-translationally regulate PHR1, meaning S6K2 may phosphorylate and regulate PHR1's activity. S6K2 was indicated to mainly localize in the nucleus, providing an appropriate site for potential phosphorylation occurrence of PHR1. The experimental evidence will be needed. It is also likely that S6K2 regulates known PHR1 regulatory proteins such as SPX proteins. SPX1 and SPX2 that share the SPX domain with yeast Pi sensor proteins were reported to physically interact with PHR1 and therefore block the P1BS binding site of PHR1 in a Pi dependent manner. Unlike PHR1, SPX1 and SPX2 were inducible by Pi starvation (Puga et al., 2014). The induction of SPX1 expression was highly reduced in *s6k2* mutant (Figure 3-9). Also, If S6K2 can phosphorylate SPX1 or SPX2, the phosphorylation status of SPX1 and SPX2 might be critical for them to bind to PHR1. Another known PHR1 regulatory protein is SUMO E3 ligase SIZ1 that sumoylates PHR1. The effect of sumoylation of PHR1 is unclear, but the *siz1* KO mutant exhibited altered Pi deficiency responses (Miura et al., 2005). More information is needed to determine if S6K can interact with SIZ1.

It is interesting to observe that lipid remodeling was halt in *s6k2* KO under Pi deprivation. Under sever Pi starvation, galactolipid DGDG increased to about 2 folds, while phospholipids such as PC, PE, PI, PG, and PA decreased largely in WT seedlings. In contrast, such lipid alternation in adaption to Pi deprivation was almost abolished in *s6k2* KO. However, the PS level in *s6k2* KO decreased similarly to WT, suggesting the enzymes that prefer PS as the substrate may not be regulated by S6K2 in the lipid conversion process. Under moderate Pi starvation, the lipid composition was compared in shoots and roots. The lipid remodeling occurred in both shoots and roots,

and the mutation of S6K2 did not completely block but highly inhibited the lipid remodeling process (Figure 3-6). Notably, DGDG level in WT roots increased dramatically by Pi starvation as galactolipids mainly localize in plastids, and the increased DGDG in roots is considered to compensate for decreased phospholipids to maintain the integrity of extraplastidial membranes (Härtel et al., 2000). Also, it is likely that the reduced lipid remodeling in roots caused by *S6K2* mutation may contribute the failure of root architecture adaption to Pi starvation. Interestingly, a recent report showed that rice S6K1 was involved in thylakoid galactolipid biosynthesis by maintaining the stable abundance of some lipid related genes such as lipid phosphate phosphatase α5 (LPPα5), MGDG synthase 1 (MGD1), and DGDG synthase 1 (DGD1). The loss of S6K1 in rice lead to pale yellow-green leaves and damaged thylakoid grana architecture. Also, similar to that in Arabidopsis, OsS6K1 was tightly regulated by RAPTOR2 and TOR (Sun et al., 2016b). Such evidence suggests that TOR-S6K pathway regulate lipid metabolism in rice. However, how S6K2 regulates lipid remodeling as a protein kinase needs further investigation in Arabidopsis.

METHODS

Plant Materials and Growth Conditions

The ecotype of *Arabidopsis thaliana* used in this paper was Columbia-0. The seeds of T-DNA insertion mutants *s6k1* (Salk_112945) and *s6k2* (Salk_026472) were obtained from *Arabidopsis* Biological Resource Center (ABRC) in Ohio State University. The homozygous *s6k* single mutant was identified by PCR using one specific primer from T-DNA (LBa1) and one specific primer from *S6K*. The primer for T-DNA lest boarder is 5'-

TGGTTCACGTAGTGGGCCATCG-3', and the primer for *S6K1* and *S6K2* were 5'-TTTCAGGTGCCATATACTCCG-3' and 5'-TGTCCTTTTCCACGAACAATC-3', respectively. For *S6K1* and *S6K2* overexpression lines, the full length CDS of *S6K1* and *S6K2* were PCR amplified and cloned from Arabidopsis WT cDNA into binary vector p35S-FAST (35S promoter, N-GFP) using restriction enzyme sites PacI and SalI. All the constructs were confirmed by sequencing and later introduced into Agrobacterium strain C58C1. The *s6k2* mutant and WT Arabidopsis plants were used for transformation by floral dip method to generate *S6K2* complementation lines and *S6K* overexpression lines, respectively (Clough and Bent, 1998). *S6K* overexpression plants were confirmed by western blot using anti-GFP antibodies (Sigma G1544).

For plants grown in soil, seeds were sowed and germinated in a plastic pot under long day condition (16 h light 22°C/8 h dark 18°C) in a growth chamber with 70% relative humidity and ~170 μmol m^{-2} s^{-1} fluorescent light intensity. For phosphate starvation treatment, seedlings were either grown in plates vertically under long day condition or in liquid medium with mild agitation under continuous light. Plant nutrient medium (PNS) was modified to adjust the Pi concentrations. The PNS medium contained 2.5 mM KH_2PO_4, 5 mM KNO_3, 2 mM $MgSO_4$, 2 mM $Ca(NO_3)$, micronutrient solution (Sigma M0529), and 0.5% sucrose. The modified PNS had indicated concentration (1 mM, 0.1 mM, 0.01 mM and 0 mM) of KH_2PO_4 as Pi source and the resulting lack of K will be supplemented with proper amount of 1 mM KCl. 0.8% agar (Sigma A8678) was added to make solid medium in plates. The PH of PNS was adjusted to PH 5.7. *Arabidopsis* seeds were surface sterilized by 70% (v/v) ethanol for 1 minute and then 30% bleach for 7 minutes. The seeds were washed 5 times by sterilized water and subject to 4°C for 2

days before sowed into agar plates or liquid medium. Seeds were germinated and grown in agar plates for indicated days. For liquid culture, seedlings were first grown in Pi sufficient (1 mM Pi) medium for 5-6 days and then transferred into Pi sufficient or Pi starvation (0 mM Pi) medium for indicated days, otherwise specified in the experiments. The liquid medium was replaced with fresh medium every 2-3 days.

RNA extraction and qRT-PCR analysis

RNA extraction and qRT-PCR analysis of gene expression were previously described (Li et al., 2011). Total RNAs were extracted form leaves or roots using a RNeasy Plant Mini Kit (Qiagen 74904) and were followed by DNase treatment using a RNase-free DNase set (Qiagen 79254). Then 1 ug RNAs were reverse transcribed into cDNAs using a qScript cDNA Synthesis Kit (Quanta 95047) according to the user's manual.
SYBR green fluorescent dye was applied in each PCR reaction and the samples were loaded into the MyiQ real-time PCR detection system (Bio-Rad)**.** The concentrations of samples were normalized based on the expression of internal control *Ubiquitin 10* (*UBQ10*). Expression levels of target genes were normalized to *UBQ10*. The qRT-PCR program was as follows: one cycle of 95°C for 3 min; 40 cycles of 95°C for 30 s, 56°C for 30 s, 72°C for 30 s; and final extension at 72°C for 10 min, followed by melting curve analysis. All the primers used were listed in the supplemental table 1.

Protein extraction and western blot

3-week old Arabidopsis leaves were collected and grounded in liquid nitrogen to extract crude protein. The total protein was then loaded into SDS-PAGE gel and followed by

western blot using anti-GFP antibodies (Sigma G1544).

Membrane lipid analysis

The lipids were extracted from fresh leaves or roots and analyzed by electrospray ionization–tandem mass spectrometry (ESI-MS/MS) as described previously (Welti et al., 2002). Briefly, the leave or root materials were collected and put into hot isopropanol (75°C) with 0.01% BHT (butylated hydroxytoluene) immediately for 15 minutes to inhibit phospholipase D activity. Then, the lipids were extracted five times by chloroform/methanol (2:1 v/v), followed by one-time wash by 1 M KCL and water, respectively. The lipids were dried under nitrogen gas and diluted appropriately based on the dry weight of materials with chloroform later on. The samples were loaded to ESI-MS/MS (API 4000) to detect phospholipids and galactolipids with certain internal standards. The final lipid profiling data was analyzed by software Analyst 1.5.1.

Root length measure

For primary root length measurement, the root tips of seedlings grown on the plates vertically were marked daily. At the end of the experiments, plates were scanned and the root length was measured by image J (http://imagej.nih.gov/ij/) or rulers.

Accession Numbers

Sequence data from this article can be found in the *Arabidopsis* Genome Initiative or GenBank/EMBL databases under the following accession numbers: *S6K1* (At3g08730);

S6K2 (At3g08720); *UBQ10* (At4g05320); *PLDζ1* (At3g16785); *PLDζ2* (At3g05630); *MGD2* (At5g20410); *MGD3* (At2g11810); *DGD1* (At3g11670); *DGD2* (At4g00550); *NPC4* (At3g03530); *NPC5* (At3g03540); *PHO1* (At3g23430); *PHO2* (At2g33770); *PHR1* (At4g28610); *PHL1* (At5g29000); *MYB62* (At1g68320); *WRKY75* (At5g13080); *ZAT6* (At5g04340); *BHLH32* (At3g25710); *PAH1* (At3g09560); *PAH2* (At5g42870).

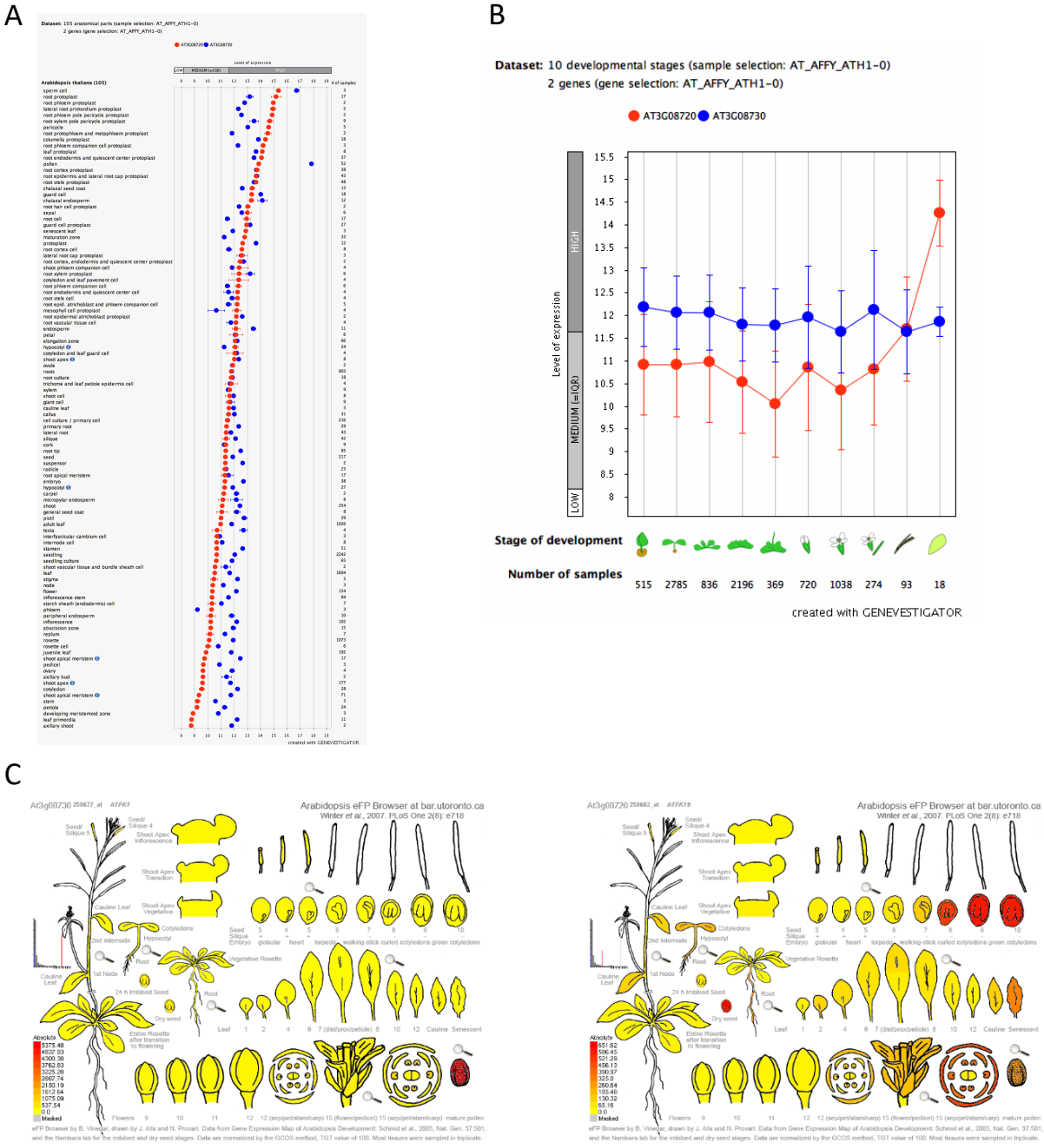

Figure S3-1. Expression pattern of *S6K1* and *S6K2* in Arabidopsis.

A. *Arabidopsis* anatomy map of *S6K* expression from genevestigator. B. *S6K* expression at different developmental stages of *Arabidopsis* from genevestigator. C. *S6K* expression pattern from *Arabidopsis* eFP browser.

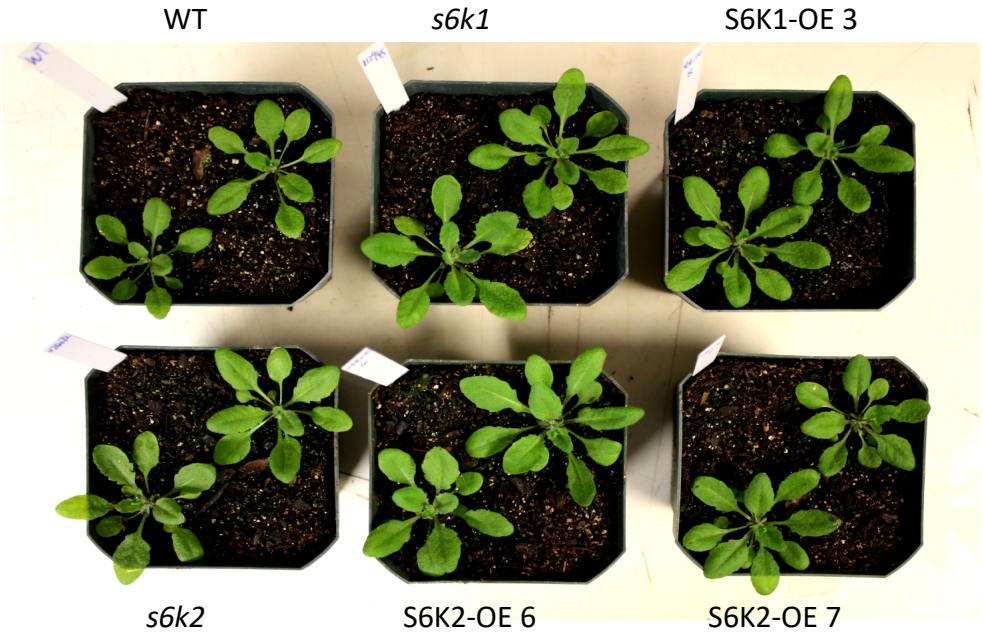

Figure S3-2. Growth phenotype of 3-week WT, *s6k* mutant and S6K-OE seedlings in soil.

WT, *s6k1*, *s6k2*, S6K1-OE and S6K2-OE seeds were germinated in soil. The 5-day old seedlings were transferred into individual plastic plots. The seedlings were well watered and supplied with sufficient nutrients.

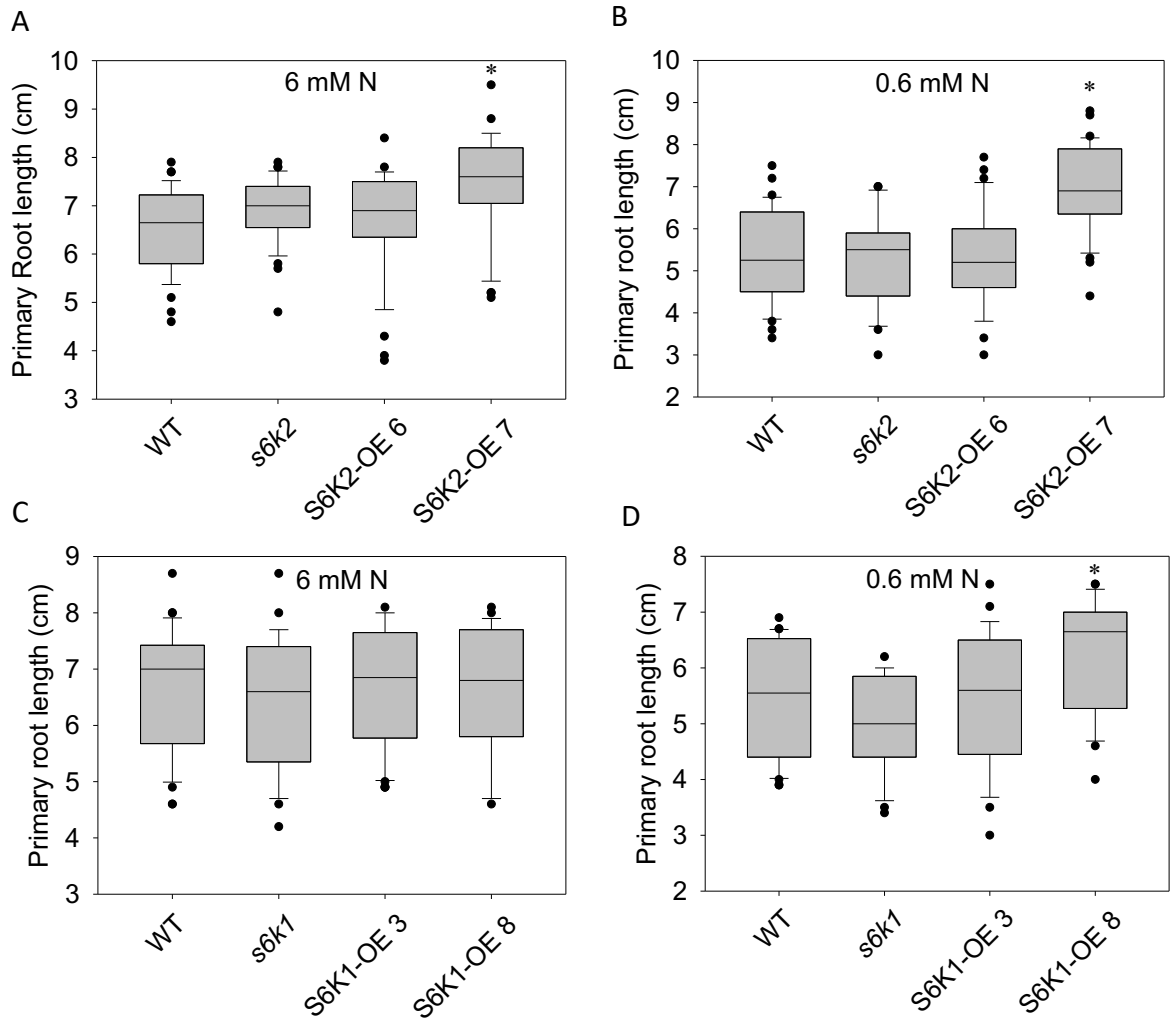

Figure S3-3. Primary root growth of WT, *s6ks* and S6K-OE seedlings in response to different N concentrations.

The primary root length of WT, *s6k* and S6K-OE seedlings grown on ½ MS plates with 6 mM N (A and C) or 0.6 mM N (B and D) for 10 days. Values are means ± SD (n ≥ 20). Asterisks indicate significant difference between WT and mutants at $P < 0.05$ based on Student's t test.

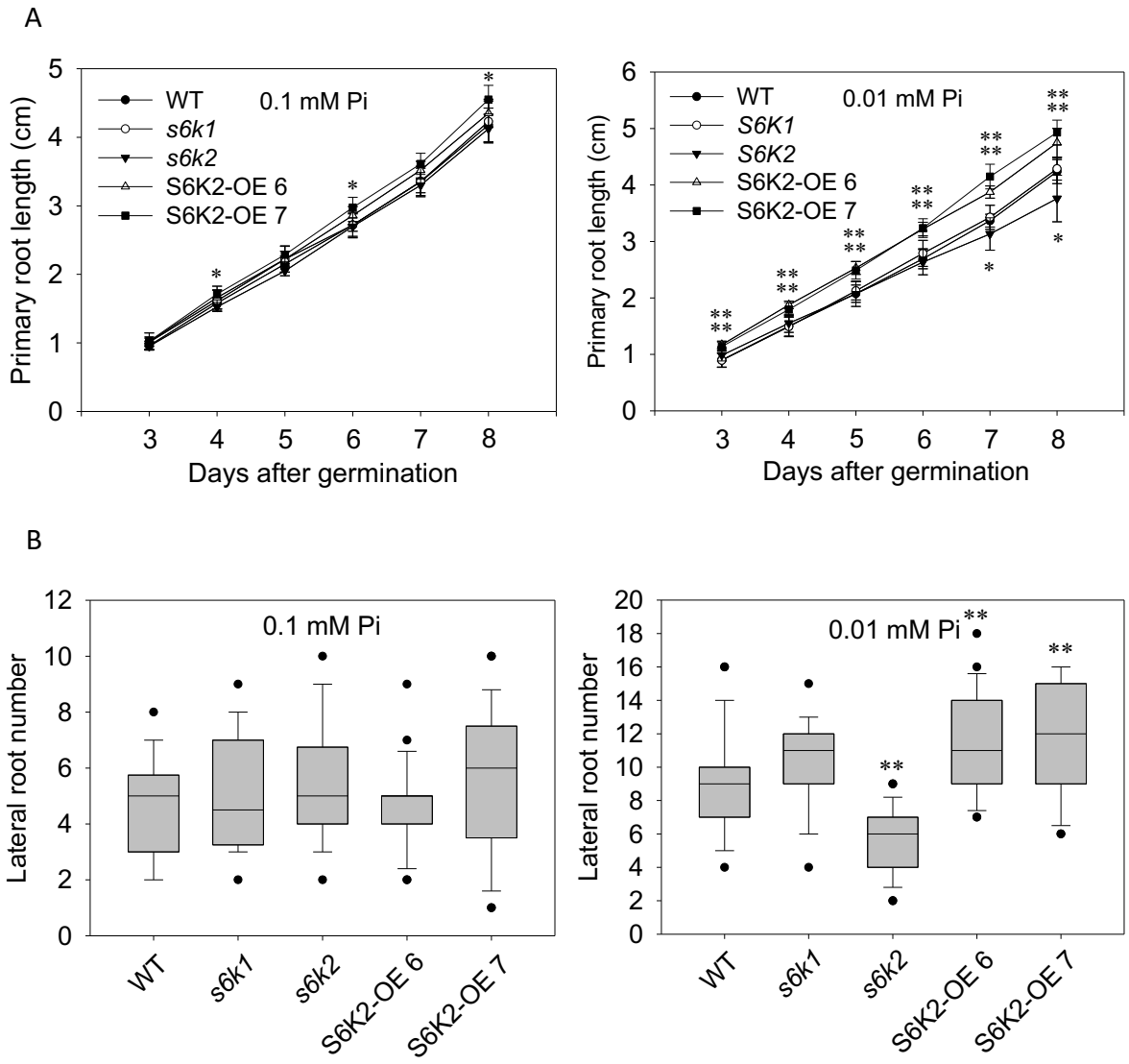

Figure S3-4. Phenotype of primary roots and later roots of WT, *s6k* and S6K-OE at 0.1 mM Pi and 0.01 mM Pi growth condition.

A. The primary root length of WT, *s6k1*, *s6k2*, S6K1-OE and S6K2-OE seedlings over 8 days. B. Later root number of seedlings at day 9 after germination. Values are means ± SD (n >= 20). Asterisks indicate significant difference between WT and mutants at P < 0.05 based on Student's t test.

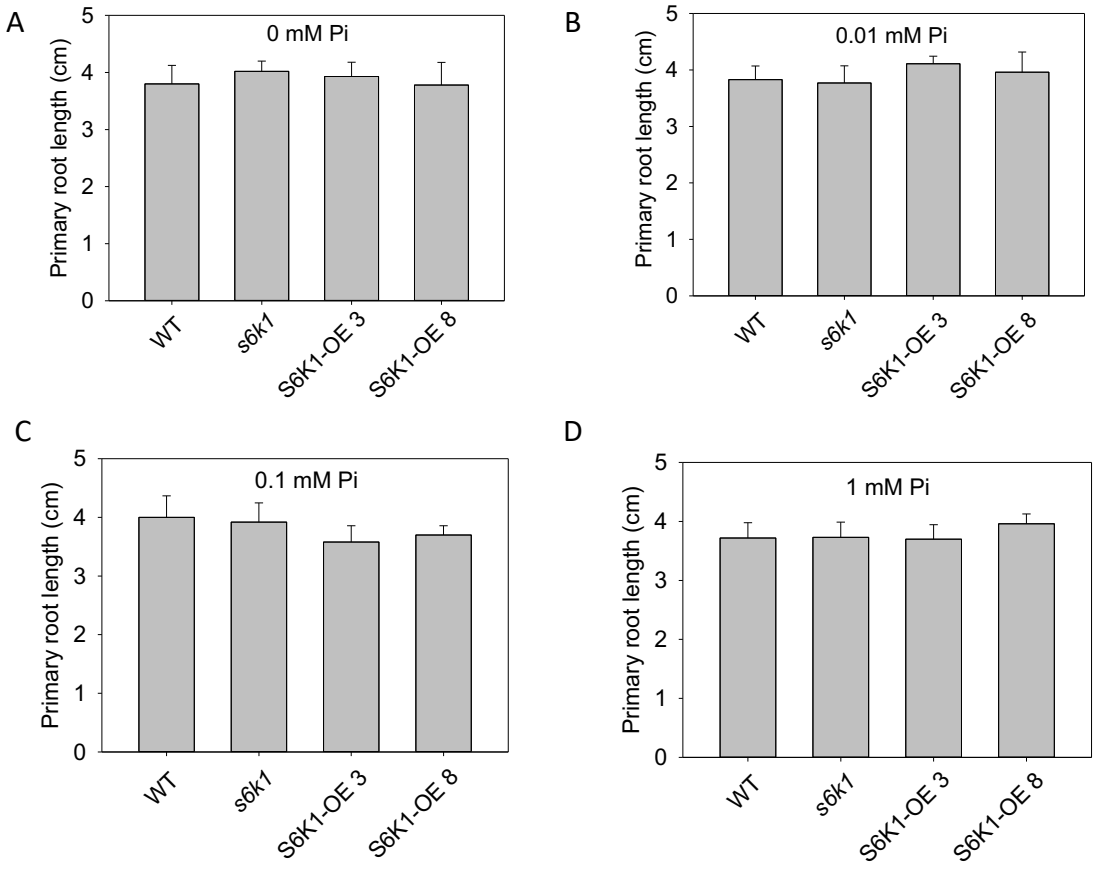

Fig. S3-5. *s6k1* knockout did not show growth difference from WT under various Pi deficient treatments.

The primary root length was measured at day 8 after germination under 0 mM (A), 0.01 mM (B), 0.1 mM (C) and 1 mM (D) Pi conditions. Values are means ± SD (n >= 10). Asterisks mark differences between the wild type and mutant at $P < 0.05$ based on Student's t test.

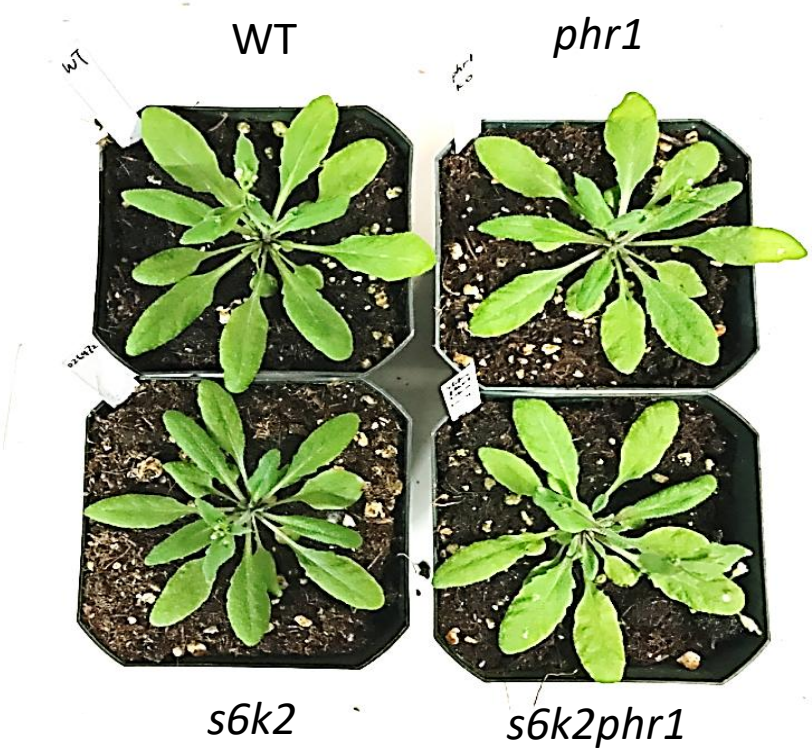

Figure S3-6. Growth phenotype of 4-week WT, *s6k2*, *phr1* and *s6k2phr1* seedlings in soil.

WT, *s6k2* and *s6k2phr1* seeds were first germinated in soil. The 5-day old seedlings were then transferred into individual plastic plots. The seedlings were well watered and supplied with sufficient nutrients.

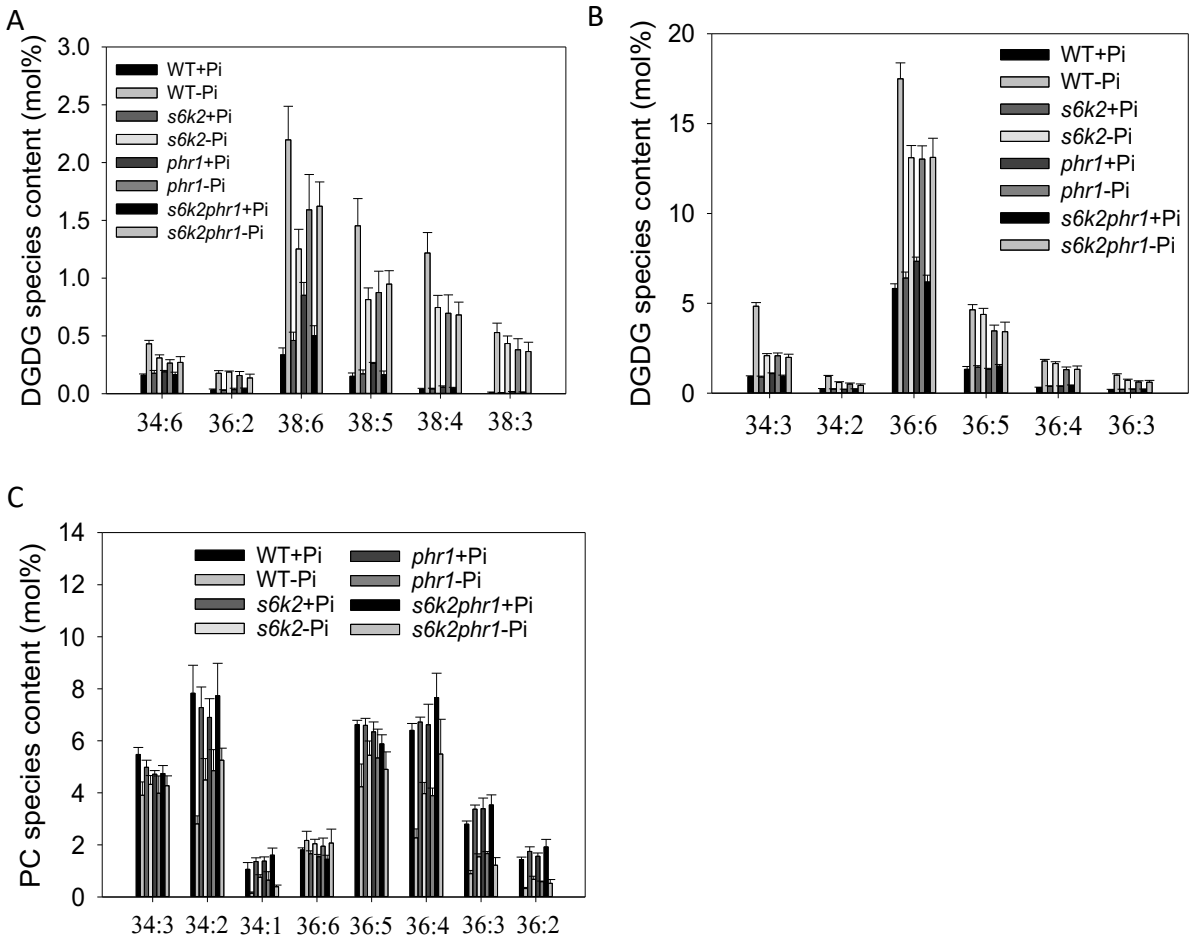

Figure S3-7. The lipid molecular species in WT, *s6k2*, *phr1*, and *s6k2phr1* seedlings.

A. Major DGDG molecular species content. B. Minor DGDG molecular species content. C. PC molecular species content. D. PE molecular species content. Values are means ± SD (n = 5).

Figure S3-8 Isolation of other *S6K2* T-DNA insertion lines.

Multiple additional T-DNA insertion lines in *S6K2* were obtained besides salk_026472.

Table S3-1. Primers used for quantitative real time PCR.

Gene ID	Gene name	Forward primer	Reverse primer
At5g20410	MGD2	AACATGTCTCCCTTAGTAGTTCTTTTGTC	GTTGATATTGTTAATGGCTAACAATAATGC
At2g11810	MGD3	GGATATCCATCATCTATCCCAACAA	GATAAAAGAATGACAAACCACTAGAGAATATAC
At3g11670	DGD1	GTGTGGGCTAAAGGATACAGAG	CATCTTCACCGTTCCCATATACA
At4g00550	DGD2	GTCTGGAGCAAAGGGTACAA	AGTCCTCTCCATCACCGTATAA
At3g03530	NPC4	TGCACAATTAAGCGAATTTCAA	TTCTTCGTTTTTGTAGTCTCCTTTT
At3g03540	NPC5	ATTACGAGAAACTCACCAAGACAA	CATTTTGACCGGATTTGACA
At3g16785	PLDζ1	TGGATGGCAACCGCAAAGACAA	ATCGTTGTGTGTCCCAGCTTCT
At3g05630	PLDζ2	TTTGAGGACGGTCCAATTGCCA	ACAACACCGATCTCAGAGTCTCGT
AT3G09560	PAH1	CTGTTGAGCATACGGGAAGTAA	CGACTCTCTGTGGTTGATTGT
AT5G42870	PAH2	GGATGCAGCAGCTCCTATTAT	TCATTCCGGTCAACAGCTATC
At3g08730	S6K1	TGATGCCAAGTTTCAAGCCGGAAGTATC	CATGTGTCAGAAGGAAACAACAACCAAAG
At3g08720	S6K2	TACAACCAAGTTTCAAGCCGGCGGTTT	ACCGTTGATTTTGTGCATGTTCATATG
At4g28610	PHR1	ATATCGGCCAGAACCATCAGAAAC	TGTAATACCTATCCCACCTTTCAAATC
AT5G29000	PHL1	CGACCGCTATGTCTTCATCTTAT	CTGACACGGTACAGGGTTATTC
At4g05320	UBQ10	TCACCGGAAAGACCATCACT	CGGTGGGATACCCTCTTTG

REFERENCES

Anderson, G.H., Veit, B., and Hanson, M.R. (2005). The Arabidopsis AtRaptor genes are essential for post-embryonic plant growth. BMC Biology 3, 1-11.

Awai, K., Maréchal, E., Block, M.A., Brun, D., Masuda, T., Shimada, H., Takamiya, K.-i., Ohta, H., and Joyard, J. (2001). Two types of MGDG synthase genes, found widely in both 16:3 and 18:3 plants, differentially mediate galactolipid syntheses in photosynthetic and nonphotosynthetic tissues in Arabidopsis thaliana. Proceedings of the National Academy of Sciences of the United States of America 98, 10960-10965.

Bates, P.D., and Browse, J. (2012). The Significance of Different Diacylgycerol Synthesis Pathways on Plant Oil Composition and Bioengineering. Frontiers in Plant Science 3, 147.

Bögre, L. (2003). Growth signalling pathways in Arabidopsis and the AGC protein kinases. Trends in Plant Science 8, 424-431.

Briat, J.F., Rouached, H., Tissot, N., Gaymard, F., and Dubos, C. (2015). Integration of P, S, Fe, and Zn nutrition signals in Arabidopsis thaliana: potential involvement of PHOSPHATE STARVATION RESPONSE 1 (PHR1). Front Plant Sci 6, 290.

Bustos, R., Castrillo, G., Linhares, F., Puga, M.I., Rubio, V., Perez-Perez, J., Solano, R., Leyva, A., and Paz-Ares, J. (2010). A central regulatory system largely controls transcriptional activation and repression responses to phosphate starvation in Arabidopsis. PLoS Genet 6, e1001102.

Clough, S.J., and Bent, A.F. (1998). Floral dip: a simplified method for Agrobacterium-mediated transformation of Arabidopsis thaliana. Plant Journal 16, 735-743.

Creff, A., Sormani, R., and Desnos, T. (2010). The two Arabidopsis RPS6 genes, encoding for cytoplasmic ribosomal proteins S6, are functionally equivalent. Plant Molecular Biology 73, 533-546.

Cruz-Ramirez, A., Oropeza-Aburto, A., Razo-Hernandez, F., Ramirez-Chavez, E., and Herrera-Estrella, L. (2006). Phospholipase DZ2 plays an important role in extraplastidic galactolipid biosynthesis and phosphate recycling in Arabidopsis roots. Proc Natl Acad Sci U S A 103, 6765-6770.

Deprost, D., Truong, H.-N., Robaglia, C., and Meyer, C. (2005). An Arabidopsis homolog of RAPTOR/KOG1 is essential for early embryo development. Biochemical and Biophysical Research Communications 326, 844-850.

Dörmann, P., and Benning, C. (2002). Galactolipids rule in seed plants. Trends in Plant Science 7, 112-118.

Gaude, N., Nakamura, Y., Scheible, W.R., Ohta, H., and Dormann, P. (2008). Phospholipase C5 (NPC5) is involved in galactolipid accumulation during phosphate limitation in leaves of Arabidopsis. Plant J 56, 28-39.

Härtel, H., Dörmann, P., and Benning, C. (2000). DGD1-independent biosynthesis of extraplastidic galactolipids after phosphate deprivation in Arabidopsis. Proceedings of the National Academy of Sciences of the United States of America 97, 10649-10654.

Henriques, R., Bogre, L., Horvath, B., and Magyar, Z. (2014). Balancing act: matching growth with environment by the TOR signalling pathway. J Exp Bot 65, 2691-2701.

Henriques, R., Magyar, Z., Monardes, A., Khan, S., Zalejski, C., Orellana, J., Szabados, L., de la Torre, C., Koncz, C., and Bögre, L. (2010). Arabidopsis S6 kinase mutants display chromosome instability and altered RBR1–E2F pathway activity. The EMBO Journal 29, 2979-2993.

Jacinto, E., and Lorberg, A. (2008). TOR regulation of AGC kinases in yeast and mammals. Biochemical Journal 410, 19-37.

Jain, A., Nagarajan, V.K., and Raghothama, K.G. (2012). Transcriptional regulation of phosphate acquisition by higher plants. Cell Mol Life Sci 69, 3207-3224.

Karthikeyan, A.S., Varadarajan, D.K., Jain, A., Held, M.A., Carpita, N.C., and Raghothama, K.G. (2007). Phosphate starvation responses are mediated by sugar signaling in Arabidopsis. Planta 225, 907-918.

Kelly, A.A., and Dörmann, P. (2002). DGD2, an Arabidopsis Gene Encoding a UDP-Galactose-dependent Digalactosyldiacylglycerol Synthase Is Expressed during Growth under Phosphate-limiting Conditions. Journal of Biological Chemistry 277, 1166-1173.

Kelly, A.A., Froehlich, J.E., and Dörmann, P. (2003). Disruption of the Two Digalactosyldiacylglycerol Synthase Genes DGD1 and DGD2 in Arabidopsis Reveals the Existence of an Additional Enzyme of Galactolipid Synthesis. The Plant Cell 15, 2694-2706.

Kobayashi, K., Awai, K., Nakamura, M., Nagatani, A., Masuda, T., and Ohta, H. (2009). Type-B monogalactosyldiacylglycerol synthases are involved in phosphate starvation-induced lipid remodeling, and are crucial for low-phosphate adaptation. Plant J 57, 322-331.

Lapis-Gaza, H.R., Jost, R., and Finnegan, P.M. (2014). Arabidopsis PHOSPHATE TRANSPORTER1 genes PHT1;8 and PHT1;9 are involved in root-to-shoot translocation of orthophosphate. BMC Plant Biology 14, 334.

Li, M., Welti, R., and Wang, X. (2006). Quantitative profiling of Arabidopsis polar glycerolipids in response to phosphorus starvation. Roles of phospholipases D zeta1

and D zeta2 in phosphatidylcholine hydrolysis and digalactosyldiacylglycerol accumulation in phosphorus-starved plants. Plant Physiol 142, 750-761.

Li, M., Bahn, S.C., Guo, L., Musgrave, W., Berg, H., Welti, R., and Wang, X. (2011). Patatin-Related Phospholipase pPLAIIIβ-Induced Changes in Lipid Metabolism Alter Cellulose Content and Cell Elongation in Arabidopsis. The Plant Cell 23, 1107-1123.

Lopez-Bucio, J., Hernandez-Abreu, E., Sanchez-Calderon, L., Nieto-Jacobo, M.F., Simpson, J., and Herrera-Estrella, L. (2002). Phosphate availability alters architecture and causes changes in hormone sensitivity in the Arabidopsis root system. Plant Physiol 129, 244-256.

Mahfouz, M.M., Kim, S., Delauney, A.J., and Verma, D.P. (2006). Arabidopsis TARGET OF RAPAMYCIN interacts with RAPTOR, which regulates the activity of S6 kinase in response to osmotic stress signals. Plant Cell 18, 477-490.

Meyuhas, O., and Kahan, T. (2015). The race to decipher the top secrets of TOP mRNAs. Biochim Biophys Acta 1849, 801-811.

Misson, J., Thibaud, M.-C., Bechtold, N., Raghothama, K., and Nussaume, L. (2004). Transcriptional regulation and functional properties of Arabidopsis Pht1;4, a high affinity transporter contributing greatly to phosphate uptake in phosphate deprived plants. Plant Molecular Biology 55, 727-741.

Misson, J., Raghothama, K.G., Jain, A., Jouhet, J., Block, M.A., Bligny, R., Ortet, P., Creff, A., Somerville, S., Rolland, N., Doumas, P., Nacry, P., Herrerra-Estrella, L., Nussaume, L., and Thibaud, M.C. (2005). A genome-wide transcriptional analysis using Arabidopsis thaliana Affymetrix gene chips determined plant responses to phosphate deprivation. Proc Natl Acad Sci U S A 102, 11934-11939.

Miura, K., Rus, A., Sharkhuu, A., Yokoi, S., Karthikeyan, A.S., Raghothama, K.G., Baek, D., Koo, Y.D., Jin, J.B., Bressan, R.A., Yun, D.-J., and Hasegawa, P.M. (2005). The Arabidopsis SUMO E3 ligase SIZ1 controls phosphate deficiency responses. Proceedings of the National Academy of Sciences of the United States of America 102, 7760-7765.

Mizoguchi, T., Hayashida, N., Yamaguchi-Shinozaki, K., Kamada, H., and Shinozaki, K. (1995). Two genes that encode ribosomal-protein S6 kinase homologs are induced by cold or salinity stress in Arabidopsis thaliana. FEBS Letters 358, 199-204.

Moreau, M., Azzopardi, M., Clement, G., Dobrenel, T., Marchive, C., Renne, C., Martin-Magniette, M.L., Taconnat, L., Renou, J.P., Robaglia, C., and Meyer, C. (2012). Mutations in the Arabidopsis homolog of LST8/GbetaL, a partner of the target of Rapamycin kinase, impair plant growth, flowering, and metabolic adaptation to long days. Plant Cell 24, 463-481.

Müller, R., Morant, M., Jarmer, H., Nilsson, L., and Nielsen, T.H. (2007). Genome-Wide Analysis of the Arabidopsis Leaf Transcriptome Reveals Interaction of Phosphate and Sugar Metabolism. Plant Physiology 143, 156-171.

Nakamura, Y. (2013). Phosphate starvation and membrane lipid remodeling in seed plants. Prog Lipid Res 52, 43-50.

Nakamura, Y., Awai, K., Masuda, T., Yoshioka, Y., Takamiya, K., and Ohta, H. (2005). A novel phosphatidylcholine-hydrolyzing phospholipase C induced by phosphate starvation in Arabidopsis. J Biol Chem 280, 7469-7476.

Nakamura, Y., Koizumi, R., Shui, G., Shimojima, M., Wenk, M.R., Ito, T., and Ohta, H. (2009). Arabidopsis lipins mediate eukaryotic pathway of lipid metabolism and cope critically with phosphate starvation. Proc Natl Acad Sci U S A 106, 20978-20983.

Otterhag, L., Gustavsson, N., Alsterfjord, M., Pical, C., Lehrach, H., Gobom, J., and Sommarin, M. (2006). Arabidopsis PDK1: identification of sites important for activity and downstream phosphorylation of S6 kinase. Biochimie 88, 11-21.

Pant, B.D., Burgos, A., Pant, P., Cuadros-Inostroza, A., Willmitzer, L., and Scheible, W.R. (2015). The transcription factor PHR1 regulates lipid remodeling and triacylglycerol accumulation in Arabidopsis thaliana during phosphorus starvation. J Exp Bot 66, 1907-1918.

Perez-Torres, C.A., Lopez-Bucio, J., Cruz-Ramirez, A., Ibarra-Laclette, E., Dharmasiri, S., Estelle, M., and Herrera-Estrella, L. (2008). Phosphate Availability Alters Lateral Root Development in Arabidopsis by Modulating Auxin Sensitivity via a Mechanism Involving the TIR1 Auxin Receptor. The Plant Cell Online 20, 3258-3272.

Poirier, Y., and Bucher, M. (2002). Phosphate transport and homeostasis in Arabidopsis. Arabidopsis Book 1, e0024.

Puga, M.I., Mateos, I., Charukesi, R., Wang, Z., Franco-Zorrilla, J.M., de Lorenzo, L., Irigoyen, M.L., Masiero, S., Bustos, R., Rodriguez, J., Leyva, A., Rubio, V., Sommer, H., and Paz-Ares, J. (2014). SPX1 is a phosphate-dependent inhibitor of Phosphate Starvation Response 1 in Arabidopsis. Proc Natl Acad Sci U S A 111, 14947-14952.

Raghothama, K.G. (1999). PHOSPHATE ACQUISITION. Annual Review of Plant Physiology and Plant Molecular Biology 50, 665-693.

Ren, M., Qiu, S., Venglat, P., Xiang, D., Feng, L., Selvaraj, G., and Datla, R. (2011). Target of rapamycin regulates development and ribosomal RNA expression through kinase domain in Arabidopsis. Plant Physiol 155, 1367-1382.

Ren, M., Venglat, P., Qiu, S., Feng, L., Cao, Y., Wang, E., Xiang, D., Wang, J., Alexander, D., Chalivendra, S., Logan, D., Mattoo, A., Selvaraj, G., and Datla, R. (2012).

Target of rapamycin signaling regulates metabolism, growth, and life span in Arabidopsis. Plant Cell 24, 4850-4874.

Robaglia, C., Thomas, M., and Meyer, C. (2012a). Sensing nutrient and energy status by SnRK1 and TOR kinases. Current Opinion in Plant Biology 15, 301-307.

Robaglia, C., Thomas, M., and Meyer, C. (2012b). Sensing nutrient and energy status by SnRK1 and TOR kinases. Curr Opin Plant Biol 15, 301-307.

Rubio, V., Linhares, F., Solano, R., Martín, A.C., Iglesias, J., Leyva, A., and Paz-Ares, J. (2001). A conserved MYB transcription factor involved in phosphate starvation signaling both in vascular plants and in unicellular algae. Genes & Development 15, 2122-2133.

Ruvinsky, I., and Meyuhas, O. (2006). Ribosomal protein S6 phosphorylation: from protein synthesis to cell size. Trends in Biochemical Sciences 31, 342-348.

Schepetilnikov, M., Dimitrova, M., Mancera-Martinez, E., Geldreich, A., Keller, M., and Ryabova, L.A. (2013). TOR and S6K1 promote translation reinitiation of uORF-containing mRNAs via phosphorylation of eIF3h. EMBO J 32, 1087-1102.

Schepetilnikov, M., Kobayashi, K., Geldreich, A., Caranta, C., Robaglia, C., Keller, M., and Ryabova, L.A. (2011). Viral factor TAV recruits TOR/S6K1 signalling to activate reinitiation after long ORF translation. EMBO J 30, 1343-1356.

Shimojima, M., and Ohta, H. (2011). Critical regulation of galactolipid synthesis controls membrane differentiation and remodeling in distinct plant organs and following environmental changes. Prog Lipid Res 50, 258-266.

Stolovich, M., Tang, H., Hornstein, E., Levy, G., Cohen, R., Bae, S.S., Birnbaum, M.J., and Meyuhas, O. (2002). Transduction of Growth or Mitogenic Signals into Translational Activation of TOP mRNAs Is Fully Reliant on the Phosphatidylinositol 3-Kinase-Mediated Pathway but Requires neither S6K1 nor rpS6 Phosphorylation. Molecular and Cellular Biology 22, 8101-8113.

Sun, L., Song, L., Zhang, Y., Zheng, Z., and Liu, D. (2016a). Arabidopsis PHL2 and PHR1 Act Redundantly as the Key Components of the Central Regulatory System Controlling Transcriptional Responses to Phosphate Starvation. Plant Physiol 170, 499-514.

Sun, L., Yu, Y., Hu, W., Min, Q., Kang, H., Li, Y., Hong, Y., Wang, X., and Hong, Y. (2016b). Ribosomal protein S6 kinase1 coordinates with TOR-Raptor2 to regulate thylakoid membrane biosynthesis in rice. Biochimica et Biophysica Acta (BBA) - Molecular and Cell Biology of Lipids 1861, 639-649.

Turck, F., Zilbermann, F., Kozma, S.C., Thomas, G., and Nagy, F. (2004). Phytohormones participate in an S6 kinase signal transduction pathway in Arabidopsis.

Plant Physiol 134, 1527-1535.

Wang, X., Devaiah, S.P., Zhang, W., and Welti, R. (2006). Signaling functions of phosphatidic acid. Progress in Lipid Research 45, 250-278.

Wang, Z., Ruan, W., Shi, J., Zhang, L., Xiang, D., Yang, C., Li, C., Wu, Z., Liu, Y., Yu, Y., Shou, H., Mo, X., Mao, C., and Wu, P. (2014). Rice SPX1 and SPX2 inhibit phosphate starvation responses through interacting with PHR2 in a phosphate-dependent manner. Proc Natl Acad Sci U S A 111, 14953-14958.

Welti, R., Li, W., Li, M., Sang, Y., Biesiada, H., Zhou, H.-E., Rajashekar, C.B., Williams, T.D., and Wang, X. (2002). Profiling Membrane Lipids in Plant Stress Responses: ROLE OF PHOSPHOLIPASE Dα IN FREEZING-INDUCED LIPID CHANGES IN ARABIDOPSIS. Journal of Biological Chemistry 277, 31994-32002.

Xiong, F., Zhang, R., Meng, Z., Deng, K., Que, Y., Zhuo, F., Feng, L., Guo, S., Datla, R., and Ren, M. (2017). Brassinosteriod Insensitive 2 (BIN2) acts as a downstream effector of the Target of Rapamycin (TOR) signaling pathway to regulate photoautotrophic growth in Arabidopsis. New Phytologist 213, 233-249.

Xiong, Y., and Sheen, J. (2012). Rapamycin and glucose-target of rapamycin (TOR) protein signaling in plants. J Biol Chem 287, 2836-2842.

Xiong, Y., McCormack, M., Li, L., Hall, Q., Xiang, C., and Sheen, J. (2013). Glc-TOR signalling leads transcriptome reprogramming and meristem activation. Nature 496, 181-186.

Chapter 4 S6 kinase binds to phosphatidic acid and affects seed oil content in Arabidopsis

SUMMARY

Phosphatidic Acid (PA) is a second signaling messenger involved in abiotic stress responses, cell growth and proliferation, and other physiological processes in diverse eukaryotes. However, little is known about how PA affects cell growth and its direct targets in plants. The 40S ribosomal protein S6 kinase (S6K) is the downstream target of Target of Rapamycin (TOR) and the TOR-S6K pathway is a conserved signaling pathway controlling growth and nutrient sensing in eukaryotes. In this study, I showed that PA binds to S6K in vitro by lipid immunoblotting, liposome binding, and surface plasmon resonance (SPR). S6K2 but not S6K1 can undergo autophosphorylation, and the autophosphorylation -was not impacted by the presence of PA or other phospholipids. In addition to being a cellular mediator, PA is a central intermediate for the synthesis of glycerolipids, including seed oil triacylglycerol. RNAi suppression of S6Ks increased triacylglycerol content, whereas overexpression of S6K decreased oil content in seeds.

INTRODUCTION

Ribosomal S6 kinase (S6K) is a Ser/Thr protein kinase that phosphorylates a 40S ribosomal subunit protein S6 (Lehman et al., 2007). It is the downstream target of TARGET OF RAPAMYCIN (TOR) and a master regulator that controls the ribosome biogenesis and translation initiation (Henriques et al., 2010; Mahfouz et al., 2006). In animals, S6K integrates growth-stimulating inputs such as available nutrients, cellular energy status and growth factors, through TOR and phosphoinositide-dependent kinase-1 (PDK-1) signaling pathway, to tightly regulate cell growth and proliferation (Henriques et al., 2010; Wullschleger et al., 2006; Fenton and Gout, 2011). The activation of S6K is through the phophorylation by PDK1 on T^{229} and T^{389} residues and several other kinases including TOR on T^{389} residue (Lehman et al., 2007). The activated S6K can then induce protein biosynthesis and initiate translation of some specific proteins involved in mitogenesis (Fenton and Gout, 2011). It is well characterized that S6K affects cell size in many organisms (Henriques et al., 2010). Knockout of S6K in mice and *Drosophila* caused severely small cell size (Montagne et al., 1999; Pende et al., 2004). Notably, the reduced cell size in mice was not due to the decreased protein synthesis, but the regulation of cell size checkpoint (Pende et al., 2004; Ruvinsky et al. 2005). Thus, S6K may play a role to ensure cells grow to a certain size before going to mitosis. In Arabidopsis, there are two S6K genes, which tandemly locate in chromosome 3. The two genes share 87% sequence identity and have similar functions as in animals (Mahfouz et al., 2006). The single knockout of S6Ks has no obvious growth defects but the homozygous *s6k2* mutants (salk_13334) showed seed abortion (~30%) (Henriques et al., 2010). Further, hemizygous *s6k1s6k2*/++ mutants

displayed reduced fertility, increased ploidy level, aborted seeds and smaller cell size in leaves compared with WT (Henriques et al., 2010). The S6K1 was indicated to interact with the Retinoblastoma-related 1 (RBR1)-E2FB complex to regulate the expression of E2F-dependent cell cycle genes (Henriques et al., 2010). In addition, ectopic over-expression (OE) of Lily S6K gene in *Arabidopsis* inhibited the cell expansion in petals and stamens by up-regulating genes involved in the flower development (Tzeng et al. 2009). All the evidence suggests that S6Ks may have conserved functions in both animals and plants. Plant S6Ks can also function in regulating cell size and proliferation through phosphorylation of S6 protein.

The TOR-S6K pathway plays important roles in cellular response to nutrients, such as amino acids and sugars (Dobrenel et al., 2016). My study described in chapter 3 showed that S6K2 affect membrane lipid remodeling in Arabidopsis response to P starvation. The mechanism by which S6K2 affects lipid remodeling is unknown. Under P starvation, the expression of PLDζ2 and NPC4 is highly induced and the two phospholipases promotes lipid remodeling. However, it is unclear whether and how the functions of S6K and the phospholipases are connected in plant response to P deficiency. The activation of PLDζ2 hydrolyzes phosphatidylcholine to produce phosphatidic acid (PA). The activity of NPC4 produces DAG that can be phosphorylated to PA. PA is a cellular mediator regulating cell growth, proliferation, and stress responses, including nutrient deficiency (Hong et al., 2009).

For example, genetic alteration of PLDε reveals the potential role of PA in cell growth

and proliferation and nitrogen sensing. PLDε OE plants accumulate more biomass and have longer primary root length, whereas pldε KO mutants displayed weaker growth and have less biomass compared with WT. The growth enhancement by increased PLDε expression is more remarkable when plants are in the N deficient condition (Hong et al., 2009). But how PLDε and its derived PA regulate cell size and growth is still elusive. In animals, PLD2-derived PA specifically bound to and activated S6K independently of TOR (Lehman et al., 2007). Also, PA acted as a leukocyte chemoattractant through S6K signaling (Frondorf et al., 2010). However, whether PA can interact with S6K in plants is unknown. This work was undertaken to investigate the interactions between PA and AtS6Ks and the possible role of S6K in the lipid metabolism.

RESULTS

PA specifically binds to S6K

To test whether PA binds to S6K, Arabidopsis S6K1 and S6K2 genes were cloned and the recombinant proteins S6K1 and S6K2 fused with His tag were expressed in *E.coli*. The purified S6K proteins were detected by immunoblotting, and the empty vector control expressed a ~30 KD Trx tag (Figure 4-1A and 4-1B). The purified S6K proteins were then used in the lipid filter binding assay. The egg yolk PC, egg yolk PA, various PA species (16:0 PA, 18:0 PA, 18:1 PA, 16:0 18:0 PA, and 16:0 18:1 PA), phosphatidylserine (PS), phosphatidylinositol (PI) and Phosphatidylethanolamine (PE) were plotted on the nitrocellulose filter. The egg yolk PC and egg yolk PA contain a mixture of different PC species and PA species, respectively. The nitrocellulose filter

was later incubated with purified S6K proteins followed by several times of washing. Finally, lipid-protein interaction was visualized by adding anti-His antibodies followed by the color develop reaction. The results showed that PA exclusively bound to both S6K1 and S6K2. Other phospholipids such as PC, PE, PI and PS could not bind to S6K (Figure 4-1C). Among various PA species, S6Ks bound to 18:1/18:1 PA and 18:2/18:2 PA

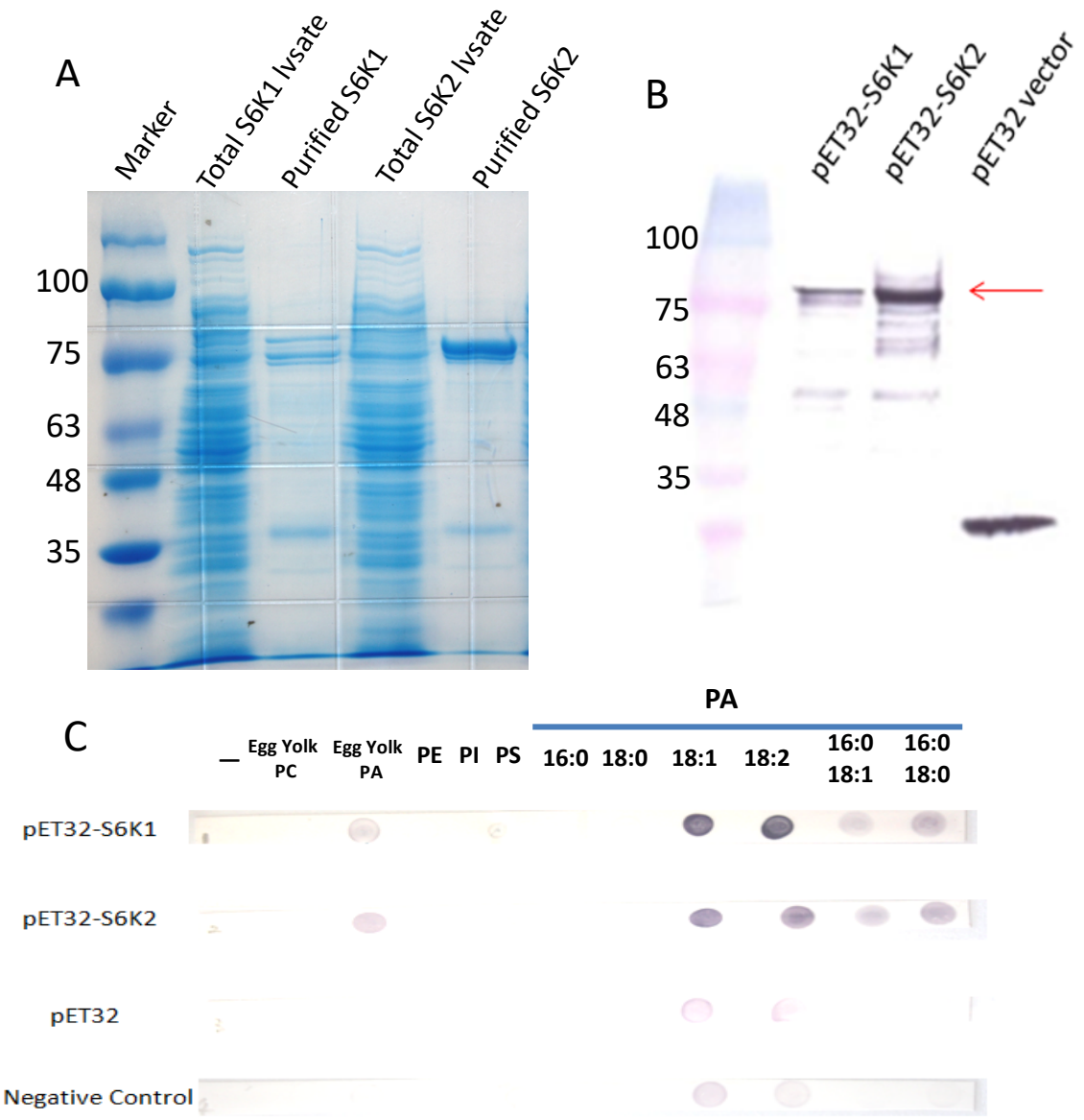

Figure 4-1 S6K protein purification and filter immunobinding.

A. Coomassie blue staining of SDS-PAGE gel of Arabidopsis S6K1 and S6K2 proteins expressed and purified from *E. coli*. B. Western blot of Arabidopsis S6K1 and S6K2 proteins expressed and purified from *E. coli*. C. Filter immunobinding of S6K with various phospholipids. Purified Arabidopsis S6K1 and S6K2 proteins specifically bind to certain PA species.

strongly, whereas bound to 16:0/18:1 PA, 16:0/18:0 PA and egg yolk PA weakly, but did not bind to 16:0/16:0 PA or 18:0/18:0 PA (Figure 4-1B).

To further verify the PA-S6K interaction, liposome binding assay was utilized. The PC liposome and PC/PA liposome were produced to mimic the physiological membrane status in cells. In the assay, purified proteins were incubated with the liposome, followed by the centrifugation. If the protein binds to the liposome, it should be present in the pellet as the liposome precipitates at the bottom after centrifugation, otherwise all the protein should be in the supernatant. To rule out the possibility that the protein tag produced by the empty vector may bind to the liposome nonspecifically due to relatively the big size of the protein tag, I used the purified protein tag from *E. coli* harboring the empty vector as the control. The results indicate that the protein tag bound neither PC nor PC/PA liposome as no protein was detected in the pellet (Figure 4-2). In contrast, S6K1 and S6K2 were detected in the PC/PA liposome pellet but not in the PC liposome pellet, indicating that S6K interacted with PA in the PC/PA liposome.

To better understand the kinetics of PA-S6K binding, surface plasmon resonance (SPR) was performed. The purified His-tagged S6K proteins were first fixed on the surface of the Biacore Ni-NTA Sensor Chip. The PA or PC liposome solution was then intruded and streamed over the surface of the chip, followed by a running buffer. The interaction between S6K and liposome was recorded by detecting the changing angles of refractive light due to the interaction. The representative sensorgram displayed an obvious and rapid increasing curve when the liposomes composed of PC and PA in a molar ratio of

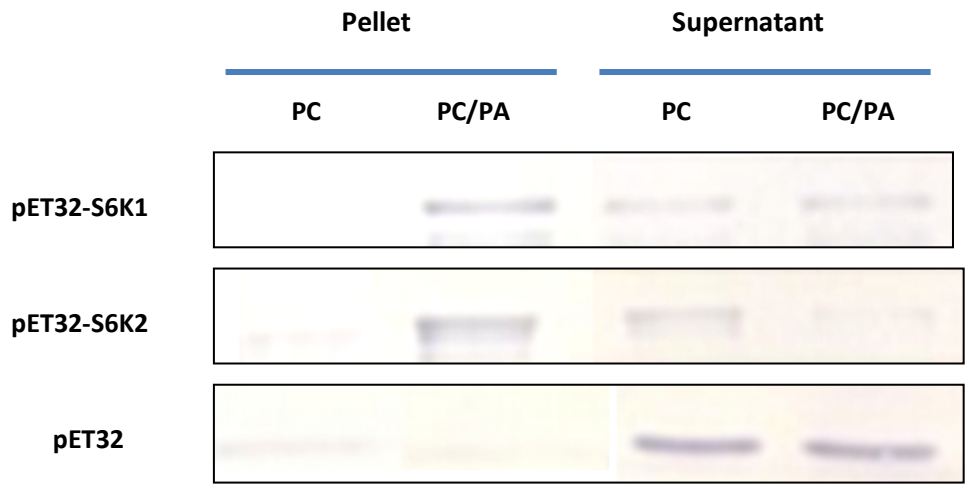

Figure 4-2 PA-S6K binding by the liposome binding assay.

Purified S6K proteins were incubated with PC or PC/PA liposomes, followed by the centrifugation. S6K1 and S6K2 were detected in the pellet with PC/PA liposome but not PC only liposome. The control protein tag was not in present in the pellet either with PC/PA liposome or PC only liposome.

3:1 was added to S6K2, whereas there was almost no increase in response units (RUs) when PC only liposome was used. In contrast, the results showed a similar but less robust binding affinity between S6K1 and PA liposome (Figure 4-3).

S6K2 rather than S6K1 undergoes autophosphorylation

Since PA binds to S6K, the effect of the binding on S6K function was investigated. It was initially intended to test if PA binding would affect S6K kinase activity. To do that, I generated a site-specific mutated version of S6K1 and S6K2, which contains a single amino acid mutation at $S6K1_{T449E}$ and $S6K2_{T455E}$. The 449^{th} threonine of S6K1 and 455^{th} threonine of S6K2 are conserved phosphorylation sites by TOR. The mutation was made to mimic the constitutive status of phosphorylated S6K and was considered as the active form. While assaying S6K phosphorylation of target proteins was unsuccessful, S6K2 but not S6K1 was found to undergo autophosphorylation. The mutations occurred at the putative TOR phosphorylation sites did not affect the S6K2 autophosphorylation (Figure 4-4). Furthermore, in order to examine if PA binding influenced S6K2 autophosphorylation, PA or PC liposome was added into S6K2 and $S6K2_{T455E}$ autophosphorylation reactions. The phosphorylated S6K2 proteins were collected at 10 min, 15 min, and 20 min. The results demonstrated that the phosphorylated S6K2 or $S6K2_{T455E}$ accumulated over time and the PA or PC addition did not affect the autophosphorylation significantly (Figure 4-5).

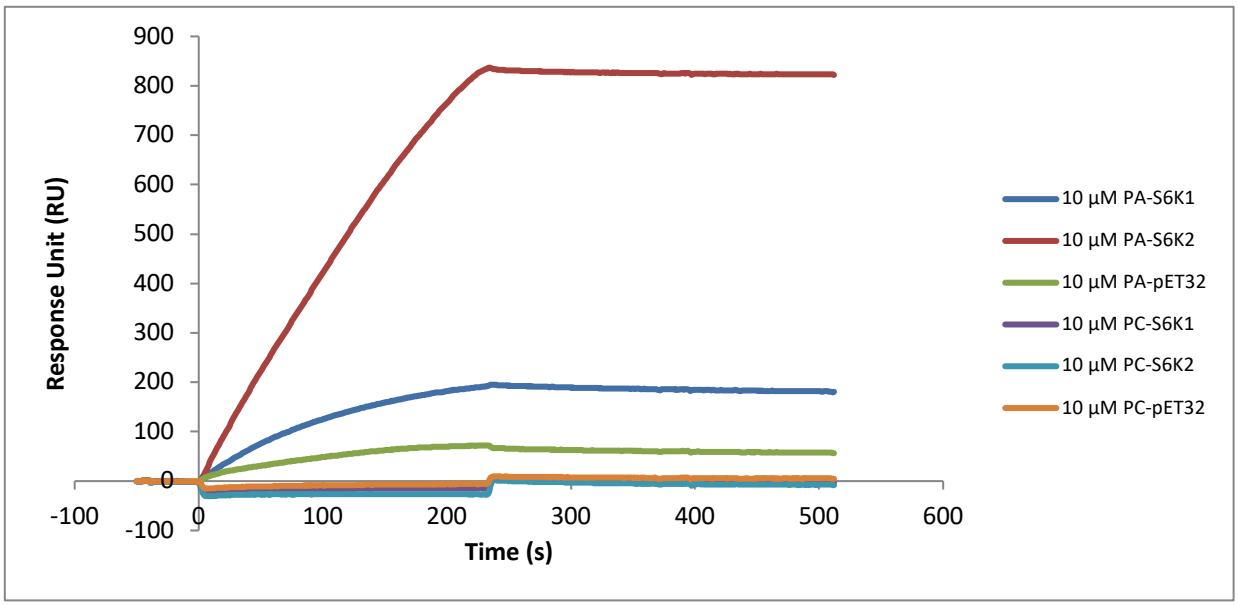

Figure 4-3 Surface plasmon resonance analysis of S6K and PA or PC liposomes.

The purified S6K-His proteins were anchored on the Biacore Ni-NTA Sensor Chip with the continuous flow of 10 uM PA or PC liposome over the surface of the chip followed by the washing buffer. S6K2 bound to PA liposome most rapidly, but not to PC liposome. Similarly, S6K1 bound to PA liposome less robustly than S6K2, but not to PC liposome either.

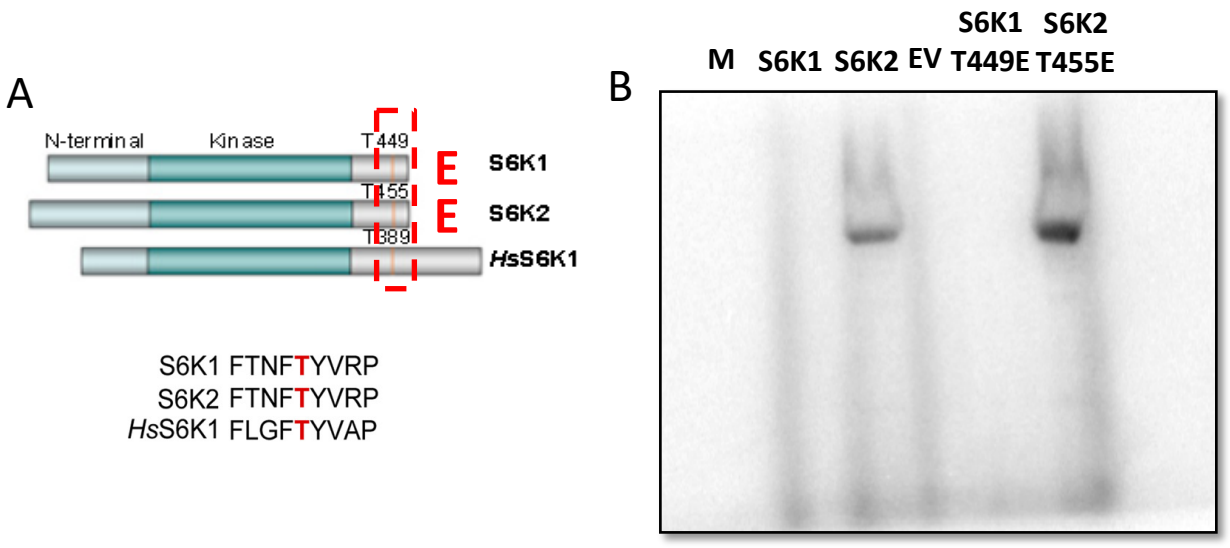

Figure 4-4 The autophosphorylation of S6K2.

A. The comparison of domain structure of S6K in Arabidopsis and human. Arabidopsis S6K and human S6K. The dash square indicates the conserved phosphorylation site T449 of S6K1 and T455 of S6K2 (Modified from Xiong and Sheen, 2012). B. The autoradiography of purified S6K1, S6K2, $S6K1_{T449E}$ and $S6K2_{T455E}$ with P^{32} labelled ATP. M, protein marker.

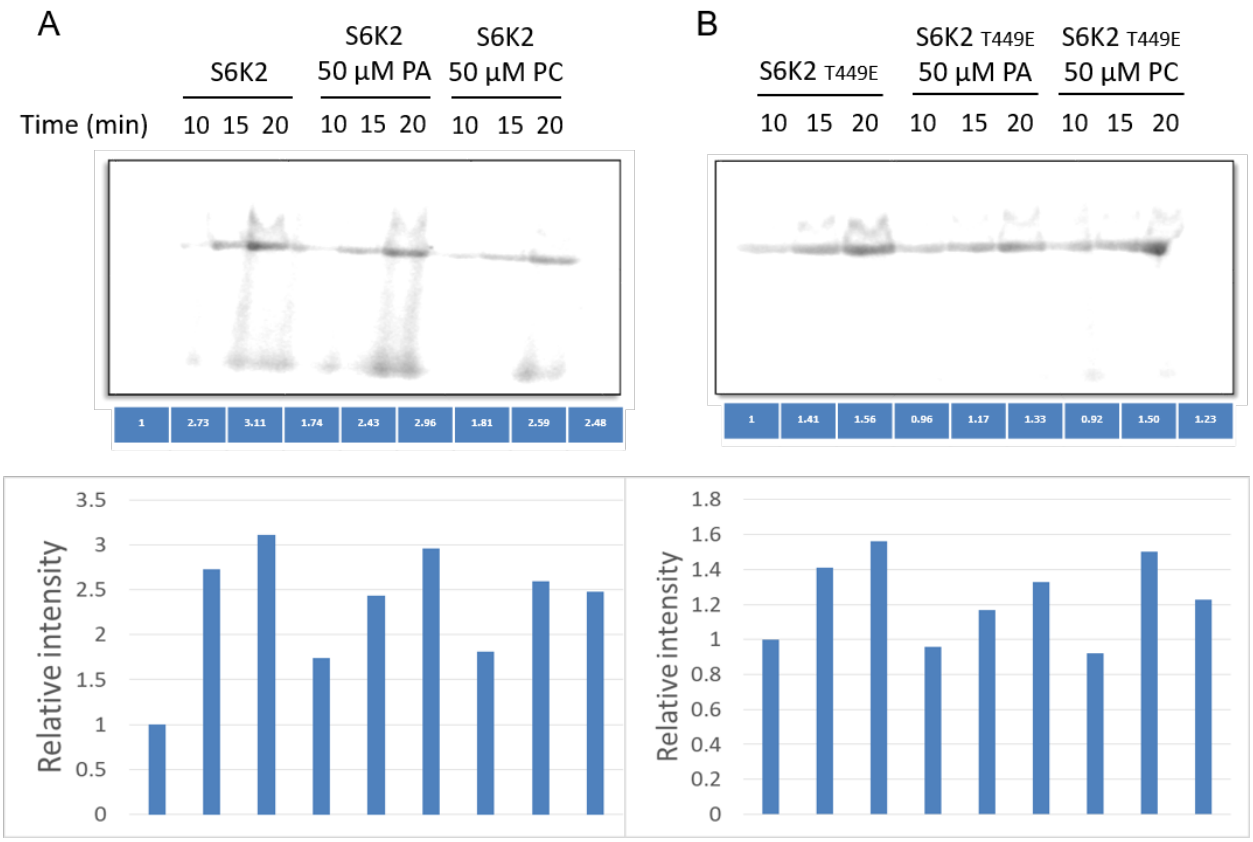

Figure 4-5 PA and PC liposome effect on S6K2 or S6K2$_{T455E}$ autophosphorylation.

Autoradiography of S6K2 (A) and S6K2$_{T455E}$ (B) autophosphorylation over 10 min, 15 min and 20 min with 50 uM PA or PC liposomes. Band intensity was quantified using image J.

S6K suppresses seed oil production

PA is not only a signaling executer, but also an important lipid metabolite involved intriacylglycerol (TAG) biosynthesis. TOR, the upstream regulator of S6K was shown to regulate storage lipid accumulation (Caldana et al., 2013). To test whether S6K affects TAG accumulation, seed oil content was analyzed and compared in WT, *s6k1*, *s6k2*, S6K1-OE, S6K2-OE and S6K-RNAi genotypes. The seed oil content in WT is about 32% of total seed dry weight, whereas the oil content in S6K1-OE 3 and S6K2-OE 6 was about 29% and 28% respectively. The mole percentage of 18:2 and 18:3 fatty acid was significantly higher in S6K1-OE 3 compared with WT, while S6K2-OE 6 had less 18:1, but more 18:2 and 18:3 fatty acid. The knockout mutant *s6k1* and *s6k2*, however, had similar fatty acid composition and oil content as WT (Figure 4-6A and 4-6B). As S6K1 and S6K2 may have redundant roles in TAG synthesis, S6K-RNAi was generated trying to eliminate S6K1 and S6K2 function at the same time. The *S6K1* expression level decreased by about 50% in S6K-RNAi in *s6k2* 8 and 10, 30% in S6K-RNAi in WT 8, while S6K2 expression level decreased by ~60% and ~65% in S6K-RNAi in *s6k2* 8 and 10, respectively (Figure 4-7). The seed oil content increased in S6K-RNAi line 8 and 10 in *s6k2* background and in S6K-RNAi line 8 in WT background, while the mole percentage of fatty acid chains did not change except for significantly increased 18:2 fatty acid in S6K-RNAi line 8 in WT background (Figure 4-6C and 4-6D).

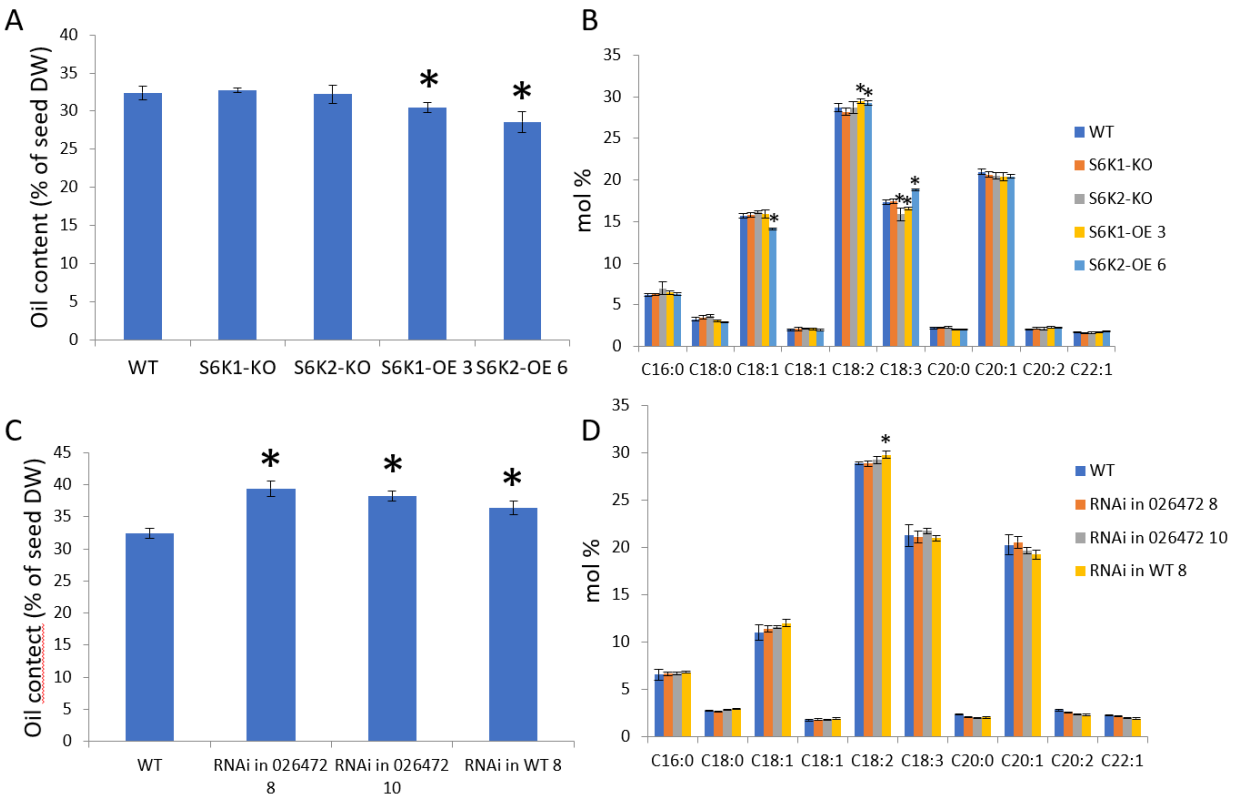

Figure 4-6 Seed oil content and fatty acid composition of WT, *s6k1*, *s6k2*, S6K1-OE, S6K2-OE and S6K-RNAi.

Oil content (A) and fatty acid composition (B) in WT, *s6k1*, *s6k2*, S6K1-OE 3 and S6K2-OE 6 seeds. Oil content (C) and fatty acid composition (D) in WT, S6K-RNAi line 8 and 10 in *s6k2* background and S6K-RNAi line 8 in WT background. Values are means ± SD (n =5). DW, dry weight. Asterisks indicate significant difference between WT and mutants at $P < 0.05$ based on Student's t test.

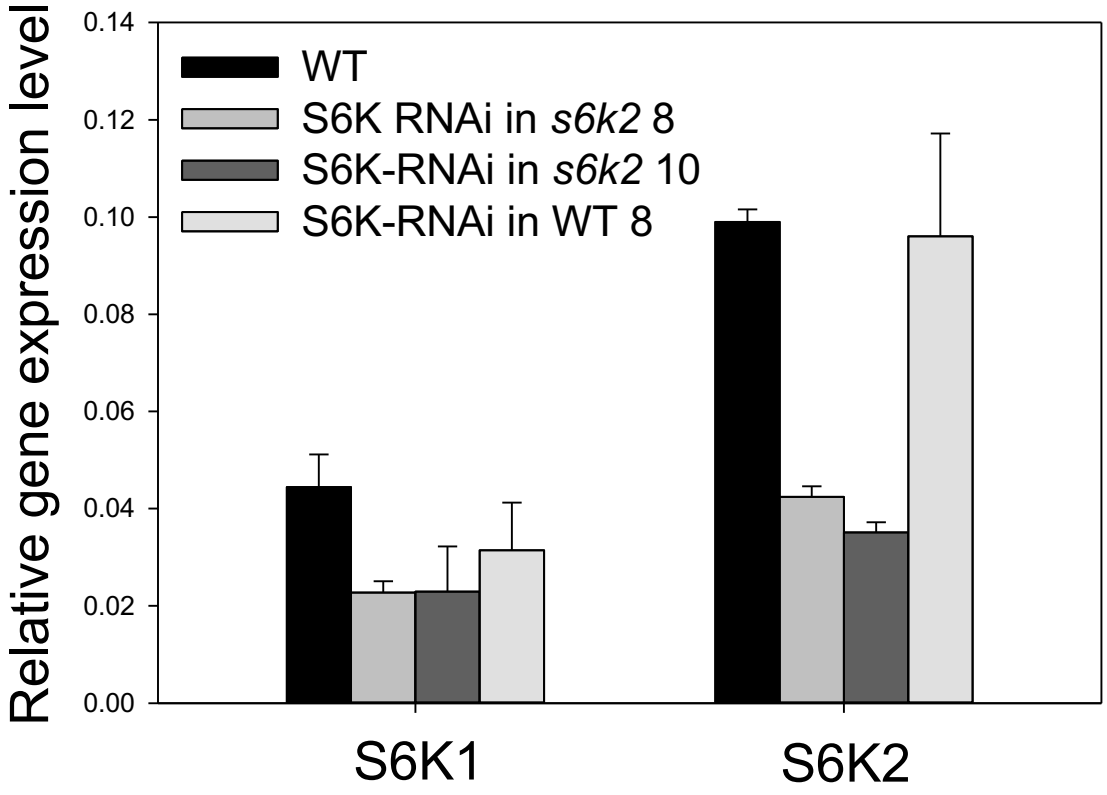

Figure 4-7 The S6K gene expression in S6K-RNAi lines.

RNAs were extracted from 10-day old WT and S6K-RNAi seedlings grown in the soil. S6K1 and S6K2 gene expression levels were detected by qRT-PCR. Values are means ± SD (n =3).

DISCUSSION

The studies of TOR-S6K pathway in yeast and animals unveiled the vital roles of the participants in the pathway in numerous physiological and metabolic processes. As the direct downstream TOR target, S6K executes its functions by interacting and phosphorylating other proteins. PLD and its product PA were shown to regulate TOR and S6K kinase activities. In contrast, Arabidopsis has very conserved TOR and S6K proteins, although not much knowledge has gained about these proteins. Our study here has demonstrated the similarity of Arabidopsis S6K as in animals, but also shed some light on the unique roles of S6K in plants.

The identification of PA-S6K binding in Arabidopsis provides the direct evidence to show that PA is involved in the TOR-S6K pathway as in animals. Interestingly, although PA binds to both S6K1 and S6K2 specifically, the kinetics of the bindings was not the same. It appeared that S6K2 had higher binding affinity with PA than S6K1 indicated by the SPR assay, suggesting the effects of PA binding on S6K1 and S6K2 may be different. It may affect S6K kinase activity as in human cells, or the endogenous PA may affect S6K cellular localizations. S6K1 is located in both cytosol and the nucleus whereas S6K2 is mainly located in the nucleus. The different cellular localizations of S6K1 and S6K2 may also contribute the distinct roles of two S6Ks. In this study, I found only S6K2 rather than S6K1 can undergo autophosphorylation, providing another piece of evidence showing the differences between S6K1 and S6K2, and also suggesting S6K2 may be in a signaling cascade to amplify the signaling by autophosphorylation. S6K1 and S6K2 proteins mainly differ at N terminus, further studies of S6K N terminal

domains may be critical to figure out the origin of differences between S6K1 and S6K2. Also, the specific binding site of S6K and PA needs further exploration. Our preliminary data showed that multiple residues on S6K may serve as important binding sites.

Recent studies discovered that TOR and S6K are involved in lipid metabolism in Arabidopsis. The storage lipid accumulated in TOR-RNAi seeds (Caldana et al., 2013). S6k1 was shown to interact with Raptor2 and affected galactolipid biosynthesis in rice (Sun et al., 2016). Since PA plays a central role in the phospholipid metabolism and thus important for the TAG biosynthesis. It is of interest to test if S6K is involved in oil production in seeds. Our results showed that the seed oil content in S6K-RNAi lines decreased while S6K-OE lines possessed higher oil content than WT. This is in consistent with the oil content data in TOR altered Arabidopsis in assumption that TOR regulates S6K positively which is implied by several reports (Xiong et al., 2013). In addition, 18:1 and 18:3 fatty acid in S6K1-OE, 18:1, 18:2 and 18:3 fatty acid in S6K2-OE and 18:3 fatty acid in S6K-RNAi were different from WT, indicating S6K is somehow involved in integrating acyl chains to TAG. It would be interesting to test if S6K affect genes in the TAG synthesis pathway. It is also possible that PA-S6K interaction serves as a signal feedback to regulate lipid metabolism which needs further investigations.

METHODS

Plant materials and growth conditions

S6K-RNAi plants were generated by transferring an RNAi vector pKANNIBAL that contains approximate 300 bp highly conserved DNA sequence fragment in a hairpin

structure between S6K1 and S6K2 to WT and S6K2-KO backgrounds, so that the transgenic S6K-RNAi plants should have decreased gene expression for both of S6K1 and S6K2. For plants grown in soil, seeds were sowed and germinated in a plastic pot under long day condition (16 h light 22°C/8 h dark 18°C) in a growth chamber with 70% relative humidity and ~170 μmol m^{-2} s^{-1} fluorescent light intensity.

Recombinant AtS6K proteins and its mutant expression and purification in *E.coli*

The cDNA of two Arabidopsis S6K genes S6K1 (At3g08730) and S6K2 (At3g08720) have been cloned and incorporated into a commercial pET32a(+) vector. The site-specific mutated $S6K1_{T449E}$ and $S6K2_{T455E}$ were generated by using QuickChange site-directed mutagenesis (Stratagene) kit under manufacturer's instructions. The constructs containing S6K cDNAs or mutated S6K cDNAs were then transformed into an *E. coli* strain (Rosetta). After the induction by 0.5 mM Isopropyl β-D-1-thiogalactopyranoside (IPTG) at 30°C for 6 hours, *E.coli* cells were harvested and S6K proteins with the His-tag were extracted and affinity purified by using Ni-nitrilotriacetic acid (NTA) agarose beads according to the manufacturer's manual (Qiagen).

Filter immunobinding assay

The purified S6K-His proteins were applied in the fatty western assay that is a general method to detect lipid-protein binding. Generally, 10 ug droplets of different phospholipids such as PC, PA, PE, PI and PS as well as various PA species (32:0, 36:0, 36:2, 36:4, 34:0, and 34:1) were added on the nitrocellulose membrane strips.

Because the lipids were dissolved in the chloroform, the chloroform solvent was used as the control. After the lipid droplets were dried in the room temperature, nitrocellulose membrane strips were blocked with the non-fat BSA for an hour and subsequently incubated with purified S6K proteins as well as the empty vector control proteins overnight. After going through several washes, anti-His antibodies and the following visualization method were utilized to recognize proteins attached to the lipid spot.

Liposome binding assay

In this assay, 3.2 umol 18:1-PC and 18:1-PC/18:1-PA mixtures in a 3:1 molar ratio (2.4 umol and 0.8 umol, respectively) were dried under nitrogen. The dried lipids were then rehydrated in the extrusion buffer and the corresponding liposomes were generated based on the standard lab protocol. The PC and PC/PA liposomes were precipitated after centrifuging by 100,000 g for 20 min at 20°C and dissolved in the binding buffer. Then, liposomes were incubated with purified S6K proteins and the empty vector control, respectively. After the centrifugation at 14,000 g for 20 min at 4°C, the supernatant was obtained while the liposome pellet was formed at the bottom. The liposome pellet was washed several times and subject to mix with the 5× SDS loading buffer. Both supernatant and pellet were then utilized to run the SDS-PAGE gel and the following immunoblotting using anti-His antibodies.

Surface plasmon resonance analysis

SPR binding assays were performed using Biacore 2000 system as described with

some modifications (Yao et al., 2013). Basically, His-tagged S6K proteins were purified and dialyzed with the running buffer (0.01 m HEPES, 0.15 m NaCl, 50 μm EDTA, pH 7.4) for 4–6 h at 4°C, and the protein concentration was determined by a protein assay kit (Bio-Rad). The purified proteins were later fixed on the Biacore sensor Ni-NTA chip that binds His-tagged proteins to immobilize the proteins. For each binding assay, 500 μm NiCl2 was injected with running buffer to saturate Ni-NTA. S6K-His (2 μm) was then used to anchor on the sensor chip via Ni2+-NTA chelation. 10 uM di18:1 PA/di18:1 PC or di18:1 PC only liposomes were suspended in the running buffer (0.01 m HEPES, 0.15 m NaCl, 50 μm EDTA, pH 7.4) and loaded in sequence over the surface of the sensor chip. The regeneration buffer (0.01 m HEPES, 0.15 m NaCl, 0.35 m EDTA, pH 8.3) was used to regenerate the sensor chip by stripping nickel from the surface.

In vitro S6K autophosphorylation assay

The purified S6K protein from *E.coli* was added into kinase buffer (20 mM HEPES, pH 7.5, 125 mM NaCl, 1 mM DTT, 10 mM MgCl2, and 5 mM MnCl2) with 100 μM cold ATP and 0.1 μCi [γ-32P]ATP. The reaction was carried out at 25°C for 30 minutes or indicated times, followed by adding 5x SDS loading buffer and boiling for 5 minutes to terminate the reaction. The samples were then loaded into SDS-PAGE gel and subject to autoradiography after gel electrophoresis.

Seed oil content and fatty acid composition analysis

Arabidopsis seed oil content and fatty acid composition analysis were measured by gas

chromatography using the acid transmethylation procedure as described by Cahoon et al. 2002. Briefly, ~5 mg Arabidopsis mature seeds were incubated with methanol containing 2.5% sulfuric acid, 0.01% (w/v) butylated hydroxytoluene, 20% toluene, and TAG-17:0 internal standard in glass tubes with Teflon-lined caps for 1 hour at 90°C water bath. Formed fatty acid methyl esters (FAME) were extracted with hexane. FAMEs in hexane were transferred into GC vials and subject to be injected into GC-FID with a SUPELCOWAX-10 (0.25 mm × 30 m) column. Each FAME was determined by the retention time compared with known standards. The quantification of individual fatty acid was calculated based on the internal standard heptadecanoic acid (17:0).

REFERENCES

Caldana, C., Li, Y., Leisse, A., Zhang, Y., Bartholomaeus, L., Fernie, A.R., Willmitzer, L., and Giavalisco, P. (2013). Systemic analysis of inducible target of rapamycin mutants reveal a general metabolic switch controlling growth in Arabidopsis thaliana. The Plant Journal 73, 897-909.

Dobrenel, T., Caldana, C., Hanson, J., Robaglia, C., Vincentz, M., Veit, B., Meyer, C. (2016) TOR Signaling and Nutrient Sensing. Annual Review of Plant Biology 67:1, 261-285.

Fang, Y., Park, I.H., Wu, A.L., Du, G., Huang, P., Frohman, M.A., Walker, S.J., Brown, H.A., and Chen, J. (2003). PLD1 regulates mTOR signaling and mediates Cdc42 activation of S6K1.Curr. Biol. 13, 2037-2044.

Fang, Y., Vilella-Bach, M., Bachmann, R., Flanigan, A., and Chen, J. (2001). Phosphatidic acid-mediated mitogenic activation of mTOR signaling. Science. 30, 1942-1945.

Fenton, T.R., and Gout, I.T. (2011). Functions and regulation of the 70 kDa ribosomal S6 kinases. The Intl J. Biochem & Cell Bio. 43, 47-59.

Henriques, R., Magyar, Z., Monardes, A., Khan, S., Zalejski, C., Orellana, J., Szabados, L., Torre, C., Koncz, C., and Bögre, L. (2010). Arabidopsis S6 kinase mutants display chromosome instability and altered RBR1-E2F pathway activity. EMBO J. 29, 2979-2993.

Hong, Y., Devaiah, S.P., Bahn, S.C., Thamasandra, B.N., Li, M., Welti, R., and Wang, X. (2009). Phopholipase Dε and phosphatidic acid enhance Arabidopsis nitrogen signaling and growth. The Plant J. 58, 376-387.

Hong, Y., Pan, X., Welti, R., and Wang X. (2008). Phospholipase Da3 Is Involved in the Hyperosmotic Response in *Arabidopsis*. The Plant Cell. 20, 803-816.

Lehman, N., Ledford, B., Fulvio, M.D., Frondorf, K., McPhail, L.C., and Gomez-Cambronero J. (2007). Phospholipase D2-derived phosphatidic acid binds to and activates p70 S6 kinase independently of mTOR. The FASEB J. 21, 1075-1087.

Mahfouz, M.M., Kim, S., Delauney, A.J., and Verma, D.P.S. (2006). *Arabidopsis* TARGET OF RAPAMYCIN interacts with RAPTOR, which regulates the activity of S6 Kinase in response to osmotic stress signals. The Plant Cell. 18, 477-490.

Montagne, J., Stewart, M.J., Stocker, H., Hafen, E., Kozma, S.C., and Thomas, G. (1999). *Drosophila* S6 Kinase: A Regulator of Cell Size. Science. 285, 2126-2129.

Pende, M., Um, S.H., Mieulet, V., Sticker, M., Goss, V.L., Mestan, J., Mueller, M.,

Fumagalli, S., Kozma, S.C., Thomas, G. (2004). S6K1(-/-)/S6K2(-/-) mice exhibit perinatal lethality and rapamycin-sensitive 5'-terminal oligopyrimidine mRNA translation and reveal a mitogen-activated protein kinase-dependent S6 kinase pathway. Mol. Cell. Biol. 24, 3112-3124.

Wullschleger, S., Loewith, R., and Hall, M.N. (2006). TOR signaling in growth and metabolism. Cell. 124, 471-484.
Reyes de la Cruz, H., Aguilar, R., and Sánchez de Jiménez, E. (2004). Functional characterization of a maize ribosomal S6 protein kinase (ZmS6K), a plant ortholog of metazoan p70(S6K). Biochemistry.43, 533-539.

Ruvinsky, I., Sharon, N., Lerer, T., Cohen, H., Stolovich-Rain, M., Nir, T., Dor, Y., Zisman, P., and Meyuhas, O. (2005). Ribosomal protein S6 phosphorylation is a determinant of cell size and glucose homeostasis. Genes. Dev. 19, 2199-2211.

Sun, L., Yu, Y., Hu, W., Min, Q., Kang, H., Li, Y., Hong, Y., Wang, X., and Hong, Y. (2016). Ribosomal protein S6 kinase1 coordinates with TOR-Raptor2 to regulate thylakoid membrane biosynthesis in rice. Biochimica et Biophysica Acta (BBA) - Molecular and Cell Biology of Lipids 1861, 639-649.

Tzeng, T.Y., Kong, L.R., Chen, C.H., Shaw, C.C., and Yang, C.H. (2009). Overexpression of the Lily $p70^{s6k}$ gene in Arabidopsis affects elongation of flower organs and indicates TOR-dependent regulation of AP3, PI and SUP translation. Plant Cell Physiol. 50, 1695-1709.

Wang, X., Devaiah, S.P., Zhang, W., and Welti, R. (2006). Signaling function of phosphatidic acid. Progress in lipid research. 45, 250-278.

Xiong, Y., McCormack, M., Li, L., Hall, Q., Xiang, C., and Sheen, J. (2013). Glc-TOR signalling leads transcriptome reprogramming and meristem activation. Nature 496, 181-186.

Chapter 5 Conclusion and perspectives

Plants, unlike animals, cannot physically move or migrate in response to the changing growth conditions. Instead, they adapt and evolve to the local environment by altering morphologies and metabolic pathways. It is of great interest to study the potential regulatory pathways involved in plant growth and stress responses. This study was focused on the process of plant response to Pi deprivation. I characterized the roles of two phospholipases PLDζ2 and NPC4 in Arabidopsis under various Pi stress durations. Later, S6K2 was discovered to function as a key regulator of plant response to Pi starvation. Furthermore, I investigated the PA-S6K binding, and the potential effect of S6K on lipid metabolism.

The main findings are summarized as follows:

1. NPC4 and PLDζ2 are strongly induced by Pi deficiency in both leaves and roots, and loss of one or both the phospholipases affect the transcript levels of other genes involved in lipid remodeling.

2. Loss of NPC4 and PLDζ2 impedes primary root growth under Pi deprivation. NPC4 promotes root hair elongation, but has no effect on root hair density, while PLDζ2 negatively regulates the root hair elongation and formation.

3. NPC4 and PLDζ2 function in a tissue and time specific manner in which NPC4 mainly contributes DGDG accumulation in 5-day roots, whereas PLDζ2 hydrolyzes PC and PE in 10-day leaves after Pi limitation.

4. S6K2 but not S6K1 is essential for the membrane lipid remodeling and Pi starvation response, and loss of S6K2 resulted in the loss of the induction of lipid-remodeling genes by Pi starvation.

5. Arabidopsis S6K2 but not S6K1 is induced by Pi starvation and this gene induction is not controlled by PHR1.

6. Double mutant *s6k2phr1* displays similar growth phenotype and lipid changes as *s6k2* and *phr1* single mutant under Pi deprivation.

7. Arabidopsis S6K1 and S6K2 binds to PA, revealing a potential molecular link between PLDζ2/NPC4 and S6K pathways.

8. S6K2 but not S6K1 can execute autophosphorylation. PA or PC addition does not affect S6K2 autophosphorylation.

9. S6Ks negatively impact seed oil accumulation as seed oil content increases in S6K RNAi plants, but decreases in S6K-OE plants.

Significance and perspectives

Phosphorus is an important fertilizer for crop production while the phosphate stock resource is limited and unrenewable. It is critical to use phosphate in a sustainable way and feed the growing world population. To accomplish the goal, one way is to

understand the mechanism of plant responses to low Pi availability and try to manipulate the candidate genes to make Pi stress resistant crops or crops with high Pi usage efficiency. This work has examined two key phospholipases PLDζ2 and NPC4 in lipid remodeling under Pi deprivation. It remains unknown that whether the root hair changes are associated with membrane lipid composition as the lipid extraction from Arabidopsis root hairs is not feasible. Alternatively, testing the relationship between the root hair growth and the lipid composition of root hair cells in larger plants such as Camelina or soybean may be more practical. It is also possible that the PLDζ2 product PA and NPC4 product DAG can mediate root hair growth through signaling pathways by interacting with transcription factors or other players that control root hair formation and elongation (Figure 2-8). Further studies are needed to test these possibilities.

In addition, a novel regulatory protein S6K2 has been discovered to affect many Pi starvation responses including lipid remodeling and root morphologies. The function of S6K2 is likely through interacting with transcription factor PHR1. The transcription of PHR1 was suppressed somehow in *s6k2* mutant at different Pi levels. Whether S6K2 physically interacts with PHR1 and phosphorylates it needs further investigation (Figure 5-1).

The discovery of PA-S6K binding and the role of S6K2 in the Pi starvation response above provides a link between PA and nutrient sensing on a molecular level in plants. It at least partially reveals the mechanism by which plants optimize nutrient resources to regulate cell growth and development. The PA-S6K binding not only shows PA has the

conserved function on S6K as in mammals, but also suggests a putative signaling pathway through which plants sense and uptake nutrients. However, the consequences of PA binding to S6K2 and whether PA generated from lipid remodeling process has a feedback to Pi signaling through S6K2 stays elusive (Figure 5-1).

It is also important to understand how the TOR-S6K pathway integrates signals from changing environmental cues and the possible role of PA in the regulation of the TOR pathway as it may activate TOR activity. In addition, the alteration of cellular PA level may act to translocate PA-target proteins to membranes and thus affect its function. Thus, it is of importance to figure out specific PA-S6K binding residues and test if the subcellular localization of S6K would change due to the changing concentrations of endogenous PA levels or if PA affects S6K kinase activity by optimizing the reaction conditions. Based on the results above, I hypothesize that S6K2 can phosphorylate PHR1 directly and regulate its activity or SK62 regulates PHR1 via interacting with PHR1 regulatory proteins. More studies need to be performed to dig into the detailed regulatory networks.

Overall, the studies in this dissertation unveil the detailed functions and regulations of key participants in Arabidopsis response to Pi limitation. The information of the regulatory network involved in Pi starvation response provided here may lead to further discoveries and serve as solid references.

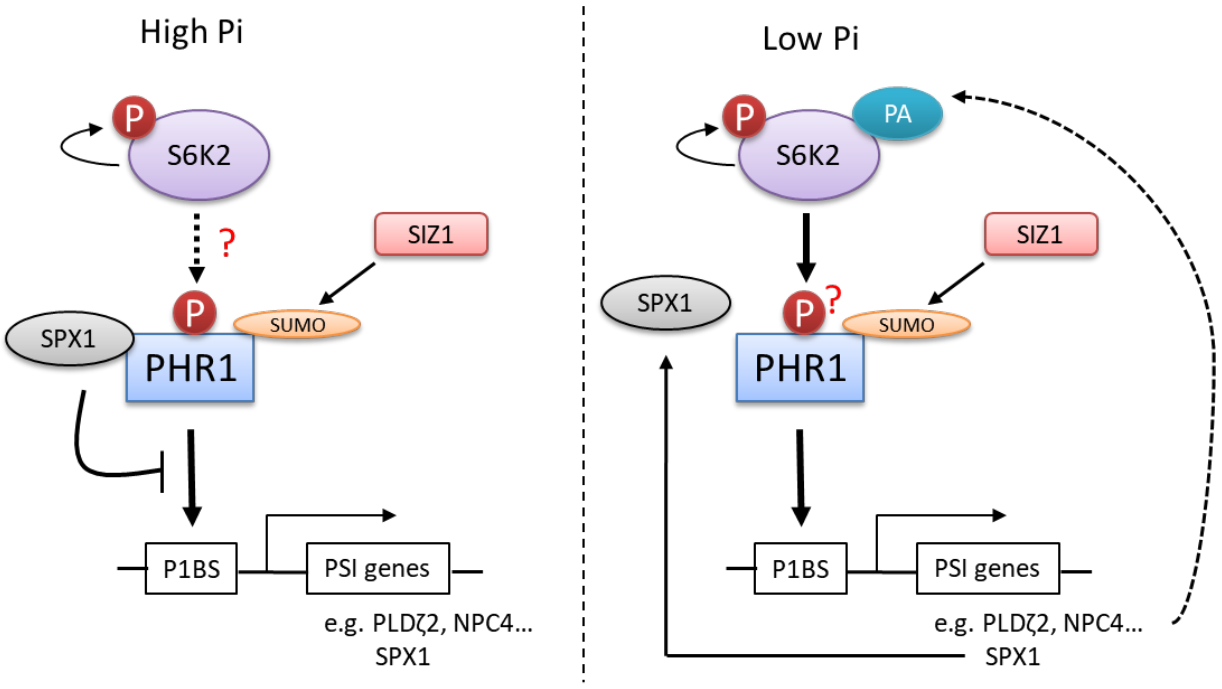

Figure 5-1 Proposed regulatory signaling pathway of lipid remodeling in plant response to P availability.

Transcription factor PHR1 is a master regulator in Pi signaling pathway. It binds to P1BS (PHR1 Binding Site) on its target gene's promoter or 5'-UTR to activate Pi starvation induced gene expression. Under sufficient Pi condition (left), SPX domain containing protein SPX1 binds to PHR1 in a Pi-dependent manner and suppress PHR1's DNA binding ability as a result. SIZ1 can sumoylated PHR1 and affect the expression of some PSI genes through unknown mechanism. Whether SK62 interacts with PHR1 needs further investigation. Under limiting Pi condition (right), SPX1 disassociates with PHR1, thus PHR1 promotes PSI (phosphate starvation induced) genes, including PLDζ2, NPC4 and SPX1. S6K2 is required for PHR1's function although the regulatory mechanism stays elusive. PA binds to S6K2, however it does not affect S6K's autophosphorylation. Whether PA formed from the dynamic lipid remodeling process binds to S6K2 and affect S6K2's subcellular localization or kinase activity needs further studies. Negative and positive regulatory effects are indicated by flat-ended lines and arrows, respectively. The thickness of arrows represents effect strength. The dashed lines indicate putative effects.